EXPERIMENTAL AND THEORETICAL CHARACTERIZATION OF ASPARAGINE SYNTHETASE INHIBITORS

By

YUN DING

A DISSERTATION PRESENTED TO THE GRADUATE SCHOOL
OF THE UNIVERSITY OF FLORIDA IN PARTIAL FULFILLMENT
OF THE REQUIREMENTS FOR THE DEGREE OF
DOCTOR OF PHILOSOPHY

UNIVERSITY OF FLORIDA

2002

To My Family

ACKNOWLEDGEMENTS

First I would like to thank my advisor, Dr. Nigel G. J. Richards, for his guidance, encouragement, support, and valuable input throughout this entire journey. It has been a wonderful experience and a pleasure to work with him. Second, I would like to thank Dr. Sheldon M. Schuster for his help and support. I would also like to thank my other committee members, Dr. Williams R. Dolbier, Jr., Dr. Eric Enholm, and Dr. Steven A. Benner, for their advice, input, and useful discussions. I could not have done it without the help from these important people. They have my appreciation and best wishes for the future.

Next, I would like to acknowledge the current and previous members of the Richards group for their friendship and support. I would also like to thank the members of Dr. Schuster's group for their initial biological evaluation of the inhibitors.

I would like to acknowledge Dr. James Deyrup for his care and support during this study. I would also like to thank the Department of Chemistry and the University of Florida for giving me the opportunity to develop myself as a professional at this institution.

Finally, I would like to thank my husband, Jianqiang Wang, for his love, encouragement and support throughout these years of graduate study. I also want to thank my mother and father, Aixian Cen and Dahua Ding, for their love and support.

TABLE OF CONTENTS

Abstract of Dissertation Presented to the Graduate School
of the University of Florida in Partial Fulfillment of the
Requirements for the Degree of Doctor of Philosophy

EXPERIMENTAL AND THEORETICAL CHARACTERIZATION OF ASPARAGINE SYNTHETASE INHIBITORS

By

Yun Ding

December 2002

Chairman: Nigel G. J. Richards
Major Department: Chemistry

Asparagine synthetase B (AS-B), a glutamine-dependent amidotransferase, catalyzes the synthesis of asparagine from aspartic acid, glutamine, and ATP. The catalytic mechanism of asparagine synthetase B is not fully understood. The X-ray structure of AS-B in complex with substrates, intermediate or inhibitors is not available. The structure of human AS is also not known. This study reports the syntheses of the substrate derivative and inhibitor of the enzyme and the molecular modeling of the structure of *E. coli* AS-B and human AS.

L-4,4-difluoroglutamic acid, a fluorinated amino acid, is an important intermediate in the preparation of L-4,4-difluoroglutamine, which can be used to investigate the mechanism of asparagine synthetase B. A new, flexible route to enantiomerically pure L-4,4-difluoroglutamic acid that exploits the addition of difluorinated nucleophiles to configurationally stable α-aminoaldehydes is reported.

Conversion of the difluorinated adducts to L-4,4-difluoroglutamic acid can be accomplished in three steps by Barton-McCombie dehydroxylation and acid hydrolysis.

Asparagine synthetase catalyzes the formation of β-aspartyl-AMP in one of its active sites. Stable analogues of acyladenylate intermediates are useful probes of the enzyme mechanism and have potential application as enzyme inhibitors. A concise, "one-pot" synthesis of β-asparaginyladenylate using a novel coupling protocol yields the target *N*-acylphosphoramidate in three steps from readily available precursors, an asparagine derivative, an adenosine derivative and benzyloxydichlorophosphine. Both D-asparagine derivative and L-asparagine derivative were tried. The initial biological evaluation showed that the L-conformation asparaginyladenylate is 200-fold more active than the D-conformation compound.

The crystal structure of *E. coli* C1A AS-B mutant in complex with AMP and glutamine has been determined. The hypothetical models of substrates, intermediate and β-asparaginyladenylate bound within the synthetase domain of bacterial asparagine synthetase are constructed. The structure of human asparagine synthetase is also modeled using the homology modeling and molecular dynamics simulation methods.

CHAPTER 1
INTRODUCTION

Chemotherapy for Acute Lymphoblastic Leukemia

L-asparaginase,[1-4] which catalyzes the hydrolysis of asparagine to aspartate and ammonia, is used in chemotherapeutic protocols in the treatment of acute lymphoblastic leukemia (ALL)[5,6] and acute myeloblastic leukemia.[7,8] However, this therapeutic approach has some limits. First, the treatment produces a wide variety of side effects[9] including granulocytopenia, thrombocytopenia, infection, stomatitis, pneumonitis and hemorrhage. Second, a large number of patients who achieve remission suffer a relapse with tumors that are resistant to further L-asparaginase therapy.[8-11] Finally, L-asparaginase enhances the growth of resistant tumors and increases their metastatic activity.[12] Because the sensitivity of tumors to L-asparaginase cannot yet be reliably predicated, the major use of this enzyme remains confined to ALL, despite estimates that 5-10% of all solid tumors, including those that appear to be smoking-related, may be sensitive to asparagine depletion.[11] The molecular basis of L-asparaginase resistance is poorly understood and remains a major clinical problem in treating relapsed patients.[13]

Given that L-asparaginase treatment is probably effective as a result of decreased levels of circulating asparagine, it is possible that AS inhibitors might prove useful as anti-leukemic agents. Such compounds would be especially valuable for cells displaying resistance to L-asparaginase treatment, which probably express endogenous asparagine synthetase. Additionally, T-cell based immunosuppression is often observed in patients

undergoing initial treatment with L-asparaginase,[14] raising the possible utility of AS inhibitors as immunosuppressive agents. The observation that L-asparaginase may be effective in treating a variety of solid tumors also provides additional stimulus to developing AS inhibitors. Such compounds might act by reducing the potential of hepatic tissue as an asparagine reservoir, enhancing the sensitivity of tumors in other organs to L-asparaginase chemotherapy.[15]

Asparagine Synthetase

To date, two families of AS enzymes[16] that do not appear to possess any sequence similarity have been described in prokaryotes and eukaryotes. Members of the first enzyme family (AS-A) which have been isolated solely from prokaryotes employ ammonia as the sole nitrogen source (Figure 1-1) and appear to be evolutionarily related to amino-acyl tRNA synthetases.[17] For the second class of asparagine synthetases (AS-B), glutamine is the preferred nitrogen source, although these enzymes can also employ ammonia as an alternate substrate (Figure 1-1). The glutamine-dependent asparagine synthetases have been cloned and/or isolated from yeast,[18] plants,[19,20] bacteria,[21-23] and mammalian sources.[24-26] Sequence analyses have indicated that these enzymes are all members of the Class II (formerly purF) glutamine amidotransferase (GAT) superfamily,[27] which also includes glutamine 5'-phosphoribosyl-1-pyrophosphate amidotransferase (GPA),[28] glutamine fructose-6-phosphate amidotransferase (GFAT)[29] and glutamate synthetase.[30]

Whereas the kinetic and chemical mechanisms employed by ammonia-dependent asparagine synthetases, such as *E. coli* AS-A, appear to be well understood,[31-33] full understanding of AS-B mechanism is an ongoing task. A key breakthrough in studying

the structure[34] and mechanism[35] of glutamine-dependent AS was our development of procedures for obtaining large amounts of AS-B, which is encoded by the *asnB* gene in *Escherichia coli*[36,37] and the successful determination of the three-dimensional structure of the ternary complex among glutamine, AMP and the C1A AS-B mutant, in which cys1 is replaced by alanine (Figure 1-2).[34] As expected on the basis of sequence comparisons,[38] glutamine-dependent AS is composed of two domains, joined together by a small peptide "linker," which possess no shared elements of secondary structure and contain distinct catalytic sites. The conversion of glutamine into glutamate and ammonia is catalyzed by the N-terminal glutaminase domain of the enzyme (blue in Figure 1-2), while the second, synthetase domain mediates the formation of βAspAMP **2** and inorganic pyrophosphate (PPi)[35] (Figure 1-1). Ammonia then travels from the glutaminase to synthetase domain along an intramolecular tunnel,[34,39,40] where it undergoes reaction with βAspAMP **2** to give asparagines and AMP. However, there are several key issues with respect to the structure and mechanistic enzymology of the glutamine-dependent enzymes that remain to be defined. The first issue is what is the structural organization of the active site involved in aspartate activation? Our recent X-ray structure of *E. coli* AS-B mutant complex has structural distortions in the synthetase domain arising from the absence of aspartate. The second issue involves the corresponding molecular basis for coordination of the two half-reactions that occur during asparagine synthesis, and the third issue deals with how the ammonia channel works?

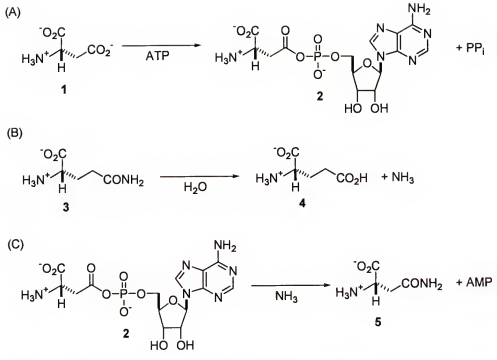

Figure 1-1 Reactions catalyzed by glutamine-dependent asparagine synthetase.

Figure 1-2 X-ray crystal structure of the *E. coli* C1A AS-B mutant in complex with AMP and glutamine.

Progress in Development of Asparagine Synthetase B Inhibitors

Potent and specific inhibitors of human AS have significant potential both as agents for treating leukemia and as tools for investigating the cellular basis of resistance to L-

asparaginase treatment. The observation that T-cell based immunosupression is often observed in patients undergoing initial treatment with L-asparaginase provides an additional stimulus to develop AS inhibitors. From a theoretical standpoint, our recent X-ray structure did not include the active site of the aspartate binding domain. More evidence was also needed to confirm the existence of the ammonia channel. Therefore, an inhibitor that is efficient against this catalytic domain is highly desirable. In order to meet our current focus to obtain information on (i) enzyme structure, (ii) the interactions that catalyze the formation and breakdown of the βAspAMP intermediate in the synthetase active site site, and (iii) the molecular mechanisms that underlie channel formation, the inhibitor should be rationally designed to mimic the βAspAMP, even though we all know that more drug-like inhibitors could be small molecules with good bio-availability.[41-43]

To date, only three inhibitors[44-46] have been reported that mimic βAspAMP, and two of them showed very potent activities as shown in Figure 1-3. Other inhibitors from random screening hundred analogues of glutamine, ATP and aspartic acid did have some inhibitory activity in either *in vivo* or *in vitro* assays, but they are either nonspecific, or are inhibitors in the millimolar range.[47-52] Some glutamine analogues acting as asparagine synthetase inhibitors are shown in Figure 1-4. These analogues irreversibly inhibit the enzyme, presumably by the formation of the covalent bond with thiolate of Cys1. For example, albizziin **9**, has been shown to inhibit AS in vitro, albeit with a K_I of 1-5 mM, causing amplification of the AS gene.[53] This compound has little potential as an antitumor agent as it inhibits many other enzymes in which glutamine is a substrate. Figure 1-5 listed some aspartic acid analogues that have been used in indirect

characterization of the aspartate binding site of asparagine synthetase B.[54-57] The studies using these competitive inhibitors with respect to the aspartate and chemical modification experiments employing 5'-O-[p-(Fluorosulfonyl)benzoyl]adenosine (FSBA),[58] an ATP analogue, (Figure 1-6) demonstrated that large steric alterations in the substrate are not tolerated by the enzyme, and that the ionizable groups are in close proximity in the bound conformation of aspartate. All these asparatic acid analogues are weak binders to AS-B (mM inhibition).

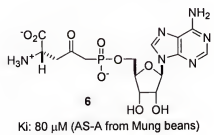

6

Ki: 80 μM (AS-A from Mung beans)

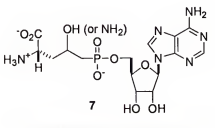

7

Ki: 100 nM (AS-A from white lupine or *E. coli*)

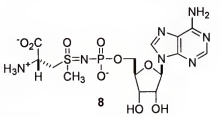

8

Ki: 67 nM (AS-A from *E. coli*)

Figure 1-3 Interesting inhibitors of AS-A that could be references for the design of AS-B inhibitors.

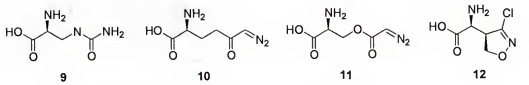

9 10 11 12

Figure 1-4 Glutamine analogues as asparagine synthetase inhibitors

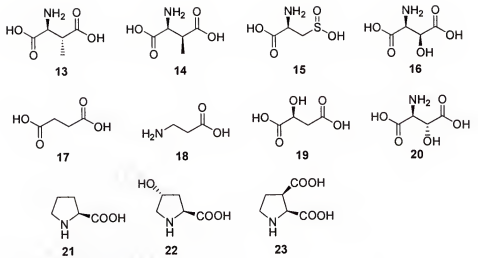

Figure 1-5 Aspartate analogues for asparagine synthetase study.

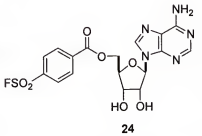

Figure 1-6 Irreversible inhibitor 5'-O-[p-(fluorosulfonyl)benzoyl]adenosine (FSBA).

As previously mentioned, the β-AspAMP mimic inhibitors with tight binding and high specificity to the aspartate catalytic domain are most relevant for this study. Compound **6** (Figure 1-3), with CH_2 as a substitute of O in β-AspAMP, had a K_i of 80 μM, which is not potent enough. However, compound **7** and **8** (Figure 1-3) demonstrated very good activities against AS-A. Compound **8**, *N*-adenylated sulfoximine, is a tight-binding inhibitor of ammonia-dependent asparagine synthetase (AS-A).[46] It is one of the most potent AS-B inhibitors reported to date. Unlike its behavior with AS-A, our recent

results[59] showed that sulfoximine derivative **8** is able to form a high-affinity complex with AS-B only when the enzyme is undergoing catalytic turnover. The inhibition is aspartate dependent. The compound does not bind free enzyme even after extended incubation. The unexpected difference in the kinetic mechanism by which **8** inhibits AS-A and AS-B is most likely a consequence of conformational changes that are unique to glutamine-dependent asparagine synthetases due to constraints imposed by the structural elements required to channel ammonia between two independent active sites.

Specific Aims

We are very interested in studying the catalytic mechanism of asparagine synthestase and discovering new inhibitors of the enzyme. The first part of the present study involved the synthesis of L-4, 4-diflutamic acid, an important intermediate in the preparation of L-4, 4-diflutamine that can be used as an alternate substrate of the enzyme. The second part of the work involved the design and synthesis of β-asparaginyladenylate. Initial biological evaluation showed that it is a potent inhibitor of *E. coli* asparagine synthetase B. The third part of the present study was using the homology modeling and molecular dynamics simulation methods to construct hypothetical models of substrates, intermediates and β-asparaginyladenylate bound within the synthetase domain of both the bacterial and human forms of asparagine synthetase.

Due to the limited previous work on the inhibitors of asparagine synthetase and their interaction with the enzyme, we studied another family of enzyme aminoacyl-tRNA synthetase, which also uses ATP and Mg^{2+} or Mn^{2+} to activate the amino acid by forming aminoacyl adenylate. This step of the reaction has been well studied and various inhibitors of aminoacyl-tRNA synthetases have been designed and synthesized. This

information is very helpful for our design of new inhibitors of asparagine synthetase. Hence, the review on the inhibitors of aminoacyl-tRNA synthetase is presented in the following chapter.

CHAPTER 2
REVIEW OF AMINOACYL-TRNA SYNTHETASES

Introduction

Aminoacyl-tRNA synthetases (aaRSs) are responsible for the correct attachment of amino acids to the 3' terminal adenosine of their cognate tRNAs through a two-step reaction.[60,61] In the presence of Mg^{2+} and ATP, the enzyme first activates the amino acid to form aminoacyl-adenylate (aa-AMP) intermediate. In the second step, the amino acid is ligated to the cogated tRNA, generating aminoacyl-tRNA (AA-tRNA). The charging of amino acids onto tRNAs is a prerequisite for protein biosynthesis. Thus, compounds that inhibit bacterial aminoacyl-tRNA synthetases specifically are potential antibacterial drugs. This concept is proven by the success of the broad-spectrum antibacterial drug mupirocin, which targets bacterial isoleucyl-tRNA synthetases.[62]

The 20 aminoacyl-tRNA synthetases are divided into two classes, class I and class II, comprising 10 members each,[61] which have distinct catalytic domain architectures with exclusive signature motifs for the ATP binding. The class I aaRSs have a catalytic domain constructured with the Rossmann fold, and display two signature amino acid motifs, "HIGH" and "KMSKS." The class II aaRSs share 3 other conserved sequence motifs and their active sites are built on an antiparallel β-sheet surrounded by α-helixes. One result of this difference in active site structure is that class I enzymes bind ATP in an extended conformation, while class II is a bent conformation.[63] The separation of aaRSs into two classes also correlates with the stereochemical modes of attack on the carbonyl

of the aminoacy-adenylate. The class I aaRSs attach amino acids to the 2'-OH of the terminal ribose at the 3'-end of tRNA and classs II enzymes attach the respective amino acids to the 3'-OH group of the terminal ribose. The only exception to this rule is phenylalanyl-tRNA synthetase (PheRS).[61,64] At present, the structure of 18 out of the 20 enzymes of the family, native or complexed with various substrates, intermediates and their analogues, are known. Nine of them belong to class I aaRSs: TyrRS,[65] GlnRS,[66,67] MetRS,[68] TrpRS,[69] GluRS,[70] IleRS,[71] ArgRS,[72] LeuRS[73] and ValRS.[74] In class II, the X-ray structures of SerRS,[75-79] GlyRS,[80,81] HisRS,[82-84] ProRS,[85] PheRS,[86-88] AsnRS,[89] LysRS,[90-92] AspRS[93-97] and ThrRS[98] have been solved.

Aminoacyl-tRNA synthetases have emerged as leading targets for the development of new antibiotics.[99-101] The explosion of structural information, coupled with complementary biochemical studies, now permits a detailed study of the first step of aminoacylation at the atomic level, which gives a lead in the design of inhibitors of synthetases as drug prototypes. This review will focus on the first step of aminoacylation: recognition of the substrates, intermediate and their analogs by two types of aaRSs and the inhibitors of aaRSs.

Structure Basis of the First Step of Aminoacylation

The first step of aminoacylation has been studied using crystal data for aaRS complexed with substrates, ATP and an amino acid. Substrate analogs, intermediates, and the aminoacyl-adenylate complex, obtained through reaction in the crystal or during crystallization, or synthetic analogs of the reaction intermediate, have also been used in these studies.

Class I aaRSs

The crystal structure of the IleRS from *Thermus thermophilus*, in complexes with Ile-AMS (Figure 2-1a) is used to exemplify the class I active site.[102]

Ile-AMS is a non-hydrolyzable analogue of Ile-AMP, in which the phosphoester bond between the isoleucyl and adenosine moieties is replaced with a sulfoamide bond. The structure of IleRS/Ile-AMS complex was compared with the adenylate complexes of the other class I aaRSs, LeuRS, TyrRS, TrpRS, ValRS and GlnRS. The result is summarized in Figure 2-1b. The amino group of the aminoacyl moiety hydrogen-bonds to the main chain carbonyl group of the residue (Pro46 in *T. thermophilus* IleRS). The carbonyl group of the aminoacyl moiety is not necessary to be recognized by any residue of the aaRSs. In IleRS, the carbonyl group of the isoleucyl moiety H-bonds to the Nε of the side chain of Gln554 H-bonds. The phosphate moiety is recognized by the main chain amide of the residue through hydrogen-bonding to one of the oxygens of the phosphate group, except for IleRS, which hydrogen-bonds to sulfamoyl group by Nε of His57, the second His of the class I specific signature motif, HIGH. The 2'-hydroxyl group of the ribose moiety is recognized through hydrogen bonding by the main chain amide of Gly (Gly551 of *T. thermophilus* IleRS), which is conserved in most of the class I aaRSs. Moreover, the carboxyl group of the acidic residue (Asp553 of *T. thermophilus* IleRS) hydrogen-bonds to the 2'-OH group. Except for IleRS and TyrRS, the main chain amide of the residue corresponding to Ile584 of the *T. thermophilus* IleRS hydrogen-bonds to N1 of adenine. Furthermore, in these aaRSs, the N6 of adenine hydrogen-bonds to the main chain carbonyl oxygen of the same residue and, in ValRS, LeuRS, and TrpRS, to

the carbonyl oxygen of the Met residue (Met592 in *T. thermophilus* IleRS) of class I specific motif, KMSKS.

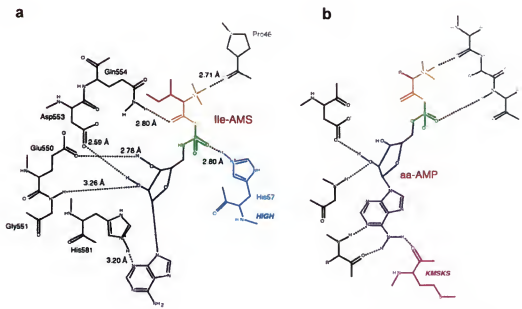

Figure 2-1 Schematic drawing of the consensus recognition model of (a) Ile-AMS by IleRS, (b) aa-AMP by the class I aaRSs.[102]

Class II aaRSs

In all class II aminoacyl-tRNA synthetases, ATP is found in a bent conformation with the β- and γ-phosphate folded toward the adenine ring into a U-shaped structure.[63] This places the α-phosphate in an ideal position to attack the carboxylate of the amino acid substrate. The binding of ATP is summarized in Figure 2-2. Specificity for the ATP adenine base is achieved by hydrogen bond interactions with the purine ring nitrogens. N1 and N6 of the purine ring make hydrogen bonds with the main chain carbonyl oxygen and nitrogen atoms of the residue that is not highly conserved in class II synthetases, Met335 of yeast AspRS and Gln271 of *E. coli* LysRS.[92] The purine moiety of ATP is

invariably sandwiched between the aromatic side chains of topologically equivalent phenylalanine and arginine residues (motif 2). A positive charge supplied by a histidine or arginine residue originating from the same loop (His270 in *E. coli* LysRS,[92] Arg231 in *Thermus thermophilus* GlyRS,[81] Arg121 in *E. coli* HisRS[83]) is well-conserved (Figure 2-3) and is always involved in enforcing the crucial bent conformation of ATP and stablization of the pyrophosphate group, together with the invariant motif 3 arginine (Arg480 in *E. coli* LysRS,[92] Arg366 in *Thermus thermophilus* GlyRS,[81] Arg311 in *E. coli* HisRS[83]) which interacts with γ-phosphate. His334 in yeast AspRS[94] does not interact with either the β- or γ-phosphate which helps the leaving of pyrophosphate. Instead, the side chain of Ser481 is involved in the stabilization of the pyrophosphate group, together with invariant Arg531. Another invariant motif 2 arginine is involved in the interaction with α-phosphate (Arg262 in *E. coli* LysRS, Arg220 in *Thermus thermophilus* GlyRS, Arg113 in *E. coli* HisRS, Arg325 in yeast AspRS). In some cases, like *Thermus thermophilus* GlyRS and *E. coli* LysRS, this arginine residue hydrogen bonds with the carboxylate of the amino acid substrate, which might help hold the α-phosphate in the right orientation to attack the carboxylate of amino acid substrate.

A cation, such as Mg^{2+} or Mn^{2+}, is always involved in the reactions catalyzed by aminoacyl-tRNA synthetases. Both kinetic[103] and structural data[78] have shown that the Mg dependence of the aminoacylation reaction differs for class I and class II enzymes, with class I enzymes requiring only one Mg^{2+}, while class II enzymes require three cations (Figure 2-2). The Mg 1 site corresponds to the bridging of the α- and β-phosphates,[78,81,89,92,97] with the exception being HisRS[83,84] where the equivalent role is

played by a conserved arginine. The two additional metals both bind the β– and γ-phosphates.

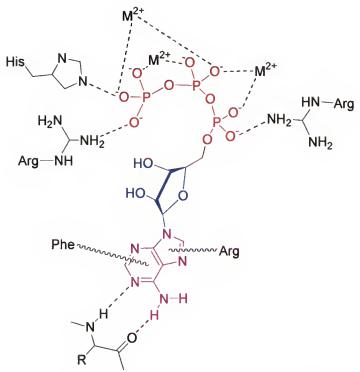

Figure 2-2 Schematic drawing of the consensus recognition model of ATP by the class II aaRSs.

Aminoacyl-adenylate adopts an extended conformation that is assumed by adenylate molecules in class II aaRSs. Comparison of the structures of lysyl-adenylate and ATP[92] shows that the mechanism for lysine activation is an in-line displacement mechanism. No enzyme residue participates directly in the reaction, and catalysis is achieved by binding both substrates (lysine and ATP) in the correct conformation. A comparison between the models of the unreacted ATP and the lysyl-adenylate intermediate also clearly illustrates the inversion of configuration at the α-phosphate, caused by the in-line nucleophilic attack. The adenosine moiety and amino acid moiety of

the intermediate bind to the synthetase in a manner similar to that of the unreacted substrates. The negative charges on the pyrophosphate moieties are stabilized through arginine and histidine residues and through the cations.

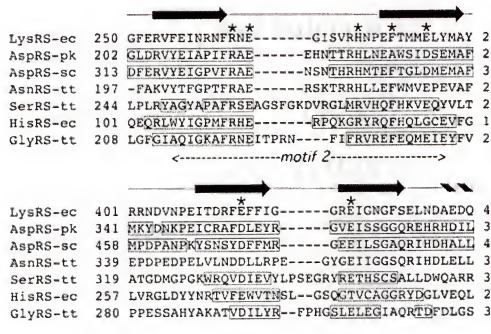

Figure 2-3 Sequence alignment of selected class II aaRSs whose three-dimensional structures have been determined in the presence of ATP or the aminoacyl adenylate intermediate.[92]

Inhibitors of Aminoacyl-tRNA Synthetases

A large number of diverse chemical structures that inhibit aminoacyl-tRNA synthetases have been identified.[104] According to their different inhibition mechanisms,

they can be divided into 3 groups: the analogues of substrates, the analogues of the reaction intermediate, and the analogues of the transition state.

Analogues of Substrates

Aminoacyl-tRNA synthetases use ATP and amino acids as their substrates. ATP analogues have been widely used in the crystallization. However, they are not targeted inhibitors because of low selectivity. The analogues of amino acids have been proven to be effective inhibitors of aaRSs.

Natural products as analogues of amino acids. Some natural products are analogues of amino acids and selectively inhibit the corresponding aminoacyl-tRNA synthetases (Figure 2-4). Cispentacin, isolated from *Bacillus cereus* and *Streptomyces setonii*, is an analogue of proline and is a weak inhibitor of prolyl-tRNA synthetase.[105] However, it has been pursued as an antifungal agent as it accumulates to high intracellular levels in several fungal species through an active transport mechanism.[105]

Furanomycin, isolated from a *Streptomyces sp.*, is a non-protein amino acid and has been found to inhibit the enzymatic activity of *E. coli* IleRS.[106] It was found to bind with *E. coli* isoleucyl-tRNA synthetase almost as tightly as the substrate L-isoleucine.[107] The conformation of IleRS-bound furanomycin, determined by NMR analysis, was similar to that of L-isoleucine bound structure, although the chemical structure of furanomycin is unlike that of L-isoleucine.

Indolmycin, produced by *streptomyces albus*, is an analogue of tryptophan. The two molecules have obvious structural similarities. In indolmycin, the α-amino acid is replaced by an uncharged 2-methylaminooxazolin-4-one ring, with a 5'-methyl substituent corresponding to the amino acid β-position. Indolmycin selectively inhibits

bacterial tryptophanyl-tRNA synthetase.[108] It has been demonstrated that indolmycin can compete for the tryptophan binding site in the synthetase-catalyzed process in which tryptophan reacts with ATP to form tryptophanyl adenylate. The unnatural diastereomer of indolmycin possesses no antibacterial activity.[109] Analogues of indolmycin were synthesized in which the methyl group on the carbon atom separating the two rings was replaced by larger or smaller groups, and by polar species including amino and carboxylic acid functionalities.[110] Their antibacterial and enzyme inhibitory potency study indicates that the methyl group binds in a small, essentially hydrophobic binding pocket and it stabilizes a particular conformation of the indole and oxazole moieties.

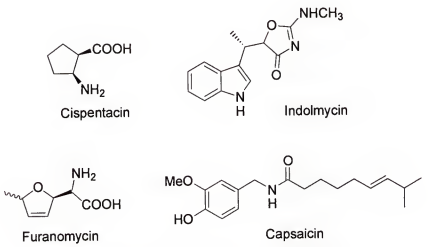

Figure 2-4 Structures of natural aaRS inhibitors.

Capsaicin, the pungent ingredient found in the fruit of the genus Capsicum (paprika, cayenne), is a structural analog of tyrosine.[111] It inhibits (K_i = 42 um) the aminoacylation of TyrRS.

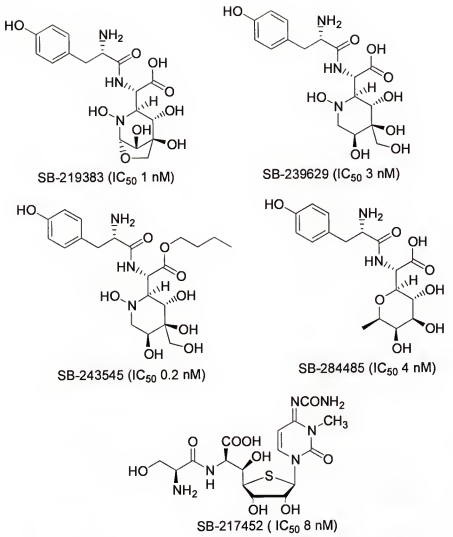

Figure 2-5 Natural products as amino acid derivatives.

There exists another kind of natural products, which are the derivatives of amino acid, and were discovered to be the inhibitors of corresponding aminoacyl-tRNA synthetases (Figure 2-5). SB-219383,[112] isolated from fermentation broth of a novel species of *Micromonospora sp.* NCIMB 40684, is the first member of a new class of compounds having inhibitory activity against tyrosyl tRNA synthetase (IC_{50} = 2 nM). SB-219383 also exhibits moderate *in vitro* activity against some Gram-positive bacteria. Some of its derivatives[113] (Figure 2-5), SB-239629, SB-243545, SB-284485, are potent

inhibitors of tyrosyl tRNA synthetase as well. SB-217452 (Figure 2-5),[114] isolated from *Streptomyces* sp. ATCC 700974, showed inhibitory activity against both *Staphylococcus aureus* and rat seryl tRNA synthetases, with similar IC_{50} values of approximately 8 nM. Its inhibition can be explained by the similarity in structure between SB-217452 and seryl adenylate.

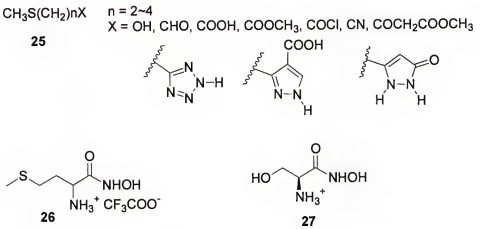

Figure 2-6 Structures of synthetic amino acid analogues.

Synthetic amino acid analogues (Figure 2-6). Methionine analogues have been reported to act as inhibitors of methionyl-tRNA synthetase.[115] Methylthioalkyl analogues **25** show little inhibitory activity. This indicates that the interaction of the amino group with the enzyme is indispensable for its inhibition. The methionine analogues containing different functionality of carboxylic acid such as an ester, amide and hydroxamate show that hydroxamate of L-methionine **26** is the best inhibitor of the enzyme (K_i = 19 μm against *E. coli* MetRS). It was concluded that amino group, nitrogen and oxygen of hydroxylamine in **26** are necessary for interacting with the enzyme because protection of each group decreased their activities. Methylthioethyl group as a side chain of methionine

seems to be necessary for inhibitory activity because modifications of the sulfur atom show little activity. Similarly, serine hydroxamate **27** has been described as a competitive inhibitor of the Seryl-tRNA toward the amino acid.[116]

Analogues of Intermediate

Aminoacyl adenylates, a mixed anhydride intermediate generated during the first step reaction, have long been recognized as the lead compounds in finding potent and selective inhibitors, because they are known to bind more tightly to the enzyme than the substrates, amino acid and ATP, generally by two or three orders of magnitude.[117]

Modifications on the amino acid moiety. Amino-alkyl adenylates are one type of aminoacyl adenylate analogues, in which the amino acid moiety is replaced by the corresponding amino alcohol to give stable esters. They are highly specific inhibitors for aminoacyl-tRNA synthetase.

Tyrosinyl adenylate is an inhibitor of tyrosyl tRNA synthetase from *Bacillus sterarothermophilus* with an IC_{50} of 11 nm.[65] The crystal structure of the enzyme complexed with tyrosinyl adenylate showes that there are a number of polar interactions between the enzyme and the inhibitor (Figure 2-7). In the tyrosine binding pocket, there are two polar groups (Tyr34 and Asp176) which form hydrogen bonds with the hydroxyl group. The side chains of Asp78, Tyr169 and Gln173 are well placed to form hydrogen bonds with the amino group of the tyrosine substrate. The phosphate group interacts with the main chain amide group of Asp38 by forming hydrogen bond. There are hydrogen bonds between 2'-OH and the main chain nitrogen of Gly192 and the side carboxylate of Asp194. Comparison of the complexes of enzyme with intermediate (tyrosyl adenylate) and the inhibitor suggests that the replacement of the carbonyl oxygen of the intermediate

by two hydrogens in the inhibitor has little effect on the mode of binding. Further modifications,[118] including replacement of the phosphate unit with α, β-unsaturated ester, removal of 3' ribose hydroxyl group or 2' ribose hydroxyl group, replacement of the adenine ring with a H, the naphthyl group or the α, β-unsaturated ester group similar to that found in mupirocin, led to substantially decreased potency.

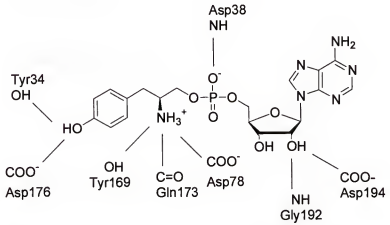

Figure 2-7 Schematic diagram showing the hydrogen bonding interaction between the tyrosyl-tRNA synthetase and tyrosinyl adenylate.[65]

Glutaminol adenylate **28** is a competitive inhibitor of *E. coli* glutaminyl-tRNA synthetase with respect to glutamine (K_i = 280 nM) and to ATP (K_i = 860 nM).[119] The corresponding methyl phosphate ester **29** is a weaker inhibitor (Ki ~ 10 μM) with respect to glutamine, which indicates that the charge of the phosphate group of glutaminol adenylate is important for its interaction with GlnRS. It is likely that the negatively charged phosphate makes a charged hydrogen bond with a residue of GlnRS, similarly to the hydrogen bond that tyrosyl adenylate makes with the main chain NH of Asp38 of *B. sterarothermophilus* tyrosyl-tRNA synthetase.[65,118] Similarly, glutamol adenylate inhibits

glutamyl-tRNA synthetase from *E. coli* with a K_i of 3 μM;[120] arginol adenylate inhibits arginyl-tRNA from *Staphylococcus aureus* with an IC_{50} of 7.5 nM;[121] isoleucol adenylate inhibits isoleucyl-tRNA synthetase from *Staphylococcus aureus* with a K_i of 50 nM.[122] All the above aminoacyl-tRNA synthetases (GluRS, GlnRS, TyrRS, IleRS, ArgRS) belong to class I. However, the aminoalkyl adenylates that correspond to the class II tRNA synthetases, such as histidinol adenylate, threonol adenylate, have very little affinity for either HisRS or ThrRS, while the aminoacyl sulfamate analogues are again potent inhibitors.[121] It seems that the carbonyl group plays a crucial role in recognition by the class II enzymes. In class I enzymes the carbonyl group is relatively exposed and does not appear to undergo any direct interaction with the protein,[65] while in class II, the carbonyl group is not only buried at the protein interface but it is also *syn* to the adjacent amino group. This results in a network of hydrogen bonds to the protein and the amine.[82]

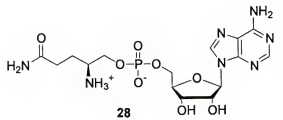

28

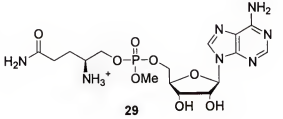

29

Another type of methylene-analogue of aminoacyl adenylates is the replacement of α-C with a CH_2 group. It is reported that methylene-analoges of phenylalanyl adenylate (Figure 2-8) are inhibitors of phenylalanyl-tRNA synthetase.[123]

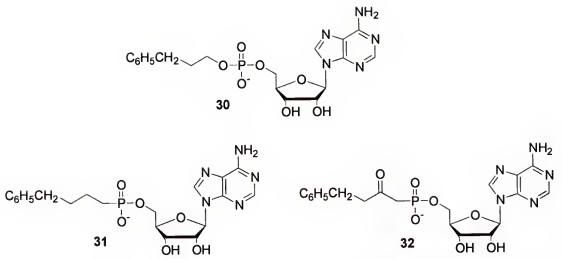

Figure 2-8 Methylene-analogues of phenylalanyl adenylate.

Modifications on the phosphonate linker. The unstable phosphate moiety can be replaced with the phosphonamide moiety, where the oxygen atom of the mixed anhydride bond is displaced with NH group. Since it is likely that the P-N bond of the N-acyl phosphoramidate linkage is stable under physiological conditions, the aa-AMP analogue bearing an N-acyl phosphoramidate linkage (aa-AMPN) can be expected to have activity as a potential specific inhibitor in the aminoacylation of tRNA.[124,125]

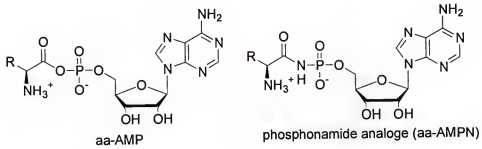

Nonhydrolyzable L-amino acid sulfamoyl adenosine (Figure 2-9) analogues have been shown to inhibit both classes of synthetases. The key structural feature of these

aminoacyl adenylate analogues is the replacement of the relatively labile phosphate ester of the natural aminoacyl adenylates with the nearly isosteric, yet hydrolytically more stable sulfamoyl linkage.[126] Such a linkage has been found in the natural product, ascamycin (Figure 2-9), which is a nucleoside antibiotics from *Streptomyces*.[127] Sulfamoyl adenosine has been widely used in the crystallization with the synthetase enzymes. For example, alanyl sulfamate,[126] seryl sulfamate,[77] glutaminyl sulfamate[67] have been reported to be complexed with the corresponding aminoacyl-tRNA synthetases in the crystal structures. The aminoacyl sulfamates are potent inhibitors of the enzymes. Arginyl sulfamate inhibits the *Staphylococcus aureus* ArgRS with an IC_{50} of 4.5 nM;[121] threonyl sulfamate has an IC_{50} of 15 nM;[121] histidyl sulfamate has an IC_{50} of 130 nM;[121] isoleucyl sulfamate has an IC_{50} of 4 nM;[122] Tyrosyl sulfamate has an IC_{50} of 26 nM;[118] Glutaminyl sulfamate inhibits GlnRS with a K_i of 1.32 μM;[67] Prolyl sulfamate inhibits the human ProRS with a K_i of 0.6 nM and *E. coli* ProRS with a K_i of 4.3 nM.[128]

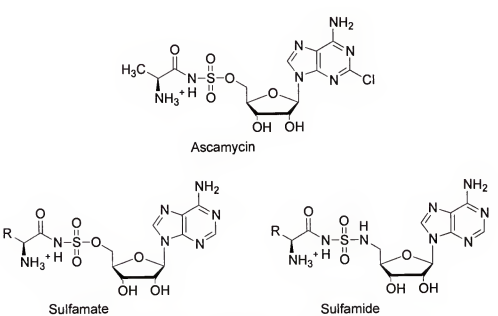

Figure 2-9 Structures of sulfamoyl adenosine analogues.

Another type of nonhydrolyzable sulfamoyl adenosine analogues is 5'-N-sulfamoyl adenosine, in which the phosphoester bond between the amino acid and adenosine moiety is replaced with a sulfoamide bond (Figure 2-9). A series of such analogues have been summarized in a recent review.[104]

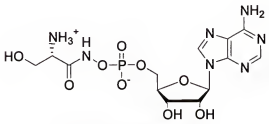

Seryl-hydroxamate-AMP

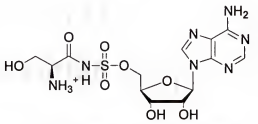

5'-O-(N-seryl--sulfamoyl)adenosine

As mentioned earlier, hydroxamate of an amino acid can inhibit the enzyme as the analogue of the amino acid. The amino acid-hydroxamate-AMP might also inhibit the enzyme as the analogue of the aminoacyl adenylate. Serine hydroxamte-AMP is reported to have very similar binding with seryl-tRNA synthetase as 5'-O-[*N*-(L-seryl)-sulfamoyl]adenosine.[77] Superposition of the two adenylate molecules shows that the extra bond in the seryl-hydroxamte-AMP molecule is accommodated by a small relative shift in the position of the phosphate group leaving the adenosine and serine moieties in the same position.

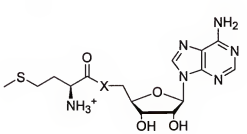

33. X = O
34. X = NH
35. X = N-OH
36. X = NH-O

The labile acylphosphate linkage of the intermediate has also been replaced with simple ester and amide bond.[129] Ester analogue **33** and amide analogue **34** of methionly adenylate were proven to be strong inhibitors of methionyl-tRNA synthetases isolated from *E. coli*, *Mycobacterium tuberculosis*, *Saccharomyces cereisiae* and human. Just as L-methionine hydroxamate is a good inhibitor of MetRS, *N*-alkyl hydorxamate analogue **35** and *O*-alkyl hydroxamate analogue **36** were proven to be good inhibitors too. Ester analogue **33** was found to be the most potent inhibitor of *E. coli* MetRS in this series and their relative activities are in the following order: **33** (ester) > **35** (N-hydroxamate) > **34** (amide) > **36** (O-hydroxamate) ≈ hydroxamate. The estimated K_i of **33** and **35** represented 10.9 μM and 13.1 μM, respectively.

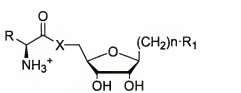

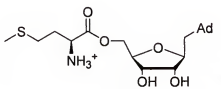

37

Modifications on the adenine and ribose moieties. Recognition of the adenine ring is significant for the inhibitor binding. Replacement of adenine of glutamol adenylate by other bases (purine, cytosine, dihydrocytosine, uridine) results in a more than 1000-fold loss in activity.[120] Introducing linkers between the 1'-position of ribose and adenine surrogates as methionyl-tRNA and isoleucyl-tRNA synthetase inhibitors has been investigated.[117] The ester analogue **37** is a potent inhibitor of *E. coli* methionyl-tRNA synthetase with an IC_{50} of 3.6 μM.

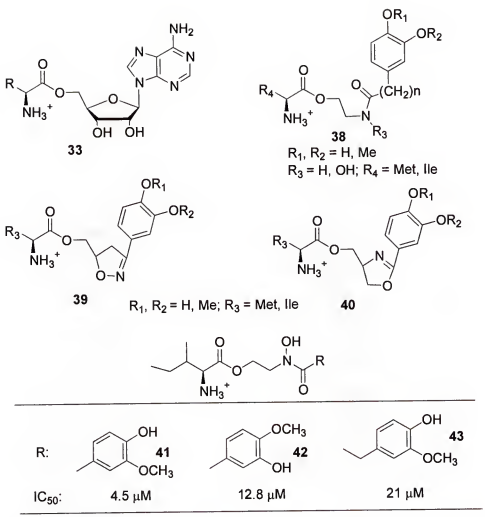

Figure 2-10 Structures and activities of vanilloid and isovanilloid analogues as inhibitors of methionly-tRNA and isoleucyl-tRNA synthetases.

Using the ester analogue of aminoacyl adenylate **33** as a lead compound, the adenine and ribose parts were modified with their appropriate bioisosters (Figure 2-10).[130] Firstly, the adenine moiety was replaced by vanilloid or isovanilloid, in which phenolic hydroxyl and the methoxy group were supposed to mimic 6-NH_2 of adenine as a hydrogen donor, and the N-1 of adenine as hydrogen acceptor, respectively. Secondly, the ribose was substituted by its biosteres, such as acyclic amide and hydroxamate (**38**),

dihydroisooxazole (**39**) and dihydrooxazole (**40**). These ribose surrogates have been successfully utilized for pharmacologically active adenylates in drug design.[131] Among IleRS inhibitors, the isovanillic hydroxamate analogue **41** is the most potent one with an IC_{50} of 4.5 μM. Concerning the MetRS inhibitors, most of the compounds display moderate inhibition to *E. coli* MetRS (IC_{50} = 32.5~163.5 μM).

Table 2-1 Tetrazole derivatives of aminoacyl adenylate as inhibitors of isoleucyl-tRNA synthetase.

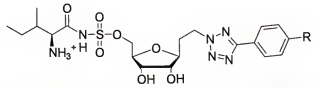

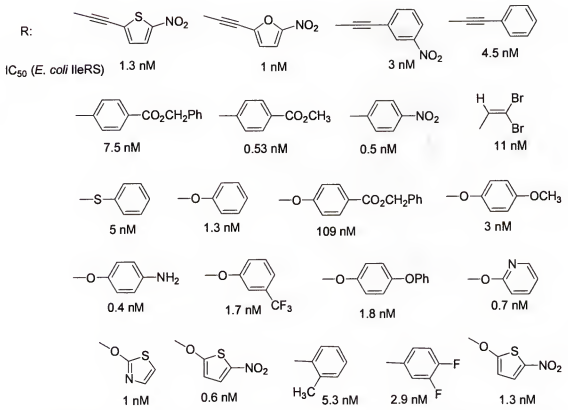

Table 2-1 continued.

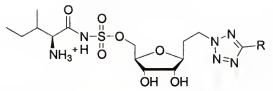

R :

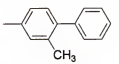

IC_{50} (E. coli IleRS) 0.6 nM

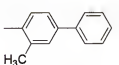

0.5 nM

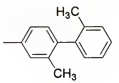

11 nM

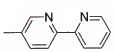

0.5 nM

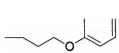

0.3 nM

8.8 nM

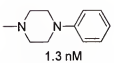

1.3 nM

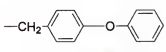

135 nM

Modification of the adenine portion of the aminoacyl adenylate with heterocycles has been reported. A series of novel tetrazole derivatives[132] of aminoacyl adenylate mimics were found to have highly potent enzyme activity and selectivity against isoleucyl-tRNA synthetases (Table 2-1).

Replacement of the adenine ring with a variety of other hecterocycles, such as thiazole derivatives, has been investigated too.[133] Isoleucine phenyl thiazole analogue **44** inhibits IleRS with an IC_{50} of 0.1 μM. It is a competitive inhibitor with respect to isoleucine (K_i = 0.031 μM) and ATP (K_i = 0.048 μM). Alanine analogue **45** exhibits inhibition of the corresponding AlaRS with an IC_{50} of 0.5 μM. Replacement of the phenyl group with the furan ring, alkenyl phenyl group, and introduction of a methyoxy group on the phenyl ring increase the inhibition. But the selectivity for bacterial IleRS

synthetases versus the human enzyme is relatively low. Leucine analogues **47** demonstrate the high selectivity of *E. Coli* LeuRS (2~16 nM) versus the human enzyme (~ 1 μM).

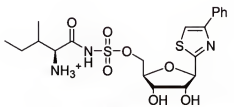

Isoleucine thiazole analogue **44**

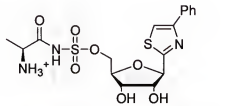

Alanine thiazole analogue **45**

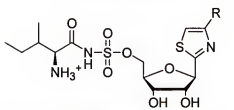

46 R: 4'-cyano-furanyl, 2'-OMe-Ph, 3'-OMe-Ph, PhOPh, 4'-OMe-Ph, 6'-OMe-2-naphthyl, CH_2CH_2Ph

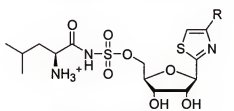

47 R : PhOPh, CH_2CH_2Ph, CH_2CH_2PhOPh

Glutamate esters[134] in which the alcohol moiety is ribose, prolinol or substituted piperidines were synthesized and tested their inhibitory potency in the aminoacylation reaction catalyzed by *E. coli* glutamyl-tRNA synthetase. It turned out that the best inhibition is obtained with piperidine derivatives (**48**, **49**).

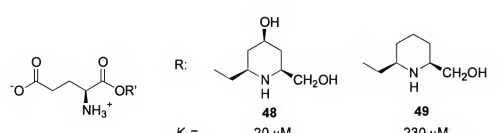

48 **49**

K_i = 20 μM 230 μM

Transition-State Analogues of Aminoacyl Adenylates

Aminophosphonyl adenylates are one type of transition-state analogues of aminoacyl adenylates.[135] They were found to be effective inhibitors of the corresponding synthetases in two reactions, ATP-PPi exchange and tRNA aminoacylation. The inhibition was specific enough and was competitive with respect to the substrate amino acids and ATP.

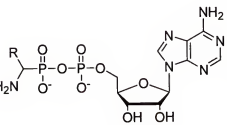

R	X	K_i ATP-PPi exchange	K_i aminoacylation
$CH(CH_3)_2$	OH	0.14 μM	0.28 μM
$-CH_2C_6H_5$	OH	0.2 μM	0.5 μM
$-(CH_2)_2SCH_3$	OH	4 μM	0.2 μM
$-CH(CH_3)_2$	OEt	4.2 μM	2.7 μM

Chimeric Synthetase Inhibitors

Consideration of structural information derived from more than one inhibitor of a synthetase proved to be important for discovering and developing more advanced synthetase-specific drugs.[104] The natural product mupirocin acts as an analogue of isoleucyl-adenylate (Ile-AMP). It blocks the binding site of Ile-AMP by binding to the catalytic domain of the *T. thermophilus* IleRS like Ile-AMS, an analogue of isoleucyl-adenylate.[136] The pyran ring and conjugated α, β-unsaturated ester of mupirocin functionally mimic the ribose and adenine moieties of Ile-AMP. Hence, these two parts were retained, while the amino acid side chain and linker were varied (Figure 2-11). A series of chimeras were synthesized and evaluated[137] for their binding activities (Table 2-

2). It demonstrates that it is possible to combine the features of the two classes of inhibitors to achieve an improvement in potency.

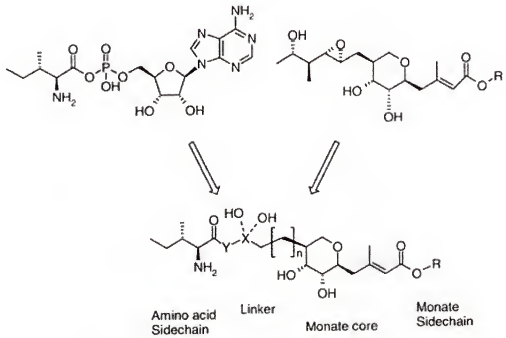

Figure 2-11 Design for combination of features of reaction intermediate and mupirocin to produce more potent hybrid inhibitors.[137]

SB-203207, isolated from *Streptomyces* NCIMB 40513, inhibits isoleucyl tRNA synthetase from *Staphylococcus aureus* Oxford and rat liver with an IC_{50} of 1.7 and <2 nM, respectively.[138,139] Substituting the isoleucine residue of SB-203207 with leucine (**50**) and valine (**51**) increase the potency of inhibition of LeuRS and ValRS by 100-fold and 25-fold, respectively.[140]

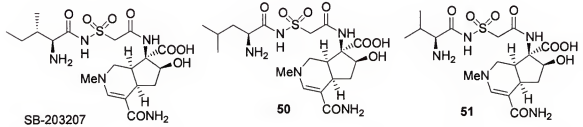

Table 2-2 Dependence of K_i on variations on aminio acid side chain and linker region.[137]

Compound	Structure	K (nM)	Compound	Structure	K (nM)
SB-234764		<0.001	SB-247186		0.55
SB-239820		0.7	SB-236838		6900
SB-241083		4.8	SB-244519		0.31
SB-251803		0.007	SB-248453		55
SB-255183		0.56	SB-244151		230
Ile-ol-AMP		50	SB-239945		2.0
Ile-NHSO$_2$-AMP		0.01	SB-252180		0.4
Et-A		0.19	SB-251109		900
SB-224736		0.02	SB-246096		0.04
SB-234764		<0.001	SB-254412		0.6
SB-226371		1.4	SB-239171		420

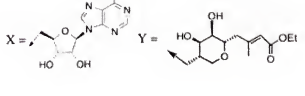

Ochratoxin A is a natural product which inhibits phenylalanyl-tRNA synthetase.[141] Analogue of ochratoxin A, in which phenylalanine is replaced by valine, is a specific inhibitor of valinyl-tRNA synthetase.[142]

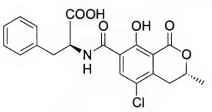

Ochratoxin A

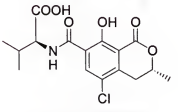

Valyl-ochratoxine A

Conclusions

Significant progress has been made in the effort to develop inhibitors of aminoacyl-tRNA synthetases. The structures of the aminoacyl-tRNA synthetase-inhibitor/substrate complexes provide valuable insights into the recognition of the substrates and inhibitors, which has great significance in further inhibitor design. Since aminoacyl-tRNA synthetases are leading targets for novel anti-infectives, the novel inhibitors would establish an operational foundation for the development of new anti-infectives for human therapy. On the other hand, it will provide valuable insights into the inhibitor design of asparagine synthetase, which has not widely developed yet.

CHAPTER 3
SYNTHESIS OF L-4,4-DIFLUOROGLUTAMATE

Fluorinated derivatives of amino acids are assuming increasing importance as probes of biological function and enzyme mechanism,[143-154] particularly because the electron-withdrawing effects of fluorine substituents[155-157] often have profound effects on reactivity and conformational preferences.[158-164] For example, fluorinated analogues of glutamic acid possess antitumor activity[165] and are modulators of folate poly-γ-glutamate biosynthesis.[166-169] Our interest in fluorinated amino acids has been stimulated by our recent efforts to characterize the structure and mechanism of asparagine synthetase (AS),[16,34,35,54] a glutamine-dependent amidotransferase[170,171] that appears to be intimately linked with progression through the cell cycle,[172] and cellular responses to amino acid starvation.[173,174] Specifically, we required L-4,4-difluoroglutamine **1** to investigate whether AS could employ this non-natural amino acid as a nitrogen source in place of L-glutamine as part of ongoing efforts to trap and structurally characterize specific intermediates formed during the kinetic mechanism.[35] Since DL-4,4-difluoroglutamic acid had been converted to a racemic mixture of the fluorinated substrate analog **1** in three steps,[175] we wished to prepare optically pure L-4,4-difluoroglutamate **2** from cheap starting materials via a route that might be easily modified to yield functionalized derivatives of 4,4-difluoroglutamine. In this regard, the elegant synthesis of L-4,4-difluoroglutamate **2**,[176] reported during our studies, seems to be less suitable for our purposes than the route we describe here. We note that the only other synthesis of L-4,4-

difluoroglutamic acid **2** in enantiomerically pure form requires the use of an expensive precursor, that is not readily available,[177] and other practical routes for the large-scale synthesis of 4,4-difluoroglutamic acid[166] and related compounds[178-185] either give the target fluorinated amino acids as racemic mixtures, or require tedious resolution procedures.[186-188] We now report the successful preparation of **2** by a strategy in which the difluorinated side chain is constructed by nucleophilic addition to the configurationally stable aldehyde **3** (Figure 3-1).[189-192]

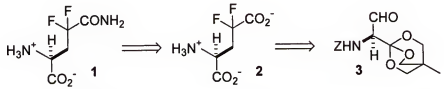

Figure 3-1 Retro-synthetic analysis of L-4, 4-difluoroglutamine.

Results and Discussion

The introduction of difluoromethylene group into amino acids has been accomplished using a variety of reagents,[193-196] including DAST,[182,183] *N*-fluorobenzenesulfonimide (NFSi),[176,197-201] and difluorobromoacetate ester.[202-205] In our initial experiments, we investigated whether 1,1-bis(dimethylamino)-2,2-difluoroethene **4**, a novel reagent for building difluoromethylene centers into molecules,[202-208] would undergo clean addition to a suitably protected chiral aldehyde. This reagent was found to condense with various substituted benzaldehydes to give good yields of the respective *N*,*N*-dimethyl-2,2-difluoro-3-hydroxy-3-arypropionamides (Figure 3-2). However, in reactions with a number of ketones or aldehydes bearing an α-H, no condensation

products were observed. In these reactions, *N*,*N*-dimethyldifluoroacetamide was obtained as the only product as reagent **4** acts as a base instead of a nucleophile.

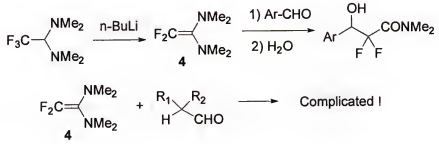

Figure 3-2

The design of a very bulky aldehyde, making the α-H very difficult to be abstracted, was hypothesized as a way to direct condensation with reagent **4**. The retro-synthetic analysis (Figure 3-3) showed that L-4,4-difluoroglutamic acid could be obtained by the coupling of intermediates **5** and **6**. Intermediate **5** could be obtained from aldehyde **7** or **8**, both of which could be easily synthesized from L-serine (Route A) or D-serine (Route B) respectively. Overall, the chiral center of serine would be used as that of L-4,4-difluoroglutamic acid.

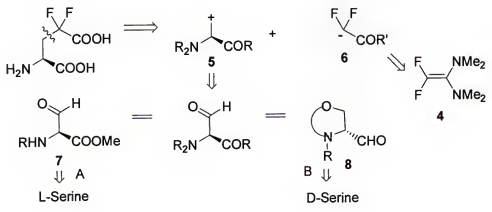

Figure 3-3

Aldehydes **7** and **8** are N-protected α-amino aldehydes. Both of these aldehydes are configurationally labile, racemizing even upon rapid chromatgtography on silica gel.[209] The 9-(9-phenylfluorenyl) (PhFl) protecting group which is more stable to solvolysis than the trityl group was reported to act as a steric pocket that shields the α-H, thereby preventing deprotection and recemization of the aldehyde.[210] Therefore, PhFl was chosen as a strategically advantageous amine protecting group. From the retro-synthetic analysis, synthetic Route A which generates aldehyde **7** starts from a cheap, readily available starting material. Therefore, Route A was chosen as the first attempt.

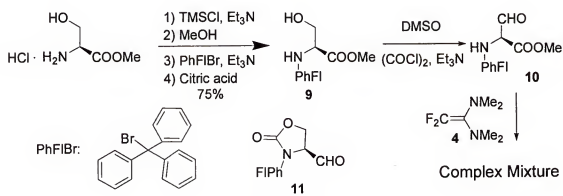

Figure 3-4

Selective nitrogen protection of L-serine methyl ester with the 9-phenylfluoren-9-yl group (Figure 3-4) requires protective silylation of both the amine and the hydroxyl groups with chlorotrimethylsilane prior to alkylation of the amine with 9-bromo-9-phenylfluorene. The trimethylsilyl group was then selectively cleaved from the amine with methanol, leaving the silyl ether intact. Alkylation of the amine with 9-bromo-9-phenylfluorene followed by acidic hydrolysis of the silyl group produced *N*-(9-

phenylfluoren-9-yl)-L-serine methyl ester **9**. Swern oxidation of *N*-PhFl L-serine methyl ester gave aldehyde **10** in high yield. However, condensation of aldehyde **10** with reagent **4** was very complicated. We proposed that this complication was caused by the active hydrogen on nitrogen. Aldehyde **11** which is synthesized from L-serine according to the literature route[211] should work better than aldehyde **10** since there is no active hydrogen except the α-H. Molecular modeling studies indicated that the PhFl protection group shields the α-H preventing its abstraction by **4**, and it is well established that racemization of the chiral center in **11** is very slow under a variety of conditions.[210,212] Although synthesis of **2** by this route ultimately requires D-serine as a starting material, we selected **11** in these early experiments in order to establish the feasibility of this synthetic approach.

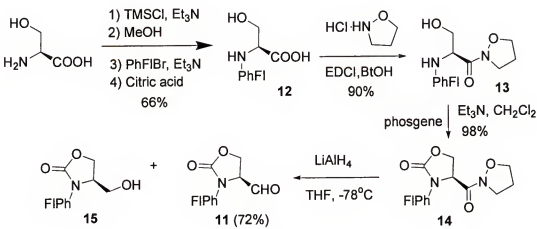

Figure 3-5

According to the literature,[211] aldehyde **11** was synthesized by the following steps (Figure 3-5). L-serine was refluxed with excess chlorotrimethylsilane and excess triethylamine in methylene chloride to insure silylation of both oxygens and nitrogen.

The trimethylsilyl group was then selectively cleaved from the amine with methanol, leaving the silyl ether and silyl ester intact. Alkylation of the amine, followed by acidic hydrolysis gave *N*-(9-phenylfluorene-9-yl)-L-serine **12** in 66% yield. *N*-PhFl-L-serine isoxazolidide **13** was prepared in high yield by coupling isoxazolidine with carboxylic acid **12** mediated by EDCI and hydroxybenzotriazole in THF. Treating amino alcohol **13** with phosgene and triethyl amine in CH_2Cl_2 gave cyclic carbamate **14** in 98% yield. Reduction of **14** with a solution of $LiAlH_4$ in THF at –78 °C produced aldehyde **11** contaminated with traces of alcohol **15**. The yield of aldehyde **11**, a white solid, was about 72% after purification by column chromatography on silica gel.

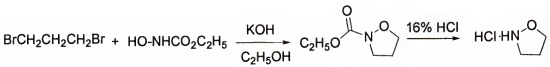

Figure 3-6

The above synthetic route of aldehyde **11** is long and more importantly, one reagent, isoxazolidine, is not commercially available. Isoxazolidine[213] was synthesized by the cyclization of 1,3-dibromopropane with *N*-hydroxyurethane mediated by KOH in EtOH, followed by acidic hydrolysis (Figure 3-6). The total yield of these two steps was 39%. The yield can be improved by using large amounts (3~5 equiv) of *N*-hydroxyurethane, which is an expensive chemical. These are big drawbacks of this synthesis.

We tried using DIBAL-H to reduce ester **16** to aldehyde **11**. Ester **16** was obtained by the cyclization of **9** with phosgene or triphosgene in CH_2Cl_2 at RT (Figure 3-7). After

reacting with DIBAL-H at –78 °C for 2~3 hrs, about equal amounts of aldehyde **11** and alcohol **15** were obtained in addition to a large amount of recovered starting ester **16**. We then intended to use $LiAlH_4$ to reduce ester **16** to alcohol, which can be further oxidized to aldehyde. After being reacted with $LiAlH_4$ at –78 °C for 12 hrs and quenched with $KHSO_4$ aqueous solution, this reaction gave 65% of aldehyde **11** and 20% of alcohol **15** after purification with column chromatography on silica gel. Shorter reaction time (2~3 hrs) improved the yield of aldehyde with only trace amounts of alcohol produced. After chromatography purification, the yield of aldehyde reached up to 92%. This is the first example of $LiAlH_4$ reducing an ester to an aldehyde. We note that esters are reduced to aldehydes at RT by $LiAlH_4$ in the presence of diethylamin.[214]

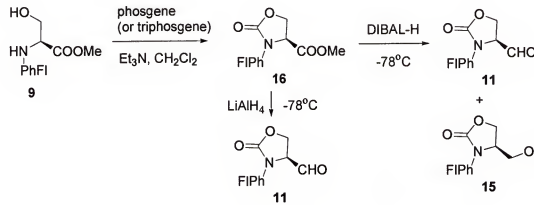

Figure 3-7

To ascertain the mechanism of this reduction and its possible application in the synthesis of amino aldehydes, more substrates were tried (Table 3-1). First, the ethyl ester and the benzoyl ester, which were synthesized by similar methods as used for the methyl ester, were treated with $LiAlH_4$ (1.0 M in THF, 1.1 equiv) at –78 °C. After reacting for around 3 hrs, the reaction was quenched with $KHSO_4$ aqueous solution. Trace amounts of

alcohol were produced in both reactions. The crude product contained 87% and 65% of aldehyde for ethyl ester and benzoyl ester respectively, according to proton NMR spectroscopy. Ester III which was synthesized by treating *N*-PhFl-L-serine methyl ester with aqueous formaldehyde under the catalysis of TsOH, gave aldehyde in 85% yield after being reacted with $LiAlH_4$ at –78 °C for 2~3 hrs. *N*-PhFl proline methyl ester and *N*-Tr proline methyl ester were treated with $LiAlH_4$ at –78 °C for 12 hrs. No aldehyde was formed and only trace amounts of alcohol were formed in both cases. After being reacted at –10 °C for 2~3 hrs, all the esters were converted to alcohols, and no trace amounts of aldehyde were formed. We proposed that the oxygen and nitrogen on serine would coordinate with Al of $LiAlH_4$, which would prevent the further reduction of the substrates to alcohols.

Table 3-1 Reduction of ester to aldehyde with $LiAlH_4$.

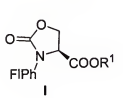

I

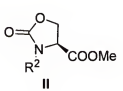

II

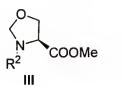

III

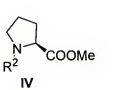

IV

	R^1	R^2	Yield of Aldehyde
I	Me	---	75 ~ 92%
	Et	---	87%
	CH_2Ph	---	65%
II	---	PhFl	75 ~ 92%
	---	Tr	> 50%
III	---	PhFl	85%
IV	---	PhFl	0
	---	Tr	0

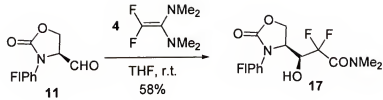

Figure 3-8

As anticipated, the difluorolefine **4** underwent smooth addition to aldehyde **11** in THF or ether at room temperature, giving an alcohol **17** as a single adduct in a purified yield of about 58% (based on **11**) (Figure 3-8). We assigned the relative and absolute stereochemistry of **17** on the basis of X-ray crystallography (Figure 3-9), assuming that no racemization had taken place at C-2 under the conditions.[210,212] The stereochemical preference for attack on **11** is consistent with that reported previously, and can be rationalized on the basis of the Felkin-Anh model in which the bulky protecting group completely hinders the *si*-face of the carbonyl group (Figure 3-10A).[215,216]

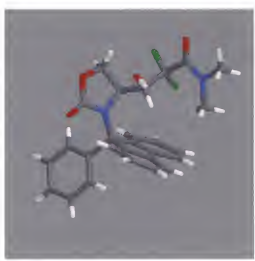

Figure 3-9 X-ray diffraction structure of adduct **17**

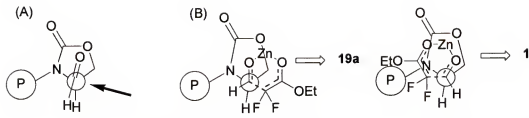

Figure 3-10 Stereochemical control of the addition reactions. (A) Felkin-Anh model for the addition reaction between difluoroolefine **4** and aldehyde **11**. (B) Models for the metal-directed addition of Reformatsky reagent **18** and aldehyde **11** leading to major and minor products **19a** and **19b**

Although this result confirmed the hypothesis that reaction of **4** and **11** proceeded with a very high level of diastereoselection and that the presence of the bulky N-protecting group suppressed deprotonation at C-2, a number of technical difficulties precluded the routine use of difluoroolefin **4** for large-scale preparations of intermediate **17**, including the need for its *in situ* preparation from 1,1-bis(dimethylamino)-2,2,2-trifluoroethane[217,218] using *n*-butyllithium. We therefore investigated whether addition of the Reformatsky reagent **18** to the chiral aldehyde **11** would proceed with equally high diastereoselectivity. Dropwise addition of ethyl bromodifluoroacetate to a solution of zinc and **11** was required for clean reaction, and gave the diastereoisomeric adducts **19a** and **19b** as a 6:1 mixture in 85% total yield after purification (Figure 3-11A). Stereochemical assignments for these compounds were based on the observation that treatment of the major isomer **19a** with lithium dimethylamide gave a single product with physical and spectroscopic properties that were identical to those of amide **17**. The loss in stereochemical control is probably associated with stabilization of the transition state leading to the minor isomer due to chelation of zinc by the oxygen in the oxazolidine ring (Figure 3-10B).[192]

Any influence of electronic effects, associated with the fluorine substituents, on product stereochemistry was ruled out by the observation that the cognate Reformatsky reagent formed from ethyl bromoacetate reacted with **11** to give a 8:1 ratio of the diastereoisomeric adducts **20a** and **20b** (Figure 3-11B). The major isomer **20a** was assigned on the basis of the ^{1}H-^{1}H coupling for the protons attached to C-4 and C-3', which is similar to the dipolar coupling observed between the cognate protons in **17** (for which the relative stereochemistry was unequivocally established). The stereochemical outcome is also consistent with the results of previous investigations into the reactions of nucleophiles with aldehyde **11**.[210-212]

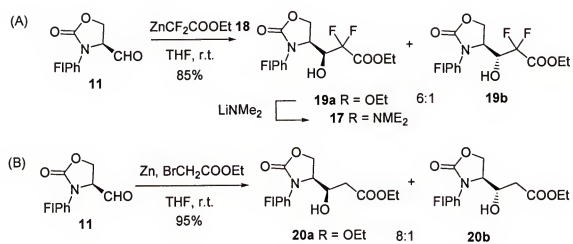

Figure 3-11

Having devised conditions for the preparation of the difluorinated secondary alcohols **17** and **19a**, we next investigated conditions for removing the hydroxyl group so as to complete the synthesis of the side chain.

Methods for accomplishing this synthetic transformation at carbon atoms adjacent to CF_2 groups, especially in highly functionalized derivatives such as **17** and **19a**, do not

seem to have been investigated in detail. To our knowledge, there is only a single published example for which no experimental details were given.[219] Given the inductive effects of the fluorine substituents, we envisaged that this reduction might be best accomplished using radical-based methods, such as the Barton-McCombie reaction.[220-223] The difluoroamide **17** was therefore converted to the *O*-pentafluorophenylthioate **21** by reaction with pentafluorophenylthiochloroformate (Figure 3-12). Relatively strong conditions were required for the synthesis of the activated *O*-pentafluorophenylthioate **21**, presumably due to steric hindrance of the secondary alcohol by the bulky *N*-protecting group. In addition, the complete conversion of starting alcohol **17** was difficult to achieve, even after adding additional amounts of pentafluorophenylthiochloroformate. Radical-mediated dehydroxylation from **21** also proved to be more difficult than anticipated. Although the desired difluorinated amide could be obtained using Bu_3SnH, with AIBN as a radical initiator, a complicated mixture of products was formed from which **22** was isolated in a disappointing 30% yield. It is possible that the secondary radical resulting from breakdown of the *O*-pentafluorophenylthioate moiety undergoes reaction with the electron-rich phenylfluorenyl-protecting group, although this remains to be established.

Efforts to optimize the yield by changing the leaving group were tried. Phenyl chlorothioformate was much less reactive than pentafluorophenyl chlorothioformate[221] and failed to give the thiobenzoyl product leaving the alcohol unchanged. We also tried converting the alcohol into xanthate. Alcohol **17** was treated with NaH, followed by CS_2 to give xanthate **26c** in 82% yield. Unfortunately, xanthate remained mostly unchanged in the attempted deoxygenation reaction with AIBN and tributyltin hydride. Alcohol **17** was

also transformed to the corresponding thioimidazolide **26d** via refluxing with thiocarbonyl bis-imidazolide in THF. However, no deoxygenation reaction occurred when treated with AIBN and tributyltin hydride.

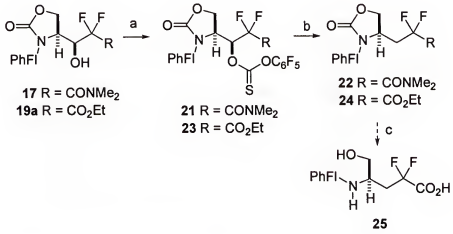

Figure 3-12 (a) $C_6F_5OC(=S)Cl$, DMAP, N-hydroxysuccinimide, toluene, 90 °C; (b) $(n\text{-}Bu)_3SnH$, AIBN, toluene, reflux; (c) KOH, EtOH or 6N HCl.

Similar results were obtained for the *O*-pentafluorophenylthioate **23** that could be prepared from alcohol **19a**. The reasons for these difficulties in using Bu_3SnH for deoxygenation remain unclear, especially in light of experiments outlined below. Having established conditions for removal of the hydroxyl group from the pentafluorophenyl derivatives **22** and **24**, albeit in low yield, we next confronted the problem of hydrolyzing the oxazolidinone ring. All attempts to prepare the acyclic material **25** by hydrolysis of either **22** or **24** under acidic or basic conditions, as previously reported,[211] gave only complex product mixtures. ^{19}F NMR analysis supports the hypothesis that these technical problems are likely associated with dehydrofluorination taking place at a rate similar to heterocyclic ring opening.

Table 3-2 Results on acylation and radical deoxygenation.

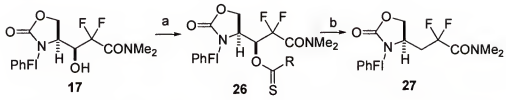

Thiocarbonyl Compound **26**	Yield of **26**	Yield of **27**
R:		
a = —O—	No reaction	---
b = —O— C_6F_5	54%	30%
c = —SMe	82%	No reaction
d = —N(imidazole)	95%	No reaction

Although we had demonstrated that addition of Reformatsky reagent **18** to configurationally stable α-aminoaldehydes preceded smoothly, these unexpected difficulties in radical-mediated deoxygenation and hydrolysis of the heterocyclic ring in either **22** or **24** caused us to re-examine our choice of starting aldehyde. In particular, we sought to avoid the use of potentially reactive nitrogen protecting groups that might participate in transformations leading to the desired difluorinated side chain. We therefore investigated reaction of the difluorinated reagent **18** with the 4-methyl-2,6,7-trioxabicyclo[2,2,2]orthoester (OBO) derivative. The above synthetic try indicated that the fully protected amine might be a good candidate for the Reformatsky reaction. *N*-phthaloylamines, a means of protecting primary amino groups, are easily crystallized, and can readily be removed by hydrazinolysis or phenylhydrazinolysis.[224] *N*-phthaloyl-L-

serine **28** was synthesized by treating L-serine with *N*-(ethyoxycarbonyl)phthalimide[225,226] in the presence of Na_2CO_3 in H_2O (Figure 3-13). Further condensation with 3-methyl-3-(hydroxymethyl)oxetane mediated by DCC and DMAP generated ester **29**. Though the yield for this esterification was good (80%), the rearrangement under boron trifluoride treatment gave only 26% of the corresponding OBO ester **30**. Many polar compounds were detected and the *N*-phthaloyl group was probably ring-opened under the acidic conditions.

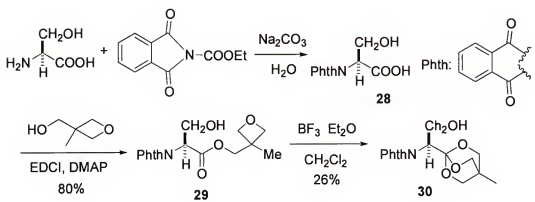

Figure 3-13

New protecting group Fmoc was tried. L-serine was selectively protected on the amine by treating with Fmoc-succinimide mediated by Na_2CO_3. Oxetane ester **32** was prepared in high yield from the addition of Fmoc-L-serine **31** to a mixture of EDCI (1.2 equiv), 3-mehtyl-3-(hydroxymethyl)oxetane (20 equiv) and DMAP (0.05 equiv) (Figure 3-14). The large excess of oxetane of alcohol can be recovered and is required to minimize esterification of the serine side chain. The oxetane ester was then converted to the OBO ester under the acidic rearrangement.[227] An essential requirement was to maintain the concentration of boron trifluoride at less than 0.1 equiv. The rearrangement

was complete after 12 hrs at room temperature with a yield of 70% after purification on silica gel. Since the ortho ester is very susceptible to ring-opening under the acidic conditions of the silica column, Et_3N (1%) was added to the eluant. Fmoc-L-serine-OBO ester **33** was oxidized under Swern conditions to give aldehyde **34** in very high yield. This aldehyde is chemically and chirally stable at room temperature.[191]

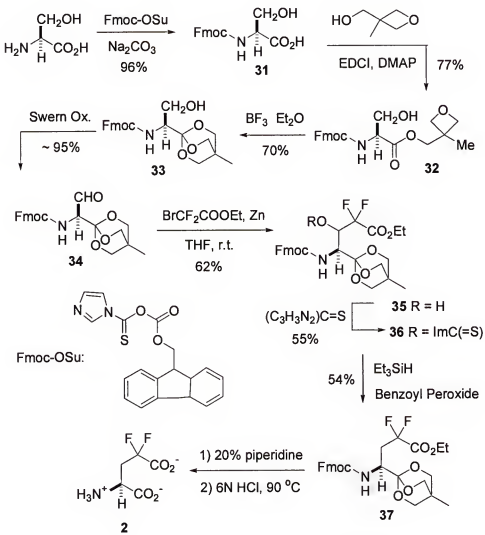

Figure 3-14

The obtained crude aldehyde (purity >90%) was pure enough for direct use in the subsequent addition reaction. Pre-activated Zn (5 eq) was mixed with the aldehyde in dried THF at room temperature, followed by the addition of ethyl difluorobromoacetate (2 eq) (Figure 3-14). The alcohol **35** was refluxed with thiocarbonyl *bis*-imidazolide in THF overnight. The obtained oxythiocarbonylimidazole **36** was mixed with triethyl silane (50 eq) in benzene at 90 °C. Benzoyl peroxide was added as an initiator. Since benzoyl peroxide is not only the source of the initiator benzoyloxy radicals, but also a trap for the triethylsilyl radicals produced during the reaction,[228] relatively high amounts of benzoyl peroxide were needed. Benzoyl peroxide (0.2 eq) was added at 30 minutes intervals. The reaction was monitored by TLC and relatively high amounts of the peroxide (1~1.2 eq.) were needed to drive the reaction to completion. The removal of the protecting groups from **37** was accomplished by a two-step, one-pot procedure. The protected amino acid was first treated with piperidine (20% in CH_2Cl_2), and then reacted with 6N HCl at 90 °C for 3 hrs. The crude product was purified by anion-exchange column chromatography. In the purification process, we found that it was very difficult to purify the final product, mostly caused by the deprotection by-product dibenzofulvene. Dibenzofulvene[229,230] is not an easily handled molecule. In the free state under ordinary conditions it undergoes rapid polymerization. It can also react with primary and secondary amine. The rotation of the final product was far lower than the literature,[188] which might be caused by impurity.

Thus, benzyl carbamate (Cbz) protecting group was tried in the synthesis (Figure 3-15). The *N*-protected derivative of L-serine **38** was converted to the ester **40** in an alterative way since the above method had a disadvantage of using 30 equivalents of 3-

methyl-3-(hydroxymethyl)oxetane. The ester **40** was obtained by treating L-serine derivative **38** with tosylate **39** in the presence of NaI. The yield was improved and the reaction was much less expensive. Using the same method as Fmoc protecting, the OBO ester **41** was formed by $BF_3 \bullet OEt_2$-catalyzed rearrangement.[227] Swern oxidation then gave the target aldehyde **3** in an excellent yield. The optical purity of this compound was verified by ^1H NMR analysis of resonance associated with the aldehyde proton in the presence of $Eu(hfc)_3$[191] (Figure 3-16).

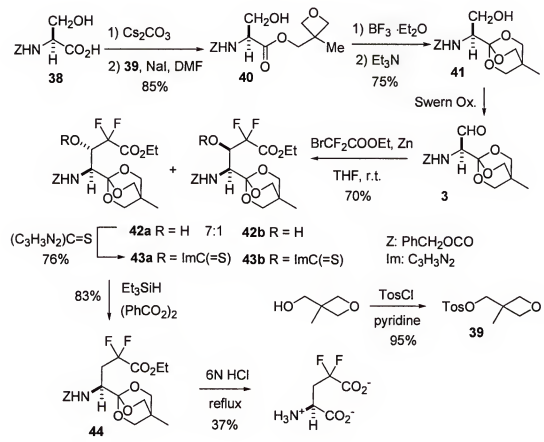

Figure 3-15

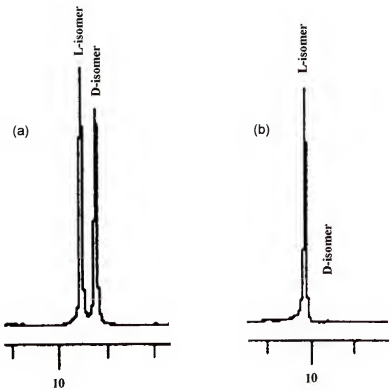

Figure 3-16 Verification of optical purity of aldehyde **3** by ^{1}H NMR (a) DL-Cbz-Ser(ald)-OBO ester and chiral shift reagent ($Eu(hfc)_3$; (b) L-Cbz-Ser(ald)-OBO ester **3** and chiral shift reagent $Eu(hfc)_3$.

Reaction of **3** with the difluorinated Reformatsky reagent again proceeded smoothly to give the enantiomerically pure alcohol **42** as a 7:1 mixture of diastereoisomers that could not be completely separated by column chromatography. The relative stereochemistry of the major isomer was assigned as **42a** by analogy to the major product obtained by reaction of **3** and the cognate, non-fluorinated Reformatsky reagent derived from ethyl bromoacetate.[191]

As reported previously, examination of the ^{1}H and ^{19}F NMR spectra revealed that there was no dipolar coupling between the protons at C-2 and C-3. Reaction of Reformatsky reagent **18** with **3** therefore proceeds via a simple Felkin-Anh model in

which the nucleophile attacks the less hindered *si*-face of the aldehyde moiety. Again the diastereoselectivity of the addition of the difluorinated reagent **18** is significantly reduced relative to that reported in other experiments employing aldehyde **3** as an electrophilic component. This may reflect stabilization of the transition state leading to **42b** through zinc-chelation, or equilibration of the initial adduct under the reaction conditions. The mixture of diastereoisomers **42** was then refluxed with thiocarbonyl *bis*-imidazolide in THF overnight to give the oxythiocarbonylimidazole derivatives **43**, which was further deoxygenated by Et_3SiH in the presence of benzoyl peroxide. The protected difluoroester **44** was obtained in 44% overall yield (for three steps) from aldehyde **3**. Conversion of **44** to L-4,4-difluoroglutamate **2** could be accomplished by heating in 6N HCl for 2 hrs, with purification using anion-exchange chromatography. Comparison of the optical and spectroscopic properties for this material with those reported previously[176,177] confirmed our observations that the synthesis had proceeded with little loss of stereochemical integrity at the chiral center. We note that this synthesis is amenable to use on large scale, and therefore represents a practical approach to the enantiospecific preparation of this difluorinated amino acid.

Experimental Section

Melting points were recorded using a Fisher-Johns melting point apparatus, and are uncorrected. Optical rotations were measured using a Polyscience Model SR-6 polarimeter. ^1H, ^{13}C and ^{19}F NMR spectra were obtained at 300, 75.4 and 282 MHz, respectively, using Varian VXR-300, Gemini-300 and Mercury-300 spectrometers. For ^1H and ^{13}C, chemical shifts are reported in ppm (δ) downfield of tetramethylsilane as an internal reference (δ 0.0), except for measurements in D_2O for which acetone (δ 2.1) was

employed as an external standard. In the case of ^{19}F, $CFCl_3$ was used as an internal standard (δ 0.0). Splitting patterns are abbreviated as follows: s, singlet, d, doublet, t, triplet, q, quartet and m, multiplet. EI, CI and FAB mass spectra were recorded on a Finnegan MAT 25Q (high resolution) spectrometer. Methane was generally employed in obtaining CI mass spectra. Analytical thin layer chromatography (TLC) was performed on silica gel 60F-254 plates. Flash chromatography was performed using standard procedures[231] on Kieselgel (230-400 mesh), and size exclusion chromatography was performed on Sephadex G-10 resin. All reagents were purchased from Aldrich or Fisher Scientific, and were used without further purification except for chromatography solvents, which were distilled before use. Moisture sensitive reactions were carried out under a nitrogen, or argon, atmosphere in glassware that was flame-dried with an inert gas sweep. THF and benzene were freshly distilled before use from sodium benzophenone ketyl.

N-(9-Phenylfluoren-9-yl)-L-serine methyl ester (**9**). A mixture of L-serine methyl ester hydrochloride (9.3 g, 60 mmol) and chlorotrimethylsilane (19.02 ml, 150 mmol) in CH_2Cl_2 (180 ml) at 0 °C was treated with triethylamine (29.16 ml, 210 mmol) and allowed to reach RT. The mixture was refluxed for 1 h, cooled to 0 °C, treated with MeOH (3.66 ml, 80 mmol) in CH_2Cl_2 (18 ml), allowed to warm to RT and stirred for 1 h. The mixture was filtered through a layer of diatomaceous earth (prewashed with Et_3N and benzene, and oven-dried) into a solution of 9-bromo-9-phenylfluorene (PhFlBr, 19.26 g, 60 mmol) in CH_2Cl_2 (50 ml). The filter was washed with CH_2Cl_2 (3 × 20 ml). Trientylamine (8.34 ml, 60 mmol) and $Pb(NO_3)_2$ (18 g, 60 mmol) were added to the solution. The reaction mixture was stirred under N_2 at RT for 4 h. TLC showed the

reaction completed. The mixture was filtered and evaporated. The remaining solid was redissolved in citric acid (5 g) in MeOH (180 ml) and vigorously stirred for 15 min. Solvent was evaporated and the remaining solid was chromatographied with EtOAc/Hexane (1/2 ~ 1/1) as eluant. Evaporation of the collected fraction provided 9 g (75%) of *N*-(9-phenylfluoren-9-yl)-L-serine methyl ester. mp 115.5 ~ 116.5 °C; ^{1}H NMR ($CDCl_3$, 300 MHz) δ 2.26 (2H, br.), 2.77 (1H, t, *J* = 5.1 Hz), 3.28 (1H, dd, *J* = 4.5, 5 Hz), 3.41 (3H, s), 3.45 (1H, dd, *J* = 4.5, 5Hz), 7.22 ~ 7.42 (11H, m), 7.69 (2H, m); ^{13}C NMR ($CDCl_3$, 75.4 MHz) δ 52.11 (q), 57.09 (d), 63.75 (t), 72.57 (s), 119.96 (d), 120.15 (d), 124.99 (d), 125.69 (d), 125.91 (d), 127.42 (d), 127.70 (d), 128.25 (d), 128.43 (d), 128.55 (d), 128.65 (d), 139.86 (s), 141.18 (s), 143.93 (s), 148.33 (s), 148.69 (s), 174.25 (s).

1-{*N*-(9-phenylfluoren-9-yl)-(1*S*)-1-amino-2-oxoethyl]-methyl ester, PhFl-L-Ser(ald)-methyl ester (**10**). DMSO (0.853 ml, 12 mmol) in CH_2Cl_2 (5 ml) was added dropwise to $(COCl)_2$ (0.537 ml, 6 mmol) at –65 °C. The mixture was kept stirring a –65 °C for 15 min. Alcohol **9** (0.85 g, 2.35 mmol) in CH_2Cl_2 (15 ml) was added. The mixture was stirred at –65 °C for 3 h. Triethylamine (2.5 ml) was added and stirred for 15 min. The mixture was warmed to RT. Water (20 ml) was added. The mixture was extracted with CH_2Cl_2 (2 × 15 ml), washed with H_2O (1 × 25 ml), sat. NH_4Cl (1 × 25 ml) and sat. NaCl (1 × 25 ml), dried and evaporated to give crude aldehyde **10** (0.86 g). This crude compound can be used without further purification. ^{1}H NMR ($CDCl_3$, 300 MHz) δ 3.11 (3H, s), 5.50 (1H, s), 7.15~7.40 (11H, m), 7.72 (2H, m), 9.56 (1H, s).

N-(9-Phenylfluoren-9-yl)-L-serine (**12**). A suspension of L-serine (4.2 g, 40 mmol) and chlorotrimethylsilane (15.74 ml, 124 mmol) in CH_2Cl_2 (50 ml) under N_2 atmosphere was refluxed for 30 min, cooled to RT, and added triethylamine (17.4 ml, 124 mmol) in

CH_2Cl_2 (40 ml) at a rate sufficient to maintain gentle reflux. The mixture was refluxed for 1 h, cooled to 0 °C, added dropwise MeOH (1.78 ml, 44 mmol) in CH_2Cl_2 (10 ml), stirred for 10 min, and allowed to warm to RT over 45 min. Stirring was stopped, and under Ar, the mixture was filtered through a layer of diatomaceous earth (prewashed with Et_3N and benzen, and oven-dried dried) into a solution of 9-bromo-9-phenylfluorene (PhFlBr, 12.84 g, 40 mmol) in CH_2Cl_2 (50 ml). The triethylamine hydrochloride that remained on the filter was washed with CH_2Cl_2 (3 × 15 ml). Triethylamine (5.58 ml, 40 mmol) and $Pb(NO_3)_2$ (13.25 g, 40 mmol) were added to the homogeneous solution. Flushed with Ar, the reaction mixture was stirred for 24 h at RT. The mixture was filtered, and the filter cake was washed with THF (3 × 50 ml). The combined organic layer was evaporated, and the residue was redissolved in THF (250 ml) and treated with 5% citric acid in H_2O (100 ml) with vigorous stirring for 5 min. Ether (250 ml) was added, and the aqueous layer was separated and extracted with 1/1 THF/Et_2O (4 × 100 ml). The combined organic layers were extracted with 1N NaOH (4 × 75 ml), and the combined NaOH extracts were washed with Et_2O (100 ml), cooled to 0 °C, and acidified with acetic acid to PH 6.5. The precipitate was extracted from the aqueous layer with 1/3 isopropyl alcohol/$CHCl_3$ (5 × 100 ml), and the combined organic layers were washed with brine, dried, and evaporated, gave 9.1 g (66%) of the compound **12**, which was used without further purification. mp 184 ~ 185 °C [lit[211] 172 ~ 174 °C]; ^{1}H NMR (CD_3OD, 300 MHz) δ 2.41 (1H, t, J = 4.5 Hz), 3.12 (1H, dd, J = 4.5, 10.8 Hz), 3.35 (1H, dd, J = 4.5, 11.1 Hz), 7.03~7.26 (11H, m), 7.57 (2H, t, J = 7.8 Hz); ^{13}C NMR (CD_3OD, 75.4 MHz) δ 59.87(d), 64.33(t), 74.32 (s), 121.16 (d), 121.35 (d), 126.77 (d), 127.01 (d), 127.13 (d), 128.74 (d), 129.04 (d), 129.19 (d), 129.60 (d), 130.21 (d), 130.47 (d), 142.05 (s), 142.15 (s), 144.16 (s), 148.00 (s).

N-(9-Phenylfluorene-9-yl)-L-serine Isoxazolidide (**13**). Isoxazolidine hydrochloride (339 mg, 3.1 mmol) was vigorously stirred in THF (5.3 ml), H_2O (0.13 ml), and DMF (0.13 ml). The mixture was treated with anhydrous K_2CO_3 (1.01 g) in three portions over 45 min. After suspension was stirred for 30 min, it was filtered under Ar into a solution of **12** (534 mg, 1.54 mmol) and hydroxybenzotriazole monohydrate (314 mg, 2.32 mmol) in THF (4 ml). The K_2CO_3 was washed with THF (3 × 1 ml). The solution was cooled to 0 °C, and EDCI (445 mg, 2.32 mmol) was added. The reaction mixture was stirred under Ar overnight at 0 °C. Water (30 ml) was added and the reaction was stirred for an additional hour. The solvent was evaporated and the crude product was purified by chromatography (eluant: 1:1 EtOAc/hexane). Evaporation of the collected fractions gave a white solid (550 mg, 90%). mp 184 ~ 185 °C [lit[211] 182 ~ 185 °C]; ^{1}H NMR ($CDCl_3$, 300 MHz) δ 1.85 (1H, m), 2.03 (1H, m), 2.65 (1H, m), 3.14 (2H, m), 3.4 ~ 3.6 (6H, m), 7.22 ~ 7.42 (11H, m), 7.68 (2H, m); ^{13}C NMR ($CDCl_3$, 75.4 MHz) δ 26.72 (t), 42.85 (t), 54.57 (t), 63.98 (d), 68.38 (t), 72.77 (s), 119.46 (d), 119.86 (d), 125.14 (d), 125.38 (d), 125.81 (d), 127.10 (d), 127.26 (d), 128.11 (d), 128.33 (d), 128.48 (d), 128.54 (d), 139.59 (s), 141.35 (s), 143.96 (s), 148.66 (s), 149.21 (s), 172.71 (s).

(4*S*)-2-Oxo-3-(9-phenylfluoren-9-yl)oxazolidine-4-carboxylic Acid Isoxazolidide (**14**). A solution of isoxazolidide **13** (0.5 g, 1.25 mmol) and triethylamine (0.436 ml, 3.13 mmol) in toluene (25 ml) was cooled to 0 °C, treated with a 20% solution of phosgene in toluene (1.3 ml, 2.5 mmol) and stirred for 15 min. Methanol (1 ml) was added, and the mixture was washed with $NaHCO_3$ (10 ml). The aqueous layer was extracted with $CHCl_3$ (3 × 5 ml) and the combined organic layer was washed with brine (2 × 5 ml), dried and evaporated to a solid, which was recrystallized from CH_2Cl_2/hexane to give **14** (522 mg,

98%). mp 224 ~ 228 °C [lit[211] 224 °C]; ^{1}H NMR ($CDCl_3$, 300 MHz) δ 2.04 (2H, m), 2.96 (1H, m), 3.35 (1H, m), 3.67 (2H, m), 4.08 (1H, m), 4.28 (2H, m), 7.11 ~ 7.87 (13H, m); ^{13}C NMR ($CDCl_3$, 75.4 MHz) δ 26.83 (t), 43.17 (t), 55.13 (t), 65.47 (d), 68.93 (t), 73.07 (s), 119.66 (d), 119.75 (d), 125.88 (d), 126.88 (d), 127.08 (d), 127.31 (d), 128.29 (d), 128.87 (d), 128.98 (d), 129.37 (d), 139.90 (s), 140.53 (s), 146.10 (s), 147.33 (s), 158.36 (s), 168.5 (s); MS (CI, CH_4) 426.1 (M, 15.4), 269.1 (9), 242.1 (18), 241.1 (100).

(4*S*)-2-Oxo-3-(9-phenylfluoren-9-yl)oxazolidine-4-carboxaldehyde (**11**) (from **14**). A solution of $LiAlH_4$ in THF (1.0 M, 5.1 ml, 5.1 mmol) was added to isoxazolidide **14** (2.0 g, 4.7 mmol) in THF (45 ml) at –78 °C. The mixture was stirred for 15 min and then $KHSO_4$ (2 g) in H_2O (45 ml) was added. The mixture was extracted with EtOAc (3 × 90 ml) and the combined organic layer was washed with brine and dried. Evaporation of the solvent gave crude product (1.327 g). ^{1}H NMR spectrum showed the purity was about 90%. So the yield was about 72%. ^{1}H NMR ($CDCl_3$, 300 MHz) δ 3.95 (1H, m), 4.12 (1H, dd, J = 9.34, 5.49 Hz), 4.34 (1H, t, J = 9.34 Hz), 7.27 ~ 7.80 (13H, m), 9.03 (1H, d, J = 3.57 Hz); MS (CI, CH_4) 356 (MH^+, 4.4), 355 (M, 2.7), 269 (6.3), 241 (100).

Isoxazolidine hydrochloride. The mixture of 1,3-dibromopropane (0.8 g, 3.96 mmol), N-hydroxyurethane (0.5 g, 4.76 mmol), KOH (0.27 g, 4.82 mmol) and EtOH (5 ml) was refluxed for 6 h. The solvent was removed, extracted with ether, condensed and provided crude product 442 mg (~77%). The crude compound was mixed with 16% HCl (15 ml) and refluxed for 2 h. Solvent was evaporated under reduced pressure and the residue oil was recrystallized from little amount of hot ethanol to provide product 168 mg (50%). ^{1}H NMR ($CDCl_3$, 300 MHz) δ 2.49 (2H, q, J = 7.2 Hz), 3.59 (2H, t, J = 2 Hz),

4.22 (2H, t, J = 6.9 Hz), 4.84 (2H, s); ^{13}C NMR ($CDCl_3$, 75.4 MHz) δ 17.957 (t), 11.772 (t), 6.977 (t).

(4*S*)-2-Oxo-3-(9-phenylfluoren-9-yl)oxazolidine-4-carboxylic methyl ester (**16**). The mixture of **9** (3.526 g, 9.82 mmol) and triethylamine (2.7 ml, 19.64 mmol) in CH_2Cl_2 (50 ml) was treated with triphosgene (0.981 g, 3.3 mmol) at 0 °C. The mixture was stirred at 0 °C for 5 min, then raised to RT and stirred for 1 h. TLC showed the reaction was completed. The mixture was filtered, evaporated, and the residue was purified by chromatography (eluant: 1:1.5 EtOAc/Hexane). Evaporation of the collected fractions provided **16**: 3.59 g, 95%; mp 113 ~ 113.5 °C; $[\alpha]^{20}_D$ = -112° (c = 1.10, $CHCl_3$); ^{1}H NMR ($CDCl_3$, 300 MHz) δ 3.28 (3H, s), 4.06 (1H, dd, J = 9, 4 Hz), 4.12 (1H, dd, J = 9, 4 Hz), 4.38 (1H, t, J = 9 Hz), 7.27 ~ 7.71 (13H, m); ^{13}C NMR ($CDCl_3$, 75.4 MHz) δ 52.35 (q), 58.14 (d), 64.81 (t), 72.67 (s), 119.80 (d), 120.08 (d), 125.35 (d), 126.37 (d), 127.49 (d), 128.05 (d), 128.45 (d), 128.58 (d), 129.30 (d), 129.61 (d), 140.03 (s), 140.18 (s), 140.29 (s), 145.82 (s), 146.01 (s), 157.53 (s), 170.74 (s); MS (CI, CH_4) exact mass calcd for M $C_{24}H_{19}NO_4$ requires 385.1314, found 385.1251 (14.7), 269.1325 (7.43), 242.1002 (27.6), 241.0939 (100).

(4*S*)-2-oxo-3-(9-phenylfluoren-9-yl)oxazolidine-4-carboxaldehyde (**11**) (from **16**). The *N*-protected methyl ester **16** (2.51 g, 6.5 mmol) was dissolved in dry THF (50 mL) under an argon atmosphere. Upon cooling to –78 °C, $LiAlH_4$ (7.8 mL of a 1 M solution in THF, 7.8 mmol) was added dropwise so that the reaction temperature did not exceed –75 °C. After further stirring for 2 h at this temperature, TLC showed complete consumption of the starting ester and the reaction was quenched by the addition of a solution of $KHSO_4$ (3 g) in H_2O (60 mL). The mixture was then allowed to warm to RT before being

extracted with EtOAc (3 x 80 mL). The combined organic extracts were washed with brine (100 mL) and dried ($MgSO_4$) before removal of the solvent under reduced pressure. The oily residue was purified using flash chromatography (eluant: 2:1 hexane/EtOAc) to give the target aldehyde **11** as a white foam: 1.96 g, 85%; $[\alpha]^{20}_D$ = -313.3° (c = 1.00, $CHCl_3$); ^1H NMR ($CDCl_3$, 300 MHz) δ 3.95 (1 H, m), 4.12 (1 H, dd, *J* = 9.3, 5.5 Hz), 4.34 (1 H, t, *J* = 9.3 Hz), 7.27-7.80 (13 H, m), 9.03 (1 H, d, *J* = 3.6 Hz); ^{13}C NMR ($CDCl_3$, 75.4 MHz) δ 61.88 (d), 63.75 (t), 72.71 (s), 120.50 (d), 124.79 (d), 125.34 (d), 126.43 (d), 127.10 (d), 127.68 (d), 128.56 (d), 128.66 (d), 128.86 (d), 129.94 (d), 130.11 (d), 139.61 (s), 139.74 (s), 140.11 (s), 145.09 (s), 146.98 (s), 157.56 (s), 196.02 (d); MS (CI, CH_4) 356 (MH^+, 4), 355 (M^+, 3), 269 (6), 241 (100).

(4*S*)-2-Oxo-3-(9-phenylfluoren-9-yl)oxazolidine-4-ethanol (**15**). The *N*-protected methyl ester **16** (0.642 g, 1.67 mmol) was dissolved in THF (10 ml). At –78 °C, DIBAL-H (1.0 M in THF, 1.67 ml, 1.67 mmol) was added dropwise. The reaction mixture was kept stirring at –78 °C for 15 min, then raised to 0 °C and stirred at 0 °C overnight. $KHSO_4$ (0.6 g) in H_2O (13 ml) was added to quench the reaction. The mixture was raised to RT and washed with EtOAc (3 × 15 ml), brine (1 × 15 ml) and dried over $MgSO_4$. The evaporated residue was chromatographied with EtOAc/hexane (1/2 ~ 1/1.5) as eluant. Evaporation of the collected fraction provided alcohol **15**; ^1H NMR (300MHz, $CDCl_3$) δ 2.82 (2H, m), 3.88 (1H, m), 4.26 (1H, m), 4.44 (1H, t, *J* = 8.24 Hz), 7.23 ~ 7.77 (12H, m), 8.17 (1H, d, *J* = 7.5 Hz); MS (CI, CH_4) exact mass calcd for MH^+ $C_{23}H_{19}NO_3$ requires 357.1365, found 357.1495 (1.2), 24.1430 (100).

N,*N*-dimethyl (4*S*,3'*S*)-2-oxo-3-(9-phenylfluoren-9-yl)oxazolidine-4-(2',2'-difluoro-3'-hydroxy)-propionamide (**17**). A solution of 1,1-*bis*(dimethylamino)-2,2-

difluoroethene **4** (11.5 mL of a 0.47 M solution in THF, 5.4 mmol) was added to the aldehyde **11** (1.3 g, 3.6 mmol) in dry THF (10 mL), and the reaction mixture was stirred at RT overnight. The reaction was quenched by the addition of a few drops of H_2O, and the organic solvent was removed under reduced pressure after drying ($MgSO_4$). The oily residue was then purified using flash chromatography (eluant:1:1 EtOAc/hexane) to yield the adduct **17** as a white solid. A portion was recrystallized (EtOAc/hexane) to give **17** as colorless plates: 998 mg, 58%; mp 244.7-245.2 °C; $[\alpha]^{20}_D$ = -464° (c = 1.22, $CHCl_3$); ^{1}H NMR ($CDCl_3$, 300 MHz) δ 2.80 (1 H, d, J = 3.5 Hz), 2.85 (3 H, s), 2.94 (3 H, dd, $^5J_{HF}$ = 2.4, 1.5 Hz), 3.46 (1 H, dt, $^3J_{HF}$ = 26.1 Hz, J = 3.4 Hz), 4.38 (2 H, m), 4.59 (1 H, dt, J = 8.3, 1.5 Hz), 7.21-7.54 (10 H, m), 7.66 (1 H, d, J = 7.5 Hz), 7.74 (1 H, d, J = 7.5 Hz), 8.20 (1 H, d, J = 7.5 Hz); ^{13}C NMR ($CDCl_3$, 75.4 MHz) δ 36.54 (q), 36.68 (q), 55.76 (d), 62.36 (t), 68.56 (ddd, $^2J_{CF}$ = 28.7, 21.2 Hz), 71.62 (s), 115.56 (dd, $^1J_{CF}$ = 268.0, 261.0 Hz), 120.09 (d), 120.54 (d), 124.69 (d), 126.05 (d), 127.19 (d), 128.00 (d), 128.12 (d), 128.37 (d), 129.04 (d), 129.51 (d), 139.12 (s), 139.61 (s), 141.65 (s), 145.01 (s), 148.04 (s), 157.92 (s), 161.92 (t, $^2J_{CF}$ = 27.5 Hz); ^{19}F NMR ($CDCl_3$, 282 MHz) -108.22 (1 F, d, $^2J_{FF}$ = 290.1 Hz), -119.56 (1 F, dd, $^2J_{FF}$ = 290.1 Hz, $^3J_{HF}$ = 25.5 Hz); MS (CI, CH_4) 479 (MH^+, 4), 478 (M^+, 11), 242 (19), 241 (100); exact mass calcd for M^+ $C_{27}H_{24}F_2N_2O_4$ requires 478.1704, found 478.1687 (CI).

Ethyl (4*S*,3'*S*)-2-oxo-3-(9-phenylfluoren-9-yl)oxazolidine-4-(2',2'-difluoro-3'-hydroxy)-prop-anoate (**19a**) and ethyl (4*S*,3'*R*)-2-oxo-3-(9-phenylfluoren-9-yl)oxazolidine-(2',2'-difluoro-3'-hydroxy)-propanoate (**19b**). Ethyl bromodifluoroacetate (658 mg, 3.25 mmol) was added slowly to a stirred mixture of aldehyde **11** (464 mg, 1.3 mmol) dissolved in dry THF (10 mL) and acid-washed zinc powder (316 mg, 4.87 mmol)

at RT under a N_2 atmosphere. The reaction mixture was stirred vigorously for 2 h until TLC analysis showed complete consumption of the aldehyde. After the addition of sat. NH_4Cl (3 mL) and sat. NaCl (3 mL), the mixture was filtered through celite. The precipitate was washed well with EtOAc (3 × 10 mL) and the organic phase separated. After extraction of the aqueous phase with EtOAc (2 x 10 mL), the combined organic extracts were dried ($MgSO_4$) and the solvent removed under reduced pressure to give an oily residue. This material was purified by flash chromatography (eluant: 3:1 hexane/EtOAc) to yield the desired adduct as a mixture of diastereoisomers **19a** and **19b** (529 mg, 85%), in a 6:1 ratio by ^{19}F NMR. This mixture was sufficiently pure for use in subsequent transformations. Careful column chromatography yielded a small amount of pure difluoroalcohol **19a**, a portion of which was recrystallized (EtOAc/hexane) to give colorless plates: mp 169-172 °C; $[\alpha]^{20}_D$ = -506° (c = 1.06, $CHCl_3$); ^1H NMR ($CDCl_3$, 300 MHz) δ 1.23 (3 H, t, J = 7.2 Hz), 1.61 (1 H, d, J = 6.6 Hz), 3.41 (1 H, dt, $^3J_{HF}$ = 20.1 Hz, J = 6.6 Hz), 4.13 (2 H, m), 4.34 (1 H, dd, J = 8.4, 1.2 Hz), 4.43 (1 H, t, J = 8.4 Hz), 4.53 (1 H, ddd, J = 9.0, 2.4, 1.2 Hz), 7.44 (10 H, m), 7.74 (2 H, m), 8.21 (1 H, m); ^{13}C NMR ($CDCl_3$, 75.4 MHz) δ 13.74 (q), 56.18 (d), 62.14 (dt, $^4J_{CF}$ = 6.9 Hz), 63.19 (t), 68.45 (dd, $^2J_{CF}$ = 28.0, 21.0 Hz), 71.70 (s), 113.56 (dd, $^1J_{CF}$ = 261.0, 254.0 Hz), 120.32 (d), 120.68 (d), 124.66 (d), 126.19 (d), 127.47 (d), 127.63 (d), 128.54 (d), 129.27 (d), 129.45 (d), 129.83 (d), 138.82 (s), 140.08 (s), 141.17 (s), 144.77 (s), 148.38 (s), 157.82 (s), 161.09 (t, $^2J_{CF}$ = 31.0 Hz); ^{19}F NMR ($CDCl_3$, 282 MHz) -112.35 (1 F, dd, $^2J_{FF}$ = 269.0 Hz, $^3J_{HF}$ = 6.2 Hz), -124.21 (1 F, dd, $^2J_{FF}$ = 269.0 Hz, $^3J_{HF}$ = 19.2 Hz); MS (CI, CH_4) 480 (MH^+, 4), 479 (M^+, 11), 242 (19), 241 (100); exact mass calcd for M^+ $C_{27}H_{24}F_2NO_5$ requires 480.1622, found 480.1623 (CI).

19b: ^{19}F NMR ($CDCl_3$, 282 MHz) -112.98 (1 F, dd, $^2J_{FF}$ = 269.0 Hz, $^3J_{HF}$ = 8.5 Hz), –122.96 (1 F, dd, $^2J_{FF}$ = 269.0 Hz, $^3J_{HF}$ = 19.2 Hz).

N,*N*-dimethyl (4*S*,3'*S*)-2-oxo-3-(9-phenylfluoren-9-yl)oxazolidine-4-(2',2'-difluoro-3'-hydroxy)-propionamide (**17**) (from **19a**). *n*-BuLi (0.08 mL of a 2.5 M solution in THF, 0.2 mmol) was added to a solution of dimethylamine (0.1 mL of a 2 M solution in THF, 0.2 mmol) at –78 °C. The reaction mixture was warmed to 0 °C and stirred for 30 min, before a solution of **19a** (76 mg, 0.16 mmol) in THF (0.5 mL) was added. The mixture was warmed to RT and stirred for a further 1.5 h, to ensure complete consumption of starting ester, before being poured into ice (2 g). The aqueous solution was then extracted with EtOAc (3 × 2 mL). The organic extracts were washed with sat. brine (2 mL), dried ($MgSO_4$) and the solvent removed under reduced pressure to give oily residue. Purification by flash chromatography (eluant: 1:1 EtOAc/hexane) gave a white solid that had identical spectroscopic properties as an authentic sample of **17**: 75 mg, 98%.

Ethyl (4*S*,3'*R*)-2-oxo-3-(9-phenylfluoren-9-yl)oxazolidine-4-(3'-hydroxy)propanoate (**20a**) and ethyl (4*S*,3'*S*)-2-oxo-3-(9-phenylfluoren-9-yl)oxazolidine-4-(3'-hydroxy)propanoate (**20b**). Ethyl bromoacetate (1.14 mL, 10 mmol) was added slowly to a mixture of aldehyde **11** (2.29 g, 6 mmol) and acid-washed zinc dust (0.78 g, 12 mmol) in dry THF (40 mL) RT under a N_2 atmosphere. The reaction mixture was stirred vigorously for 2 h before the addition of aq. NH_4Cl (20 mL) and aq. NaCl (20 mL). After filtration through celite, the precipitate was washed well with EtOAc (4 × 10 mL) and the organic phase separated. After extraction of the aqueous phase with EtOAc (4 x 10 mL), the combined organic extracts were dried ($MgSO_4$) and the solvent removed

under reduced pressure to give an oily residue. This material was purified by flash chromatography (eluant: 4:1 hexane/EtOAc). The major diastereoisomer **20a** was eluted as the first material from the column, followed by **20b**. Both compounds were obtained as colorless oils.

20a: 2.244 g, 84%; ^{1}H NMR ($CDCl_3$, 300 MHz) δ 1.11 (3 H, t, J = 7.2 Hz), 1.50 (1 H, d, J = 4.4 Hz), 1.71 (1 H, dd, J = 15.6, 4.8 Hz), 2.05 (1 H, dd, J = 15.6, 8.9 Hz), 3.28 (1 H, m), 3.90 (3 H, m), 4.27 (1 H, dd, J = 8.8, 2.7 Hz), 4.34 (1 H, t, J = 8.6 Hz), 7.18-7.42 (9 H, m), 7.51 (1 H, dt, J = 7.6, 0.6 Hz), 7.69 (1 H, d, J = 7.6 Hz), 7.77 (1 H, d, J = 7.6 Hz), 8.20 (1 H, d, J = 7.3 Hz); ^{13}C NMR ($CDCl_3$, 75.4 MHz) δ 13.88 (q), 37.06 (t), 60.06 (d), 60.63 (d), 61.86 (t), 65.88 (t), 71.52 (s), 120.31 (d), 120.52 (d), 124.63 (d), 124.73 (d), 125.98 (d), 127.21 (d), 127.32 (d), 128.03 (d), 128.37 (d), 129.08 (d), 129.68 (d), 139.04 (s), 140.01 (s), 141.46 (s), 145.01 (s), 148.22 (s), 157.73 (s), 169.93 (s); MS (CI, CH_4) 443 (M^+, 16), 241 (100); exact mass calcd for MH^+ $C_{27}H_{26}NO_5$ requires 444.1811, found 444.1812 (CI).

20b: 281 mg, 11%; ^{1}H NMR ($CDCl_3$, 300 MHz) δ 1.26 (3 H, t, J = 7.2 Hz), 1.42 (1 H, d, J = 4.6 Hz), 1.75 (1 H, dd, J = 15.4, 5.0 Hz), 2.15 (1 H, dd, J = 15.4, 8.4 Hz), 3.28 (1 H, m), 3.90 (1 H, ddd, J = 8.4, 2.4, 1.5 Hz), 4.11 (2 H, q, J = 7.2 Hz), 4.29 (1 H, dd, J = 8.7, 2.7 Hz), 4.37 (1 H, t, J = 8.7 Hz), 7.20-7.42 (9 H, m), 7.52 (1 H, m), 7.70 (1 H, m), 7.79 (1 H, m), 8.21 (1 H, m); ^{13}C NMR ($CDCl_3$, 75.4 MHz) δ 14.15 (q), 36.88 (t), 51.84 (d), 60.08 (d), 61.88 (t), 65.95 (t), 71.66 (s), 120.44 (d), 120.68 (d), 124.71 (d), 124.79 (d), 126.07 (d), 127.35 (d), 127.38 (d), 128.09 (d), 128.49 (d), 129.17 (d), 129.83 (d), 139.20 (s), 140.12 (s), 141.46 (s), 145.14 (s), 148.34 (s), 157.75 (s), 170.39 (s); MS (CI, CH_4) 443 (M^+, 12), 241 (100).

N,*N*-dimethyl (4*S*,3'*S*)-2-oxo-3-(9-phenylfluoren-9-yl)oxazolidine-4-(2',2'-difluoro-3'-oxythio-carbonylpentafluorophenyl)-propionamide (**21**). The difluorinated alcohol **17** (372 mg, 0.78 mmol) was dissolved in toluene together with DMAP (220 mg, 1.8 mmol) and *N*-hydroxysuccinimide (45 mg, 0.39 mmol). After the addition of pentafluorophenylthiochloroformate (408 mg, 1.5 mmol), the reaction was heated at 90 ^{o}C overnight. The solution was then filtered through celite and dried ($MgSO_4$). After removal of the solvent under reduced pressure, the crude product was purified using flash chromatography (eluant: 1:2 EtOAc/hexanes) to yield **21** as a yellowish foam: 296 mg, 54% (74% based on recovered **17**); ^{1}H NMR ($CDCl_3$, 300 MHz) δ 2.78 (6 H, s), 4.58 (1 H, m), 4.74 (2 H, m), 5.04 (1 H, m), 7.15-7.50 (10 H, m), 7.70 (2 H, m), 8.13 (1 H, d, J = 7.6 Hz); ^{13}C NMR ($CDCl_3$, 75.4 MHz) δ 37.19 (qt, $^{4}J_{CF}$ = 6.8 Hz), 37.57 (q), 55.41 (dt, $^{3}J_{CF}$ = 5.0 Hz), 63.19 (t), 72.11 (s), 80.27 (dt, $^{2}J_{CF}$ = 24.1 Hz), 114.01 (dd, $^{1}J_{CF}$ = 268.0, 261.0 Hz), 120.21 (d), 120.46 (d), 124.64 (d), 126.77 (d), 127.47 (d), 128.38 (d), 128.44 (d), 128.59 (d), 129.45 (d), 129.71 (d), 129.83 (d), 137.00 (m), 139.65 (s), 139.83 (s), 140.28 (m), 140.93 (m), 141.54 (s), 144.44 (s), 147.33 (s), 157.21 (s), 159.99 (t, $^{2}J_{CF}$ = 26.0 Hz), 189.97 (s); ^{19}F NMR ($CDCl_3$, 282 MHz) –107.37 (2 F, d, $^{3}J_{HF}$ = 10.7 Hz), –151.84 (2 F, d, $^{3}J_{FF}$ = 17.1 Hz), –156.58 (1 F, t, J = 21.3 Hz), -162.16 (2 F, dt, $^{3}J_{FF}$ = 21.3, 17.1 Hz); MS (CI, CH_4) 705 (MH^+, 5), 704 (M^+, 14), 242 (20), 241 (100); exact mass calcd for M^+ $C_{34}H_{23}F_7N_2O_5S$ requires 704.1216, found 704.1224 (CI).

Further elution gave unreacted alcohol **17**: 102 mg.

N,*N*-dimethyl (4*S*)-2-oxo-3-(9-phenylfluoren-9-yl)oxazolidine-4-(2',2'-difluoro)-propionamide (**22**). A solution of the difluorinated derivative **21** (295 mg, 0.42 mmol) dissolved in toluene (8 mL) was degassed for 15 min, before being heated to reflux under

an Ar atmosphere. A mixture of Bu_3SnH (0.45 mL, 1.68 mmol) and AIBN (42 mg, 0.26 mmol) dissolved in toluene (4 mL) was then added dropwise to the hot solution. After heating for an additional 15 min, the reaction mixture was cooled to RT and quenched by the addition of H_2O (0.1 mL). The solvent was then removed under reduced pressure, and the residue was purified using flash chromatography (eluant: 5:2 hexane/EtOAc) to yield the deoxygenated amide **22** as a white foam. A portion was recrystallized from EtOAc/hexane: 76 mg, 39%; mp 211-211.5 °C; $[\alpha]^{20}_D$ = -638° (c = 0.1, $CHCl_3$); ^1H NMR ($CDCl_3$, 300 MHz) δ 2.78 (3 H, s), 2.89 (3 H, t, $^5J_{HF}$ = 1.8 Hz), 3.64 (1 H, ddd, $^3J_{HF}$ = 21.3, 12.3 Hz, J = 8.4 Hz), 4.51 (1 H, dd, J = 9.0, 8.4 Hz), 4.61 (1 H, t, J = 8.6 Hz), 4.85 (1 H, dd, J = 16.2, 8.1 Hz), 6.58 (2 H, m), 6.70 (1 H, s), 6.84-7.04 (6 H, m), 7.18 (1 H, m), 7.39 (1 H, m), 7.52 (2 H, m), 7.76 (1 H, m); ^{13}C NMR ($CDCl_3$, 75.4 MHz) δ 36.90 (q), 37.24 (q), 49.21 (t, $^2J_{CF}$ = 22.0 Hz), 58.24 (d), 61.69 (t), 65.60 (s), 119.15 (t, $^1J_{CF}$ = 257.0 Hz), 125.42 (d), 126.01 (d), 126.08 (d), 127.28 (d), 127.59 (d), 128.15 (d), 128.79 (d), 129.09 (d), 130.39 (d), 130.58 (d), 133.37 (s), 136.42 (s), 138.21 (s), 139.85 (s), 141.43 (s), 158.29 (s), 162.10 (t, $^2J_{CF}$ = 26.0 Hz); ^{19}F NMR ($CDCl_3$, 282 MHz) –89.86 (1 F, dd, $^2J_{FF}$ = 281.4 Hz, $^3J_{HF}$ = 12.7 Hz), -93.43 (1 F, dd, $^2J_{FF}$ = 281.4 Hz, $^3J_{HF}$ = 21.4 Hz); MS (CI, CH_4) 463 (MH^+, 100), 462 (M^+, 18), 443 (72), 241 (10); exact mass calcd for MH^+ $C_{27}H_{25}F_2N_2O_3$ requires 463.1833, found 463.1828 (CI).

Ethyl (4*S*,3'*S*)-2-oxo-3-(9-phenylfluoren-9-yl)oxazolidine-4-(2',2'-difluoro-3'-oxythiocarbonylpenta-fluorophenyl)-propanoate (**23a**) and ethyl (4*S*,3'*R*)-2-oxo-3-(9-phenylfluoren-9-yl)oxazolidine-4-(2',2'-difluoro-3'-oxythiocarbonylpentafluorophenyl)-propanoate (**23b**). The mixture of diastereoisomeric fluorinated alcohols **19** (1.66 g, 3.5 mmol) was dissolved in toluene (50 mL), together with DMAP (885 mg, 7 mmol) and *N*-

hydroxysuccinimide (403 mg, 3.5 mmol). After the addition of pentafluorophenylchlorothioformate (408 mg, 1.5 mmol), the reaction mixture was heated to 90 °C and stirred overnight. The solution was then filtered through celite and dried ($MgSO_4$). After removal of the solvent under reduced pressure, the crude product was purified using flash chromatography (eluant: 1:6 EtOAc/hexane) to yield the desired pentafluorophenyl ester as a mixture of diastereoisomers **23a** and **23b**: 1.47 g, 60%; ^{13}C NMR ($CDCl_3$, 75.4 MHz) δ 13.60 (q), 55.09 (d), 63.07 (t), 64.07 (t), 72.21 (s), 79.76 (ddd, $^2J_{CF}$ = 21.7, 30.2 Hz), 111.09 (dd, $^1J_{CF}$ = 258.4, 261.7 Hz), 120.39 (d), 120.69 (d), 124.78 (d), 126.42 (d), 127.51 (d), 127.73 (d, $^1J_{CF}$ = 225.6 Hz), 128.21 (d), 128.41 (d), 128.57 (d), 129.56 (d), 129.70 (d), 129.74 (d), 137.96 (m), 139.61 (s), 139.87 (s), 140.18 (m), 141.02 (s), 144.32 (s), 146.94 (s), 149.40 (s), 157.12 (s), 160.84 (t, $^2J_{CF}$ = 29.7 Hz), 189.58 (s).

23a: ^1H NMR ($CDCl_3$, 300 MHz) δ 1.25 (3 H, t, J = 7.2 Hz), 4.10 (2 H, m), 4.58 (3 H, m), 5.03 (1 H, dd, $^3J_{HF}$ = 15.9 Hz, J = 8.4 Hz), 7.20-7.48 (10 H, m), 7.71 (2 H, m), 8.07 (1 H, m); ^{19}F NMR ($CDCl_3$, 282 MHz) δ -111.76 (1 F, dd, $^2J_{FF}$ = 264.7 Hz, $^3J_{HF}$ = 8.5 Hz), -116.83 (1 F, dd, $^2J_{FF}$ = 264.7 Hz, $^3J_{HF}$ = 16.9 Hz), -151.93 (2 F, d, J = 19.2 Hz), -156.38 (1 F, t, J = 21.5 Hz), -161.9 (2 F, dt, $^3J_{FF}$ = 21.5, 19.2 Hz); MS (CI, CH_4) 705 (M^+, 7), 704 (16), 241 (100).

23b: ^1H NMR ($CDCl_3$, 300 MHz) δ 1.25 (3 H, t, J = 7.2 Hz), 4.10 (2 H, m), 4.58 (4 H, m), 7.20-7.48 (10 H, m), 7.71 (2 H, m), 8.07 (1 H, m); ^{19}F NMR ($CDCl_3$, 282 MHz) δ –113.29 (1 F, dd, $^2J_{FF}$ = 266.7 Hz, $^3J_{HF}$ = 8.5 Hz), -118.72 (1 F, dd, $^2J_{FF}$ = 266.7 Hz, $^3J_{HF}$ = 15.0 Hz), –152.57 (2 F, d, J = 16.9 Hz), -156.75 (1 F, t, J = 21.5 Hz), -161.87 (2 F, dt, $^3J_{FF}$ = 21.5, 16.9 Hz).

Ethyl (4*S*)-2-oxo-3-(9-phenylfluoren-9-yl)oxazolidine-4-(2',2'-difluoro)-propanoate (**24**). A solution of the difluorinated derivative **23** (490 mg, 0.695 mmol) dissolved in toluene (15 mL) was degassed for 15 min, before being heated to reflux under an Ar atmosphere. A mixture of Bu_3SnH (0.56 ml, 2.09 mmol) and AIBN (30 mg, 0.15 mmol) dissolved in toluene (1 mL) was then added dropwise to the hot solution. After heating for an additional 10 min, the reaction mixture was cooled to RT and quenched by the addition of H_2O (0.1 mL). The solvent was removed under reduced pressure, and the residue was purified using flash chromatography (eluant: 5:2 hexane/EtOAc) to yield the deoyxygenated ester **24** as a white foam. A portion was recrystallized (EtOAc/hexane) to give **24** as white crystals: 119 mg, 37% (49% based on recovered **23**); mp 182.0-183.5 °C; $[\alpha]^{20}_D$ = -41.8° (c=1.02, $CHCl_3$); ^1H NMR ($CDCl_3$, 300 MHz) δ 0.84 (3 H, t, J = 7 Hz), 3.57 (2 H, ddd, $^3J_{HF}$ = 24.3, 12.9 Hz, J = 8.4 Hz), 3.87 (2 H, m), 4.69 (3 H, m), 6.54 (2 H, m), 6.71 (1 H, s), 6.87-7.01 (5 H, m), 7.13 (1 H, m), 7.33 (1 H, m), 7.54 (2 H, m), 7.73 (1 H, m); ^{13}C NMR ($CDCl_3$, 75.4 MHz) δ 13.29 (q), 47.18 (tt, $^2J_{CF}$ = 18.0 Hz), 57.57 (d), 61.65 (t), 62.69 (t), 65.51 (s), 116.90 (dd, $^1J_{CF}$ = 254.0, 259.0 Hz), 125.27 (d), 126.11 (d), 127.61 (d), 127.85 (d), 128.40 (d), 128.93 (d), 129.18 (d), 130.01 (d), 130.59 (d), 131.61 (d), 131.75 (d), 133.42 (s), 136.36 (s), 138.11 (s), 139.60 (s), 141.68 (s), 158.13 (s), 161.50 (t, $^2J_{CF}$ = 32 Hz); ^{19}F NMR ($CDCl_3$, 282 MHz) δ –89.47 (1 F, dd, $^2J_{FF}$ = 262.5 Hz, $^3J_{HF}$ = 13.0 Hz), -111.37 (1 F, dd, $^2J_{FF}$ = 262.5 Hz, $^3J_{HF}$ = 25.7 Hz); MS (CI, CH_4) 464 (MH^+, 100), 463 (M^+, 40), 254 (22), 241 (21); exact mass calcd for MH^+ $C_{27}H_{24}F_2NO_4$ requires 464.1673, found 464.1670 (CI).

Further elution gave the unreacted pentafluorophenyl derivative **23**: 116 mg.

N-phthaloyl-L-serine (**28**). A mixture of L-serine (5.25 g, 0.05 mol), *N*-ethoxycarbonylphthalimide (14.27 g, 0.0625 mol), Na_2CO_3 (5.3 g, 0.05 mol) in H_2O was vigorously stirred at RT for 1 h. Filtering out the unreacted starting materials, the solution was acidified with 3N HCl to PH ~ 4. The aqueous solution became cloudy and it was extracted with Et_2O (3 × 100 ml). The combined extracts were washed with sat. NaCl and condensed to give a little yellowish oil: 9.4 g, ~80%; ^{1}H NMR ($CDCl_3$, 300 MHz) δ 4.30 (1H, m), 4.42 (1H, m), 5.07 (1H, dd, J = 4.5, 5.7 Hz), 6.58 (2H, br.), 7.75 (2H, m), 7.88 (2H, m); ^{13}C NMR ($CDCl_3$, 75.4 MHz) δ 60.90 (t), 61.57 (d), 123.76 (d), 131.61 (s), 134.45 (d), 168.14 (s), 171.26 (s).

N-phthaloyl-L-serine 3-methyl-3-(hydroxymethyl)oxetane Ester (**29**). *N*-phthaoloy-L-serine **28** (460 mg, 1.96 mmol, 1 eqiv) was dissolved in CH_2Cl_2 (20 ml) and added dropwise over 1 h to a stirred solution of EDCI (564 mg, 2.94 mmol, 1.5 eqiv), DMAP (24 mg, 0.196 mmol, 0.1 eqiv), 1-hydroxybenzotriazole (26.5 mg, 0.196 mmol, 0.1 eqiv) and 3-methyl-3-(hydroxymethyl)-oxetane (2 g, 19.6 mmol, 10 eqiv) cooled to 0 °C. After 3 h following completion of adding, the solution was warmed to RT and stirred overnight. The reaction mixture was washed with 1% NH_4Cl (2 × 50 ml) and 5% $NaHCO_3$ (1 × 50 ml), dried ($MgSO_4$) and evaporated to dryness, yielding white foam. The aqueous fraction was saved for recovery of oxetane alcohol. The product was further purified by flash chromatography (eluant: 1:1 EtoAc/hexane), yielding 5.0 g (65%) of a white solid. Oxetane alcohol was recovered by evaporating the aqueous fraction to near dryness and then extracting with EtOAC (3 × 50 ml). The organic fractions were combined, dried ($MgSO_4$) and evaporated to a viscous liquid, which can be reused in esterification. ^{1}H NMR ($CDCl_3$, 300 MHz) δ 1.27 (3H, s), 3.81 (1H, m), 4.25 (4H, m),

4.33 (2H, m), 4.46 (2H, m), 5.09 (1H, m), 7.77 (2H, m), 7.88 (2H, m); ^{13}C NMR ($CDCl_3$, 75.4 MHz) δ 20.75 (q), 38.94 (s), 54.82 (t), 60.78 (d), 69.67 (t), 79.18 (t), 123.60 (d), 131.49 (s), 134.43 (d), 167.78 (s), 167.96 (s).

1-[*N*-phthaloyl-(1*S*)-1-amino-2-hydroxyethyl]-4-methyl-2,6,7-trioxabicyclo[2,2,2] octane (**30**). *N*-phthaloyl-L-serine-oxetane ester **29** (139 mg, 0.435 mmol) was dissolved in freshly distilled CH_2Cl_2 (3 ml) and cooled to 0 °C under Ar. A solution of BF_3•OEt_2 (8 µl of a 20% (v/v) solution in CH_2Cl_2, 0.013 mmol, 0.03 eqiv) was added, and the solution was stirred and allowed to warm to RT. After 8 h, Et_3N (23 µl, 0.162 mmol, 0.44 eqiv) was added and the solution was evaporated to dryness. The residue was purified by flash column chromatography (eluant: 1.5:1 EtOAc/hexane), giving 36 mg (26%) of a white foam; ^{1}H NMR ($CDCl_3$, 300 MHz) δ 0.79 (3H, s), 2.67 (1H, m), 3.90 (6H, s), 4.31 (2H, m), 4.54 (1H, dd, J = 6.3, 6.9 Hz), 7.71 (2H, m), 7.84 (2H, m); ^{13}C NMR ($CDCl_3$, 75.4 MHz) δ 14.26 (q), 30.42 (s), 56.35 (t), 59.07 (d), 72.63 (t), 108.24 (s), 123.3 (d), 131.78 (s), 133.83 (d), 168.11 (s).

N-(9-Fluorenylmehtyloxycarbony)-L-serine (**31**). L-serine (5.235 g, 49.857 mmol) and Na_2CO_3 (5.813 g, 54.84 mmol, 1.1 equiv) were dissolved in H_2O (62 ml) and added dropwise to a stirred solution of Fmoc-succinimide (15.976 g, 47.364 mmol, 0.95 eqiv) in dioxane (115 ml) cooled in ice bath. The solution was allowed to warm to RT overnight and was poured into H_2O (100 ml) after 24 h. The solution was washed with CH_2Cl_2 (3 × 100 ml), cooled by ice-bath and acidified by con. HCl to pH 7. Lots of white precipitate was produced. Filter out the precipitate and the filter was washed with cold H_2O. The filtrate was further acidified to pH ~2 and extracted with $CHCl_3$/*iso*-propanol 3/1 (3 × 100 ml). The combined organic fractions were washed by sat. NaCl, dried by $MgSO_4$,

and condensed to give white solid. Combination gave 14.8 g (96%) of product. mp 97.5 ~99.0 °C [lit[191] 74 ~ 86 °C]; ^{1}H NMR (acetone-d_6, 300 MHz) δ 3.90 (1H, dd, J = 11.0, 3.8 Hz), 3.98 (1H, dd, J = 11.1, 4.6 Hz), 4.40 ~ 4.21 (4H, m), 6.61 (1H, d, J = 8.4 Hz), 7.43 ~7.13 (4H, m), 7.74 (2H, d, J = 7.2 Hz), 7.86 (2H, d, J = 7.5 Hz); ^{13}C NMR (acetone-d_6, 75.4 MHz) δ 47.87 (d), 57.15 (d), 62.95 (t), 67.27 (t), 120.72 (d), 126.11 (d), 127.86 (d), 128.44 (d), 141.97 (s), 144.98 (s), 156.95 (s), 172.14 (s).

N-(9-Fluorenylmethyloxycarbonyl)-L-serine 3-methyl-3-(hydroxymethyl)oxetane Ester (**32**). Fmoc-L-serine (5.18 g, 15.844 mmol) was dissolved in CH_2Cl_2 (130 ml) and added dropwise over 2 h to a stirred solution of EDCI (3.04 g, 23.77 mmol, 1.5 eqiv), DMAP (200 mg, 1.634 mmol, 0.1 eqiv), and 3-methyl-3-(hydroxymethyl)-oxetane (31.4 ml, 316.9 mmol, 20 eqiv) cooled to 0 °C. After 3 h folllowing completion of adding, the solution was warmed to RT and stirred overnight. The reaction mixture was washed with 1% NH_4Cl (2 × 250 ml) and 5% $NaHCO_3$ (1 × 250 ml), dried ($MgSO_4$) and evaporated to dryness, yielding white foam. The aqueous fraction was saved for recovery of oxetane alcohol. The product was further purified by flash chromatography (eluant: 2:1 EtOAc/hexane), yielding 5.0 g (77%) of white foam. Oxetane alcohol was recovered by evaporating the aqueous fraction to near dryness and then extracting with EtOAC (3 × 100 ml). The organic fractions were combined, dried ($MgSO_4$) and evaporated to a viscous liquid, which can be reused in esterification. ^{1}H NMR ($CDCl_3$, 300 MHz) δ 1.29 (3H, s), 3.10 (1H, br), 3.95 (1H, m), 4.09 ~ 4.13 (2H, m), 4.22 (1H, t, J = 6.9 Hz), 4.41 ~ 4.56 (8H, m), 5.80 (1H, br, d, J = 6.9 Hz), 7.30 (2H, t, J = 7.5 Hz), 7.39 (2H, t, J = 7.5 Hz), 7.60 (2H, d, J = 6.3 Hz), 7.75 (2H, d, J = 7.5 Hz); ^{13}C NMR ($CDCl_3$, 75.4 MHz) δ

20.70 (q), 39.61 (s), 47.06 (d), 56.32 (d), 63.26 (t), 67.13 (t), 68.83 (t), 79.43 (t), 119.93 (d), 125.03 (d), 127.02 (d), 127.68 (d), 141.21 (s), 143.62 (s), 156.18 (s), 170.65 (s).

1-[*N*-(9-Fluroenylmethyloxycarbonyl)-(1*S*)-1-amino-2-hydroxyethyl]-4-methyl-2,6,7-trioxabicyclo[2,2,2] octane (**33**). Fmoc-L-serine-oxetane ester **32** (310 mg, 0.755 mmol) was dissolved in freshly distilled CH_2Cl_2 (5 ml) and cooled to 0 °C under Ar. A solution of $BF_3 \bullet OEt_2$ (14 µl of a 20% (v/v) solution in CH_2Cl_2, 0.023 mmol, 0.03 eqiv) was added, and the solution was stirred and allowed to warm to RT. After 8 h, Et_3N (46 µl, 0.332 mmol, 0.44 eqiv) was added and the solution was evaporated to dryness. The residue was purified by flash column chromatography (eluant: 1.5:1 EtOAc/hexane, containing 1% Et_3N), giving 197 mg (64%) of a white foam, which can be recrystallized to give white crystals. mp 143 ~145 °C [lit[191] 14 ~ 147 °C]; ^{1}H NMR($CDCl_3$, 300 MHz) δ 0.80 (3H, s), 2.60 (1H, br.), 3.70 (1H, m), 3.97 ~ 3.86 (8H, m), 4.25 (1H, t, J = 6.6 Hz), 4.38 (2H, d, J = 6.9 Hz), 5.41 (1H, d, J = 9.3 Hz), 7.28 ~ 7.42 (4H, m), 7.61 (2H, t, J = 7.2 Hz), 7.75 (2H, d, J = 7.2 Hz); ^{13}C NMR ($CDCl_3$, 75.4 MHz) δ 14.20 (q), 30.50 (s), 47.11 (d), 55.19 (d), 61.85 (t), 66.95 (t), 72.65 (t), 108.46 (s), 119.85 (d), 125.15 (d), 126.95 (d), 127.56 (d), 141.19 (s), 143.82 (s), 144.03 (s), 156.42 (s).

1-[*N*-(9-Fluorenylmethyloxycarbonyl)-(1*S*)-1-amino-2-oxoethyl]-4-methyl-2,6,7-trioxabicyclo[2,2,2]octane (**34**). Fmoc-L-serine-OBO ester **33** (990 mg, 2.409 mmol) was dissolved in 7 ml of freshly distilled CH_2Cl_2 under Ar and cooled to –78 °C. Oxalyl chloride (0.34 ml, 3.85 mmol, 1.6 eqiv) was added to 40 ml of CH_2Cl_2 in a separate flask under Ar and the solution was cooled to –78 °C. Dry DMSO (0.56 ml, 7.95 mmol, 3.3 eqiv) was added to the oxalyl chloride solution and the mixture was stirred at –78 °C for 10 min. The alcohol solution was then transferred by syringe. The resulting solution was

stirred for 80 min at –78 °C, after which DIPEA (2.1 ml, 12.05 mmol, 5 eqiv) was added. The solution was warmed to 0 °C and stirred for an additional 20 min. CH_2Cl_2 (150 ml) was added, the solution was washed with ice-cold 3% NH_4Cl (2 × 150 ml) and sat. NaCl (1 × 150 ml), dired ($MgSO_4$), and evaporated to dryness, yielding 0.98 g (80%) of a white solid foam. The aldehyde was reasonably pure and was used without further purification. mp 153.5 ~ 155.0 °C [lit[191] 163 ~ 164.5 °C]; ^{1}H NMR($CDCl_3$, 300 MHz) δ 0.84 (3H, s), 3.97 (6H, s), 4.25 (1H, t, *J* = 7.2 Hz), 4.33 ~ 4.42 (2H, m), 4.65 (1H, d, *J* = 9.0 Hz), 5.42 (1H, d, *J* = 9.0 Hz), 7.31 (1H, t, *J* = 7.2 Hz), 7.32 (1H, t, *J* = 7.2 Hz), 7.40 (2H, t, *J* = 7.2 Hz), 7.63 (2H, d, *J* = 7.2 Hz), 7.76 (2H, d, *J* = 7.5 Hz), 9.72 (1H, s); ^{13}C NMR ($CDCl_3$, 75.4 MHz) δ 14.26 (q), 30.87 (s), 47.01 (d), 63.23 (d), 67.39 (t), 72.89 (t), 107.17 (s), 119.90 (d), 125.20 (d), 127.02 (d), 127.04 (d), 127.64 (d), 141.22 (s), 143.83 (s), 156.19 (s), 195.70 (s).

1-[*N*-(9-fluorenylmethyloxycarbonyl)-(1*S*)-1-amino-3,3-difluoro-3-ethoxylcarbonyl-4-hydroxypropyl]-4-methyl-2,6,7-trioxabicyclo[2.2.2]octane (**35**). Ethyl bromodifluoroacetate (2.1 ml, 14.5 mmol, 5 eqiv) was added slowly to a stirred solution of aldehyde **34** (1.186 g, 2.9 mmol, 1 eqiv) and acid-washed zinc dust (1.414 g, 21.75 mmol, 7.5 eqiv) in dry THF (30 ml) at RT under argon. The reaction mixture was stirred for 2 h and TLC showed the reaction had completed. Quench the reaction with aqueous solution of 3% NH_4Cl (15 ml) and sat. NaCl (15 ml). The mixture was filtered, extracted with ethyl acetate, washed with sat. NaCl and dried over $MgSO_4$. The evaporated residue was chromatographied with EtOAc/hexane (1/1, containing 1% Et_3N) to give 0.958 g (62%) of a white foam. ^{1}H NMR ($CDCl_3$, 300 MHz) δ 0.81 (3H, s), 1.33 (3H, t, *J* = 7.2 Hz), 3.29 (1H, br.), 3.94 (6H, s), 4.28 ~ 4.40 (6H, m), 4.70 (1H, dd, *J* = 5.7 Hz, $^3J_{HF}$ =

18.3 Hz), 5.50 (1H, d, J = 10.0 Hz), 7.31 (2H, m), 7.39 (2H, t, J = 7.5 Hz), 7.62 (2H, t, J = 7.5 Hz), 7.75 (2H, d, J = 7.5 Hz); ^{13}C NMR ($CDCl_3$, 75.4 MHz) δ 13.79 (q), 14.11 (q), 30.66 (s), 47.04 (d), 51.83 (d), 63.10 (t), 67.16 (t), 68.50 (dd, $^2J_{CF}$ = 22.2, 30.7 Hz), 72.80 (t), 108.48 (s), 113.63 (dd, $^1J_{CF}$ = 251, 262.6 Hz), 119.80 (d), 125.20 (d), 126.95 (d), 127.51 (d), 141.13 (s), 143.90 (s), 143.95 (s), 156.00 (s), 163.14 (dd, $^2J_{CF}$ = 29.7, 32.7 Hz); ^{19}F NMR ($CDCl_3$, 282 MHz) δ major isomer: -112.73 (1F, dd, $^2J_{FF}$ = 264.6 Hz, $^3J_{HF}$ = 6.4 Hz), -125.18 (1F, dd, $^2J_{FF}$ = 264.6 Hz, $^3J_{HF}$ = 17.1 Hz); minor isomer: -111.97 (1F, dd, $^2J_{FF}$ = 262.5 Hz, $^3J_{HF}$ = 6.4 Hz), -124.63 (1F, dd, $^2J_{FF}$ = 262.5 Hz, $^3J_{HF}$ = 18.0 Hz); MS (FAB) exact mass calcd. For MH^+ $C_{27}H_{30}NF_2O_8$ requires 534.1939, found 534.1921.

1-[*N*-(9-fluorenylmethyloxycarbonyl)-(1*S*)-1-amino-3,3-difluoro-3-ethoxycarbonyl-4-oxythiocarbonyl-imidazole-propyl]-4-methyl-2,6,7-trioxabicyclo[2.2.2]octane (**36**). The mixture of alcohol ester **35** (537 mg, 0.99 mmol) and thiocarbonyldiimidazole (311 mg, 1.57 mmol, 1.6 eqiv) were dissolved in THF (15 ml) under argon. The solution was stirred at RT overnight. The reaction mixture was washed with 5% NH_4Cl (1 × 15 ml), sat. $NaHCO_3$ (1 × 15 ml) and sat. NaCl (1 × 15 ml), and dried ($MgSO_4$). The evaporated residue was chromatographied with EtOAc/hexane (1/2 ~1/1.5, containing 1% Et_3N) as eluant. Evaporation of the collected fractions provided white foam: 428 mg, 55%; ^{1}H NMR ($CDCl_3$, 300 MHz) δ 0.76 (3H, s), 1.26 (3H, t, J = 7.2 Hz), 3.79 ~ 3.84 (6H, m), 4.24 ~ 4.45 (6H, m), 4.65 (1H, dd, J = 1.2, 10.5 Hz), 5.26 (1H, br.), 6.65 (1H, m), 7.08 (1H, m), 7.28 ~ 7.41 (4H, m), 7.62 (2H, m), 7.76 (2H, m), 8.38 (1H, s); ^{13}C NMR ($CDCl_3$, 75.4 MHz) δ 13.62 (q), 14.00 (q), 30.75 (s), 46.96 (d), 52.15 (d), 63.65 (t), 67.29 (t), 72.87 (t), 75.45 (dd, $^2J_{CF}$ = 26.2, 27.2 Hz), 107.17 (s), 111.78 (dd, $^1J_{CF}$ = 259.3, 258.9 Hz), 119.91 (d), 124.96 (d), 124.99 (d),

126.99 (d), 127.63 (d), 141.18 (s), 141.22 (s), 143.65 (s), 143.75 (s), 155.8 (s), 161.55 (dd, $^2J_{CF}$ = 30.7, 31.2 Hz), 182.59 (s); ^{19}F NMR ($CDCl_3$, 282 MHz) δ -114.38 (1F, d, $^2J_{FF}$ = 10.7 Hz), -114.77 (1F, d, $^2J_{FF}$ = 12.8 Hz); MS (FAB) exact mass calcd. For MH^+ $C_{31}H_{32}SF_2N_3O_8$ requires 644.1878, found 644.1871.

1-[*N*-(9-fluorenylmethyloxycarbonyl)-(1*S*)-1-amino-3,3-difluoro-3-ethoxycarbonyl-propyl]-4-methyl-2,6,7-tri-oxa-bicyclo[2.2.2]octane (**37**). Thioester **36** (418 mg, 0.65 mmol) and Et_3SiH (5.2 ml, 32.5 mmol, 50 eqiv) were dissolved in freshly distillated benzene (8 ml). After being degassed for about 15 min, the reaction mixture was heated to reflux. One portion of benzoyl peroxide (31.5 mg, 0.13 mmol, 0.2 eqiv) in benzene (0.2 ml) was added. Every 30 min, add another portion of benzoyl peroxide and totally 1.2 eqiv of benzoyl peroxide was added. Stop heating and evaporate the solvent to dryness. The residue was purified by flash column chromatography (eluant: 1:2.5 EtOAc/hexane, containing 1% Et_3N), giving product (113 mg, 34%). ^{1}H NMR ($CDCl_3$, 300 MHz) δ 0.81 (3H, s), 1.27 (3H, t, *J* = 7.2 Hz), 2.32 (1H, m), 2.60 (1H, ddd, *J* = 3 Hz, $^3J_{HF}$ = 15, 30 Hz), 3.93 (6H, s), 4.17 ~ 4.34 (5H, m), 4.43 (1H, m), 4.85 (1H, br., d, *J* = 10.5 Hz), 7.31 (2H, m), 7.40 (2H, t, *J* = 7.2 Hz), 7.60 (2H, t, *J* = 6.3 Hz), 7.76 (2H, d, *J* = 7.5 Hz); ^{13}C NMR ($CDCl_3$, 75.4 MHz) δ 13.85 (q), 14.26 (q), 30.69 (s), 34.77 (dd, $^2J_{CF}$ = 23.3, 24.4 Hz), 47.08 (d), 49.88 (d), 62.86 (t), 67.00 (t), 72.80 (t), 107.83 (s), 115.28 (dd, $^1J_{CF}$ = 248.9, 252.3 Hz), 119.89 (d), 125.10 (d), 125.21 (d), 126.95 (d), 126.99 (d), 127.57 (d), 141.20 (s), 143.83 (s), 144.04 (s), 155.8 (s), 163.86 (dd, $^2J_{CF}$ = 32.2, 32.7Hz); ^{19}F NMR ($CDCl_3$, 282 MHz) δ -102.91 (1F, ddd, $^2J_{FF}$ = 266.8 Hz, $^3J_{HF}$ = 14.9, 12.8 Hz), -106.01 (1F, ddd, $^2J_{FF}$ = 266.8 Hz, $^3J_{HF}$ = 14.9, 19.2 Hz); MS (FAB) exact mass calcd. For MH^+ $C_{27}H_{30}NF_2O_7$ requires 518.1990, found 518.1963.

L-4,4-Difluoroglutamic Acid (**2**). Fmoc-L-F_2Glu-OBO ester **37** (140 mg, 0.27 mmol) was stirred with 3.5 ml of 20% piperidine in CH_2Cl_2 for 40 min. at RT. The solvent was removed under vacuum to give white residue. The residue was redissolved in 5 ml 6N HCl and heated at 90 °C for 3 h. Removal of the solvent left the crude L-4,4-difluoroglutamic acid hydrochloride. The hydrochloride was dissolved in ddH_2O and applied to a column of Bio-Rad AG3-X4 resin which had been equilibrated with ddH_2O. The column was eluted with ddH_2O and then an increasing gradient of TFA up to 0.25 N. The eluant was evaporated to dryness under vacuum to give 60 mg (75%) of the final product. ^{1}H NMR (D_2O, 300 MHz) δ 2.56 (1H, m), 2.79 (1H, m), 4.04 (1H, dd, J = 2.9, 9.8 Hz); ^{13}C NMR (D_2O, 75.4 MHz) δ 35.43 (t, $^2J_{CF}$ = 24.5 Hz), 49.72 (t, $^3J_{CF}$ = 0.04 Hz), 116.82 (dd, $^1J_{CF}$ = 250.9, 251.2 Hz), 169.54 (t, $^2J_{CF}$ = 27.7 Hz), 173.15 (s); ^{19}F NMR (D_2O, 282 MHz) δ -103.45 (1F, ddd, $^2J_{FF}$ = 253.97 Hz, $^3J_{HF}$ = 21.34, 12.81 Hz), -104.59 (1F, ddd, $^2J_{FF}$ = 253.97 Hz, $^3J_{HF}$ = 21.34, 14.94 Hz); ^{19}F NMR (D_2O, 282 MHz) δ -27.70 (1F, ddd, $^2J_{FF}$ = 248.4 Hz, $^3J_{HF}$ = 11.6, 23.2 Hz), -28.90 (1F, ddd, $^2J_{FF}$ = 248.7 Hz, $^3J_{HF}$ = 14.1, 21.2 Hz) (CF_3COOH as reference)

3-Methyl-3-(toluenesulfonyloxymethyl)oxetane Oxetane Tosylate (**39**). Tosyl chloride (23.05 g, 0.12 mol) was dissolved in dry pyridine (150 ml) under argon. 3-methyl-3-(hydroxymethyl)oxetane (8.224 g, 0.081 ml) was added slowly, and the solution was stirred for 1.5 h. Crushed ice (150 g) was then added to the vigorously stirring mixture, which was allowed to stir for an additional 0.5 h. The white precipitate was collected and washed with cold H_2O. The filtrate was condensed and redissolved in H_2O (100 ml). The solution was extracted with EtOAc (3 × 100 ml). The combined extracts were washed with sat. NaCl, dried over $MgSO_4$ and condensed to give white

solid. The combined white solid was 19.58 g (94%). mp 59.0 ~ 59.5 °C [lit[232] 49.5 ~ 51 °C]; ^{1}H NMR($CDCl_3$, 300 MHz) δ 1.37 (3H, s), 2.53 (3H, s), 4.19 (2H, s), 4.42 (4H, m), 7.37 (2H, d, J = 8.1 Hz), 7.81 (2H, d, J = 8.4 Hz); ^{13}C NMR ($CDCl_3$, 75.4 MHz) δ 20.18 (q), 21.21 (q), 38.77 (s), 73.92 (t), 78.40 (t), 127.48 (d), 129.63 (d), 132.06 (s), 144.77 (s).

N-Benzyloxycarbonyl-L-serine 3-Methyl-3-(hydroxy-methyl)oxetane Ester, Cbz-Serine Oxetane Ester (**40**). Cbz-L-Serine (5.04 g, 0.021 mol) and Cs_2CO_3 (3.432 g, 0.0105 mol, 0.5 eqiv) were combined and dissolved in H_2O (45 ml). The water was then removed in vacuo, and the resulting oil was lyophilized for 24 h to give a white solid. To this solid were added oxetane tosylate **39** (5.376 g, 0.021 mol, 1 equiv) and NaI (0.63 g, 4.2 mmol, 0.2 equiv). They were then mixed with DMF (150 ml) and allowed to stir under Ar for 48 hr. The DMF was removed in vacuo, and the resulting solid was dissolved in EtOAc (270 ml) and H_2O (90 ml), extracted with 10% $NaHCO_3$ (2 × 50 ml) and sat. NaCl (1 × 50 ml), and dried over $MgSO_4$. The solvent was removed to yield yellow oil that was further purified by chromatography to give thick oil in 85% yield (5.76 g). ^{1}H NMR ($CDCl_3$, 300 MHz) δ 1.26 (3H, s), 3.67 (1H, br.), 3.81 ~ 3.87 (1H, br., m), 4.00 ~ 4.11 (2H, m), 4.31 ~ 4.52 (6H, m), 5.10 (2H, s), 6.10 (1H, d, J = 7.8 Hz), 7.31 (5H, m); ^{13}C NMR ($CDCl_3$, 75.4 MHz) δ 20.63 (q), 39.17 (s), 56.17 (d), 62.85 (t), 66.91 (t), 68.79 (t), 79.25 (t), 127.91 (d), 128.02 (d), 128.34 (d), 135.98 (s), 156.17 (s), 170.63 (s).

1-[*N*-benzyloxycarbonyl-(1*S*)-1-amino-2-hydroxyethyl]-4-methyl-2,6,7-trioxabicyclo[2,2,2]oxetane, Cbz-L-Ser OBO Ester (**41**). Cbz-Ser oxetane ester **40** (3.3078 g, 10.24 mmol) was dissolved in dry CH_2Cl_2 (85 ml) and cooled to 0 °C under Ar. BF_3• OEt_2 (0.26 ml, 10% v/v in CH_2Cl_2, 0.205 mmol, 0.02 equiv) was added to the

reaction flask. The reaction was allowed to warm to RT. After 6 h, Et_3N (0.29 ml, 2.05 mmol. 0.2 equiv) was added and the reaction solution was evaporated to dryness to give thick oil. The crude product was purified by flash column chromatography (eluant: 2:1 EtOAc/hexane, containing 1% Et_3N), giving 2.7 g (82%) of white thick oil. $[\alpha]^{20}_D$ = -24.5° (c = 1.05, EtOAc) [lit[232] –24.8° (c = 1.00, EtOAc)]; ^{1}H NMR($CDCl_3$, 300 MHz) δ 0.79 (3H, s), 2.66 (1H, br., dd, *J* = 4.6, 8.3 Hz), 3.63 ~ 3.72 (1H, m), 3.80 ~ 3.96 (8H, m), 5.11 (2H, m), 5.38 (1H, d, *J* = 9.1 Hz), 7.29 ~ 7.36 (5H, m); ^{13}C NMR ($CDCl_3$, 75.4 MHz) δ 14.14 (q), 30.42 (s), 55.26 (d), 61.79 (t), 66.79 (t), 72.56 (t), 108.33 (s), 127.94 (d), 128.01 (d), 128.34 (d), 136.33 (s), 156.32 (s).

1-[*N*-benzyloxycarbonyl-(1*S*)-1-amino-2-oxoethyl]-4-methyl-2,6,7-trioxabicyclo[2,2,2]octane, Cbz-L-serine(ald)-OBO Ester (**3**). Cbz-Ser OBO ester **41** (1.866 g, 5.778 mmol) was dissolved in freshly distilled CH_2Cl_2 (16 ml) under Ar in flask 1. Oxalyl chloride (0.81 ml, 9.24 mmol, 1.6 equiv) was added to CH_2Cl_2 (25 ml) in a separate round-bottom flask 2 under Ar and cooled to –78 °C. Dry DMSO (1.46 ml, 19.07 mmol, 3.3 equiv) was added to the oxalyl chloride solution and the mixture was stirred at –78 °C for 15 min. The alcohol solution was transferred slowly to flask 2 and the resulting mixture was stirred for 80 min at –78 °C. DIPEA (5.01 ml, 28.89 mmol, 5 equiv) was added and the solution was stirred for 30 min at –78 °C and 10 min at 0 °C. Ice-cold CH_2Cl_2 (40 ml) was added, and the solution was washed with ice-cold 3% NH_4Cl (3 × 40 ml) and saturated NaCl (1 × 40 ml), dried ($MgSO_4$), and evaporated to dryness. The reaction yielded a slightly yellowish solid (1.87g, 101%). Without further purification, the aldehyde was used for the next step. ^{1}H NMR($CDCl_3$, 300 MHz) δ 0.81 (3H, s), 3.93 (6H, s), 4.60 (1H, d, *J* = 9.0 Hz), 5.11 (2H, d, *J* = 1.46 Hz), 5.41 (1H, d, *J* =

8.8 Hz), 7.32 ~ 7.36 (5H, m), 9.68 (1H, s); ^{13}C NMR ($CDCl_3$, 75.4 MHz) δ 14.2 (q), 30.68 (s), 63.11 (d), 67.02 (t), 72.71 (t), 106.97 (s), 127.97 (d), 128.31 (d), 135.97 (s), 156.03 (s), 195.59 (s).

1-[*N*-benzyloxycarbonyl-(1*S*,2*R*)-1-amino-3,3-difluoro-3-ethoxycarbonyl-4-hydroxypropyl]-4-methyl-2,6,7-trioxabicyclo[2.2.2]octane (**42a**) and 1-[*N*-benzyloxycarbonyl-(1*S*,2*S*)-1-amino-3,3-difluoro-3-ethoxycarbonyl-4-hydroxypropyl]-4-methyl-2,6,7-trioxabicyclo[2.2.2]octane (**42b**). Ethyl bromodifluoroacetate (8 mL, 62.4 mmol) was slowly added to a well-stirred mixture of acid-washed zinc dust (6.08 g, 93.6 mmol) and aldehyde **3** (5 g, 15.6 mmol) dissolved in dry THF (150 mL) at RT, under an argon atmosphere. The reaction mixture was stirred for 2 h, after which time TLC analysis showed complete consumption of aldehyde. After the addition of 3% aq. NH_4Cl (80 mL) and saturated aq. NaCl (80 mL), the mixture was filtered to remove solid materials. The solution was then extracted with EtOAc (3 x 150 mL), washed with saturated aq. NaCl (150 mL), and the combined organic extracts dried ($MgSO_4$). After removal of the solvent under reduced pressure and column chromatography (eluant: 2:3 EtOAc/hexane containing 1% Et_3N) the desired adduct was obtained as a 7:1 mixture of diastereoisomers **42a**:**42b**, based on ^{19}F NMR, as a white foam: 4.85 g, 70%; ^{13}C NMR ($CDCl_3$, 75.4 MHz) δ 14.10 (q), 14.41 (q), 30.95 (s), 52.11 (t), 63.39 (d), 67.17 (t), 68.84 (ddd, $^2J_{CF}$ = 31.0, 22.9 Hz), 73.08 (t), 108.74 (s), 113.97 (dd, $^1J_{CF}$ = 261.9, 250.9 Hz), 128.25 (d), 128.67 (d), 136.67 (s), 156.30 (s), 163.47 (dd, $^2J_{CF}$ = 32.7, 29.7 Hz); MS (FAB) 446 (MH^+, 58), 138 (64), 137 (100), 136 (85); exact mass calcd for MH^+ $C_{20}H_{26}F_2NO_8$ requires 446.1626, found 446.1614 (FAB).

42a: ^{1}H NMR ($CDCl_3$, 300 MHz) δ 0.80 (3 H, s), 1.32 (3 H, t, J = 7.1 Hz), 3.24 (1 H, br. s), 3.92 (6 H, s), 4.26-4.35 (3 H, m), 4.66 (1 H, dd, $^{3}J_{HF}$ = 18.3, J = 5.4 Hz), 5.13 (2 H, m), 5.43 (1 H, d, J = 10.3 Hz), 7.32 (5 H, m); ^{19}F NMR ($CDCl_3$, 282 MHz) –112.69 (1 F, dd, $^{2}J_{FF}$ = 264.6 Hz, $^{3}J_{HF}$ = 6.4 Hz), -125.35 (1 F, dd, $^{2}J_{FF}$ = 264.6 Hz, $^{3}J_{HF}$ = 19.2 Hz).

42b: ^{19}F NMR ($CDCl_3$, 282 MHz) –112.33 (1 F, d, $^{2}J_{FF}$ = 262.5 Hz), -124.68 (1 F, dd, $^{2}J_{FF}$ = 264.6 Hz, $^{3}J_{HF}$ = 17.1 Hz).

1-[*N*-benzyloxycarbonyl-(1*S*,2*R*)-1-amino-3,3-difluoro-3-ethoxycarbonyl-4-oxythiocarbonyl-imidazole-propyl]-4-methyl-2,6,7-trioxabicyclo[2.2.2]octane (**43a**) and 1-[*N*-benzyloxycarbonyl-(1*S*,2*S*)-1-amino-3,3-difluoro-3-ethoxycarbonyl-4-oxythiocarbonylimidazole-propyl]-4-methyl-2,6,7-trioxabicyclo[2.2.2]octane (**43b**). Thiocarbonyldiimidazole (349 mg, 1.76 mmol) and the diastereoisomeric mixture of adducts **42a** and **42b** (491 mg, 1.1 mmol) were dissolved in dry THF (15 mL) and stirred at RT, under an argon atmosphere, for 10 h. The resulting reaction mixture was then washed with 5% aq. NH_4Cl (15 mL), saturated aq. $NaHCO_3$ (15 mL) and saturated aq. NaCl (15 mL). After drying ($MgSO_4$), the solvent was removed to yield an oily residue that was purified by column chromatography (eluant: 1:3 EtOAc/hexane containing 1% Et_3N). The mixture of thioester derivatives **43a** and **43b** was obtained as a white foam: 465 mg, 76%; ^{13}C NMR ($CDCl_3$, 75.4 MHz) δ 13.63 (q), 14.00 (q), 30.72 (s), 52.11 (t), 63.60 (d), 67.34 (t), 72.82 (t), 75.51 (dt, $^{2}J_{CF}$ = 27.2 Hz), 107.12 (s), 111.75 (t, $^{1}J_{CF}$ = 258.9 Hz), 118.17 (d), 128.19 (d), 128.45 (d), 130.96 (d), 135.92 (s), 137.19 (d), 155.80 (s), 161.54 (dd, $^{2}J_{CF}$ = 31.2, 30.7 Hz), 182.63 (s); MS (FAB) 556 (MH^+, 33), 154 (70), 91 (100); exact mass calcd for MH^+ $C_{24}H_{28}F_2N_3O_8S$ requires 556.1565, found 556.1560 (FAB).

43a: ^{1}H NMR ($CDCl_3$, 300 MHz) δ 0.76 (3 H, s), 1.27 (3 H, t, J = 7.1 Hz), 3.77-3.86 (6 H, m), 4.24 (2 H, m), 4.62 (1 H, dd, J = 10.8, 1.0 Hz), 5.13-5.19 (3 H, m), 6.74 (1 H, m), 7.04 (1 H, m), 7.36 (5 H, m), 7.62 (1 H, m), 8.34 (1 H, m); ^{19}F NMR ($CDCl_3$, 282 MHz) –113.87 (1 F, dd, $^{2}J_{FF}$ = 269.0 Hz, $^{3}J_{HF}$ = 9.7 Hz), -115.19 (1 F, dd, $^{2}J_{FF}$ = 269.0 Hz, $^{3}J_{HF}$ = 11.7 Hz).

43b: ^{19}F NMR ($CDCl_3$, 282 MHz) –113.45 (1 F, dd, $^{2}J_{FF}$ = 270.0 Hz, $^{3}J_{HF}$ = 9.6 Hz), -115.78 (1 F, dd, $^{2}J_{FF}$ = 270.0 Hz, $^{3}J_{HF}$ = 11.8 Hz).

1-[*N*-benzyloxycarbonyl-(1*S*)-1-amino-3,3-difluoro-3-ethoxycarbonyl-propyl]-4-methyl-2,6,7-tri-oxa-bicyclo[2.2.2]octane (**44**). The diastereoisomeric mixtures of thioester derivatives **43** (430 mg, 0.78 mmol) and Et_3SiH (6.2 mL, 39 mmol) were dissolved in freshly distilled benzene (10 mL). After degassing the solution for 15 min. using dry argon, a solution of benzoyl peroxide (37.5 mg, 0.15 mmol) in dry benzene (0.2 mL) was added, and the reaction mixture heated to reflux. At 30 min intervals, additional portions of benzoyl peroxide were added to a total amount of 0.8 equivalents. The reaction mixture was then refluxed for a further 30 min and then allowed to cool to RT. The solvent was removed under reduced pressure and the residue was purified by flash chromatography (eluant: 4:1 hexane/EtOAc containing 1% Et_3N) to give the dehydroxylated OBO ester **44** as a white foam: 276 mg, 83%. A portion was recrystallized (EtOAc/hexane) to give **44** as colorless needles. mp 78.0-78.8 °C; $[\alpha]^{20}_{D}$ = -37.6° (c = 1, EtOAc); ^{1}H NMR ($CDCl_3$, 300 MHz) δ 0.79 (3 H, s), 1.27 (3 H, t, J = 7.0 Hz), 2.17-2.36 (1 H, m), 2.58 (1 H, ddd, $^{3}J_{HF}$ = 29.8, 14.9 Hz, J = 2.3 Hz), 3.87 (6 H, s), 4.13-4.27 (3 H, m), 4.84 (1 H, d, J = 10.5 Hz), 5.11 (2 H, m), 7.29-7.34 (5 H, m); ^{13}C NMR ($CDCl_3$, 75.4 MHz) δ 13.77 (q), 14.14 (q), 30.57 (s), 34.80 (ddt, $^{2}J_{CF}$ = 24.4, 23.3

Hz), 49.78 (t), 62.76 (d), 66.78 (t), 72.69 (t), 107.73 (s), 115.24 (dd, $^1J_{CF}$ = 252.1, 248.9 Hz), 127.99 (d), 128.03 (d), 128.37 (d), 136.34 (s), 155.76 (s), 163.90 (dd, $^2J_{CF}$ = 32.7, 32.2 Hz); ^{19}F NMR ($CDCl_3$, 282 MHz) –102.76 (1 F, ddd, $^2J_{FF}$ = 266.8 Hz, $^3J_{HF}$ = 14.9, 12.8 Hz), -106.29 (1 F, ddd, $^2J_{FF}$ = 266.7 Hz, $^3J_{HF}$ = 19.2, 14.9 Hz); MS (FAB) 430 (MH^+, 93), 307 (59), 136 (100), 107 (48); exact mass calcd for MH^+ $C_{20}H_{26}F_2NO_7$ requires 430.1677, found 430.1671 (FAB).

L-4,4-Difluoroglutamic Acid (**2**). The *N*-protected OBO ester **44** (190 mg, 0.44 mmol) was dissolved in 6N aq. HCl (20 mL) and the solution heated at 90 °C for 2 h. The solvent was removed under vacuum to yield viscous oil that was re-dissolved in doubly deionized (dd) H_2O. After adjusting the solution pH to 7 using aq. $NaHCO_3$, the solution was applied to an anion-exchange column (BioRad AG3-X4 resin) that had been equilibrated with ddH_2O. Elution was then carried out using ddH_2O and an increasing gradient of TFA up to a final concentration of 0.25 M. Ninhydrin positive fractions were then pooled and lyophilization yielded the crude product **2** as a solid. L-4,4-Difluoroglutamic acid **2** was then obtained by recrystallization from H_2O/^{i}PrOH as white needles: 35 mg, 37%; mp 174.5-176.5 °C dec [lit.[176] 173-176 °C dec]; $[\alpha]^{20}_D$ = 6.5° (c = 1, ddH_2O) [lit.[177] $[\alpha]^{20}_D$ = 5.4° (c = 1.04, H_2O)]; ^{1}H NMR (D_2O, 300 MHz) δ 2.55-2.92 (3 H, m), 4.32 (1 H, dd, *J* = 8.4, 3.8 Hz); ^{13}C NMR (D_2O, 75.4 MHz) δ 34.79 (tt, $^2J_{CF}$ = 24.7 Hz), 48.53 (d), 116.42 (dd, $^1J_{CF}$ = 251.8, 251.3 Hz), 169.00 (dd, $^2J_{CF}$ = 28.2, 27.7 Hz), 171.26 (s); ^{19}F NMR (D_2O, 282 MHz) –103.36 (1 F, ddd, $^2J_{FF}$ = 251.8 Hz, $^3J_{HF}$ = 21.3, 12.8 Hz), -104.45 (1 F, ddd, $^2J_{FF}$ = 251.8 Hz, $^3J_{HF}$ = 19.2, 14.9 Hz). MS (CI, CH_4) exact mass calcd for MH^+ $C_5H_8F_2NO_4$ requires 184.0421, found 184.0410.

X-ray diffraction structure determination of *N*,*N*-dimethyl (4*R*,3'*S*)-2-oxo-3-(9-phenylfluorenyl-9-yl)oxazolidine-4-(2',2'-difluoro-3'-hydroxy)-propionamide (**17**). Data were collected at 173 K on a Siemens SMART PLATFORM equipped with A CCD area detector and a graphite monochromator utilizing Mo Kα radiation (λ = 0.71073 Å). Cell parameters were refined using 5720 reflections. A hemisphere of data (1381 frames) was collected using the ω-scan method (0.3° frame width). The first 50 frames were remeasured at the end of data collection to monitor instrument and crystal stability (maximum correction on *I* was < 1 %). Absorption corrections by integration were applied based on measured indexed crystal faces. The structure was solved by the Direct Methods in *SHELXTL5,*[39] and refined using full-matrix least squares. The non-H atoms were treated anisotropically, whereas the hydrogen atoms were calculated in ideal positions and were riding on their respective carbon atoms, except the O3' hydroxyl and the water molecule protons which were obtained from a Difference Fourier map and refined without any constraints. There is a water molecule of solvation present in the asymmetric unit. A total of 340 parameters were refined in the final cycle of refinement using 3880 reflections with $I > 2\sigma(I)$ to yield R_1 and wR_2 of 4.04% and 7.63%, respectively. Refinement was done using F^2.

CHAPTER 4
SYNTHESIS OF β-ASPARAGINYL ADENYLATE

Based on our current focus to obtain information of asparagine synthetase on (i) enzyme structure, (ii) the interactions that catalyze the formation and breakdown of the βAspAMP intermediate in the synthetase active site, and (iii) the molecular mechanisms that underlie channel formation, the inhibitor should be rationally designed to mimic βAspAMP. D. C. Pike's inhibitor[44] with replacement of O with CH_2 is a good intermediate mimic but didn't show potent inhibition. What we thought is that keeping a hetero-atom such as N between carbonyl group and phosphorous group may be essential for stronger binding of such an intermediate inhibitor. So we designed inhibitor **45** as shown in Figure 4-1.

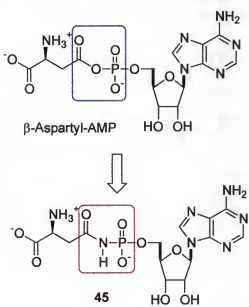

Figure 4-1 *N*-acylphosphoramidate linkage is a good mimic of acylphosphorate.

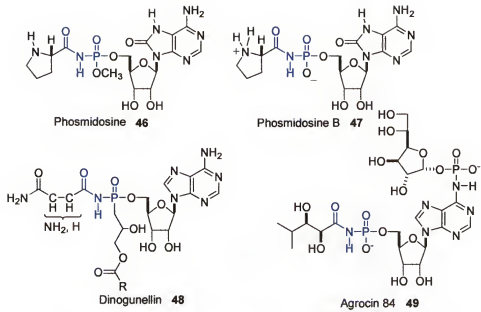

Figure 4-2 Structures of Phosmidosine, Dinogunellin and Agrocin 84.

N-acylphosphoramidate is a rather stable bond linkage that could be found in some natural nucleotide antibiotics (Figure 4-2) such as Phosmidosine **46**, **47**,[233] Dinogunellin **48**[234] and Agrocin-84 **49**.[235] In the particular case of Phosmidosine **46** and **47**, they have *N*-acylphosphoramidate linkages that connect a nucleoside analogue, 8-oxoadenosine, with a L-proline residue. Syntheses of *N*-acylphosphoramidate derivatives are summarized as outlined in Figure 4-3, by either acylation of a phosphoramidate group,[236,237] reaction of carboxamide salts with phosphorochloridates,[238,239] esterification of *N*-acylphosphoramidic acids (or derivatives),[240] reaction of trialkyl phosphates with *N*-haloamides,[241] or Grandas'[242] and Sekine's[124,125] approaches.

The acylation of neutral phosphoramidates (Figure 4-3, eq. 1) has been studied under different conditions and has been found to be accompanied by cleavage of the P-N bond and formation of a carboxamide.[236] The reaction of acyl halides with the conjugate base of phosphoramidates gives a mixture of products,[237] and consequently, it is also not

practical for preparative purposes. Phosphorochloridate esters and the conjugate base of primary or secondary carboxamides[238,239] react to give the desired *N*-acylphosphoramidate (eq 2). This synthetic method requires the use of strong bases (sodium, butyllithium) for the preparation of the amide anion and thus is only compatible with base-stable substrates.

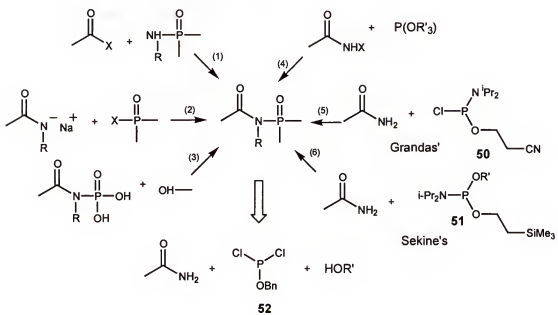

Figure 4-3 Existing approaches for the synthesis of *N*-acylphosphoramidate.

N-Acylphosphoramidic acids or chloroacylphosphoramidates (ClP(O)(OH)NHCOR'') can be esterified with an alcohol to *N*-acylphosphoramidates[240] (eq 3). The inconvenience of the method lies in the preparation of the dichloroacylphosphoramidate precursors (or their corresponding monochloro or acid derivatives), which can only be obtained from aromatic carboxamides or aliphatic amides with electron-withdrawing substituents at the α-carbon. With other substrates, a large or nearly quantitative amount of dehydration takes place. With respect to the Arbuzov

reaction between *N*-haloamides and trialkyl phosphates (eq 4), *N*-acylphosphoramidates can only be obtained from cyclic haloamides or cyclic haloimides.[241]

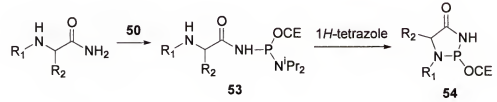

Figure 4-4 Side reaction of Grandas' phosphilylation.

Grandas' phosphilylation[242] of the carboxamide by reaction with chloro-2-cyanoethyl-*N*,*N*-diisopropylphosphoroamidite **50** followed by condensation with nucleoside derivative is a more general method for the preparation of peptide-nucleotide hybrids linked through an *N*-acylphosphoramidate. But it was found that if carboxamide has an α-amino group, the further reaction of the phosphorodiamidite **53** with adenosine derivative in the presence of 1*H*-tetrazole activator gave a cyclized derivative **54** (Figure 4-4).[124] Our target amide, asparagine derivative, contains an α-amino group, which prevents its use of this method.

Grandas' method was further improved by Sekines' approach,[124,125] that is, construction the *N*-acyl phosphoramidate linkage by the reaction of carboxamides with nucleoside phosphoramidite derivatives (Figure 4-5). Diisopropylammonium tetrazolide was used as an activating catalyst in the first step of coupling. In the second step of coupling of the nucleoside 3'-phosphoramidate derivatives with the carboxamide derivatives, most of the commonly used activators, like 1*H*-tetrazole, are not satisfactory. The best activator is 5-(3,5-dinitrophenyl)-1*H*-tetrazole.[124] They also found that the fully

protected *N*-acyl-2-cyanoethylphosphoramidate **58**, either with 2-(trimethylsilyl) ethyl group (TSE) or 2-cyano ethyl group (CE), are extremely unstable and easily decompose with the cleavage of the P-N bond during silica gel column chromatography. Therefore, TSE was used as the phosphate protecting group, which can be removed selectively by treatment with Bu_4NF after construction of the P-N bond.

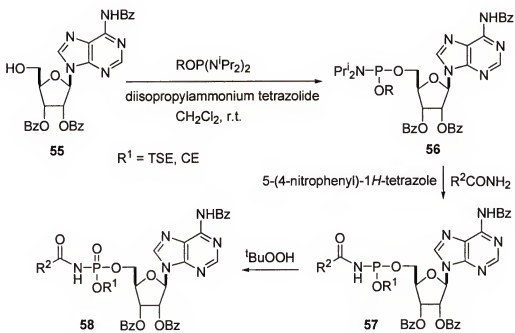

Figure 4-5 Sekine's approach to construct *N*-acylphosphoramidate linkage.

Exploration of new methods for the construction of *N*-acylphosphoramidate linkage is important, not only for the synthesis of our desired inhibitor, but also for the synthesis of aminoacyladenylate analogue that contains *N*-acylphosphoramidate linkage. Such aminoacyladenylate analogue can be expected to have activity as a potential specific inhibitor in aminoacylation of tRNA. Moreover, it will have great significance in the synthesis of the natural products containing the phosphoramidate linkage.

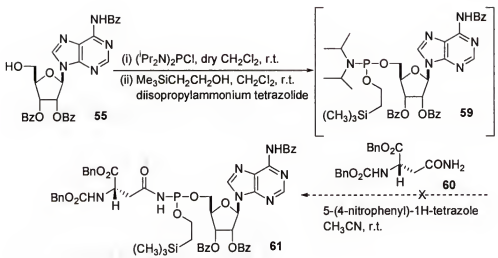

Figure 4-6 Synthesis of β-*N*-aspartylphosphoramidate via Sekine's approach.

We attempted to prepare the target *N*-acylphosphoramidite **61** following Sekine's approach (Figure 4-6). Reaction of *N*-benzoyl-2',3'-di-*O*-benzoyladenosine **55**[243] with the reagent bis-(*N*,*N*-diisopropylamino)-chlorophosphine yielded a reactive intermediate that was immediately treated with 2-(trimethylsilyl)ethanol in the presence of diisopropylammonium tetrazolide to generate 5'-*O*–phosphoramidite derivative **59**. Unfortunately, reaction of the reactive intermediate **59** with the L-asparagine derivative **60**[244] in the presence of 5-(4-nitrophenyl)-1*H*-tetrazole[245,246] failed to give the desired *N*-acylphosphoramidite product **61** under a variety of literature protocols. This was an unexpected setback given the reported success of these procedures in other studies. We note, however, that all previous examples employ carboxamides that lack ester functionality. And for our substrate, coupling reactions employing 5-(4-nitrophenyl)-1*H*-

tetrazole may proceed sluggishly, leading to extended reaction time and competing hydrolysis of the newly formed P-N bond.

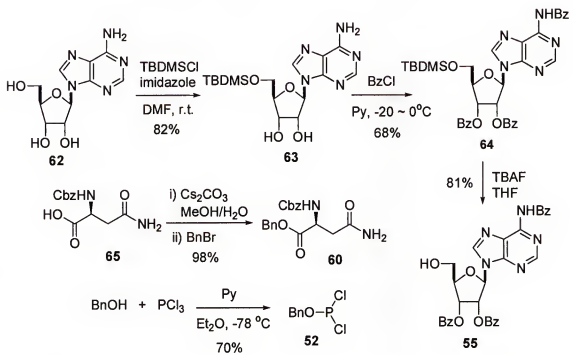

Figure 4-7 Synthesis of starting materials for "one-pot" coupling reaction.

We therefore examined use of more reactive phosphine derivatives in the coupling reaction, and noted that benzyloxydichlorophosphine **52**, prepared by reaction of PCl_3 with benzyl alcohol at –78 °C in pyridine (Figure 4-7),[247,248] appeared suitable for the preparation of functionalized phosphoramidates.[247] The fully protected asparagine derivative **60** was obtained from *N*-protected asparagine by treating it with Cs_2CO_3 and benzyl bromide. 2',3'-Dibenzoyladenosine **55** was synthesized from adenosine: selectively protection 5'-OH with *tert*-butyl dimethyl silyl (TBDMS) group, then protection the 2',3'-OH with benzoyl group and finally deprotection the TBDMS group. The chose of benzyl and benzoyl protection groups simplified the final deprotection step.

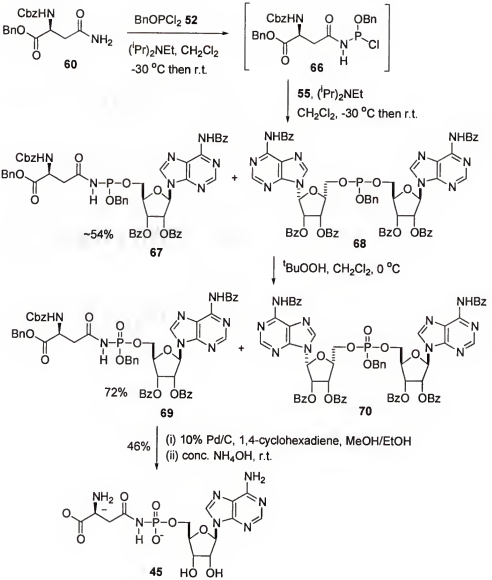

Figure 4-8 "One-pot" synthesis of L-β-asparaginyladenylate **45**.

As anticipated, this reagent could be employed in a novel "one-pot" procedure to prepare the protected *N*-acylphosphoramidite **67** (Figure 4-8), an advanced precursor of β-asparaginyladenylate **45**. Thus, the L-asparagine derivative **60** was slowly added to a solution of the electrophilic phosphine **52** in CH_2Cl_2 at low temperature, followed by adding diisopropylamine. Presumably this procedure yields the monochlorophosphine

intermediate **66**, which is sufficiently deactivated to prevent further reaction with primary amide **60**. After this initial step was complete, *N*-benzoyl-2',3'-di-*O*-benzoyladenosine **55** and additional diisopropylamine were added to the solution, allowing the more reactive primary alcohol to couple with **66** to yield **67** (Figure 4-8). The observation of a signal at 132.48 & 133.57 ppm, in the ^{31}P NMR spectrum of the crude material confirmed that the coupling reaction had taken place to give **67**,[124] and, remarkably, this highly functionalized phosphine derivative was sufficiently stable for its partial purification from a by-product that was assigned to be **68** with the observation of a single resonance at 141.7 ppm in the ^{31}P NMR spectrum, and the known nitrile **72** (Figure 4-9).[249-251] Similar P(III) intermediates in which the benzyl group is replaced by either a 2-cyanoethylene or 2-trimethylsilyl have been reported to be too unstable for purification by silica chromatography.[125] The purification can be accomplished by rapidly eluting the crude reaction mixture through a short plug of silica using $CHCl_3$/EtOAc. The symmetrical phosphine **68** was presumably formed by reaction of two molecules of **55** with unreacted benzyloxydichlorophosphine **52**, implying that there had been incomplete coupling of the phosphine **52** with the amide **60** in the reaction. Having established conditions for the preparation of **67**, this intermediate was easily oxidized using *t*-BuOOH in anhydrous CH_2Cl_2 at 0 °C to give compound **69** in 72% yield from **67**. This stable *N*-acylphosphoramidate **69** could then be readily purified from the symmetrically coupled contaminant **70** by column chromatography. The decomposition with the cleavage of the P-N bond wasn't observed during purification, unlike the TSE or CE protected N-acylphosphoramidate.[124,125] We noted that the oxidation reaction can, in

principle, be performed without isolation of the intermediate *N*-acylphosphoramidite **67**, further simplifying this synthetic approach.

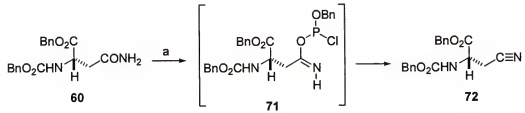

Figure 4-9 Bn = $PhCH_2$. (a) $BnOPCl_2$ **52**, $(^iPr)_2NEt$, CH_2Cl_2, -30 °C.

Table 4-1 Optimization of the "one-pot" coupling reaction.

Entry	Base (eq)[1]	Solvent	Temperature[1]	**67** (%)	**72** (%)	**60** (%)
1	1.08	CH_2Cl_2	r.t.	54	42	56
2	1.5	CH_2Cl_2	r.t.	45	30	49
3	3.0	CH_2Cl_2	r.t.	0	39	41
4	1.08	THF	0 °C	46	50	61
5	1.08	THF	r.t.	37	51	52
6	1.08	THF	60 °C	tiny	96	50
7	1.08	1,4-Dioxane	r.t.	48	45	48
8	1.08	DME	r.t.	33	59	61

[1]Base and temperature used in the step of coupling **52** with **60**

The formation of nitrile **72** suggested there was a side reaction presumably via elimination from the *O*-phosphitylated amide that is the likely kinetic product when the primary amide **60** reacts with the phosphine **52** (Figure 4-9).[252] The formation of the by-product **68** suggested that reaction of the primary amide **60** with the dichlorophosphine **52** had not gone to completion prior to the addition of alcohol **55** under our initial

conditions. We therefore carried out a series of studies in which base concentration, temperature and solvent were systematically varied so as to evaluate their effects on the yield of **67** in our "one-pot" synthetic procedure. In these experiments, the production of **67** via its oxidation form **69** and nitrile **72** were monitored. Studies showed that the yield of the coupled product **67** was highly dependent upon the ratio of diisopropylamine to amide **60** and the temperature before alcohol **55** was added. The low temperature and using less base concentration are crucial in obtaining more **67** over **72**. With 1.08 eq of isopropylamine in CH_2Cl_2 at –30 °C to RT gave a better yield (~54% from **60**) of **67** and reduced amount of nitrile **72** (42% from **60**). Thus, protected *N*-acylphosphoramidate **69** was obtained from **60** in 39% yield. Solvent has no big influence on the coupling. Many aprotonic solvents that make the substrate soluble, such as CH_2Cl_2, THF, 1,4-dioxane and DME are suitable for the reaction. The sequence in which the reagents were added in this "one-pot" synthesis was also important to obtaining good yield of the coupled derivative **67**. For example, alcohol **55** must be added to the reaction mixture prior to addition of diisopropylamine in the second stage of the coupling procedure. Other amide substrates were also tested with such a strategy and got similar results as summarized in Table 4-2.

Catalytic hydrogenation and subsequent ammonolysis to remove the protecting groups of **69** afforded the target *N*-acylphosphoramidate **45** in 46% yield (for two steps) after RP-HPLC purification. The cleavage of the C-N bond or N-P bond was not observed in the final deprotection reaction. A similar sequence of reactions, using N-protected D-asparagine derivative **78** as the starting amide, could be used to obtain the diastereoisomeric *N*-acylphosphoramidate **82** in 15% overall yield (Figure 4-10).

Table 4-2 Results of the "one-pot" coupling from different amide substrates.

Substrate	 Yield %	R-CN Yield %	 Yield %
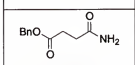	40 (**73**)	37 (**74**)	25
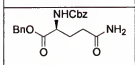	37 (**75**)	45 (**76**)	40
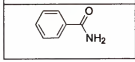	38 (**77**)	-	-

This concise "one-pot" approach offers some potential advantages over existing methods for the preparation of *N*-acylphosphoramidates. First, benzyloxydichlorophosphine **52** is sufficiently reactive at low temperatures for reaction with relatively unreactive amides, leading to reduced reaction time and minimizing breakdown of the P-N bond. Our approach therefore obviates the need to select the correctly functionalized tetrazole that is required to catalyze coupling of *N,N*-diisopropylaminophosphochloridite intermediates with the carboxamide. It is clear from previous studies that the nature of the tetrazole catalyst plays a significant role in determining the yield of the desired *N*-acylphosphoramidite.[124,125] Second, phosphine **52** does not react with esters, which should allow the application of this method in using more expanded range of functionalized amides to prepare *N*-acylphosphoramidates. Finally, the presence of the benzyloxy group as a substituent on phosphorus not only simplifies the final deprotection strategy needed to obtain the target *N*-acylaminoadenylate, but also appears to yield P (III) derivatives that are sufficiently stable for purification using column chromatography.

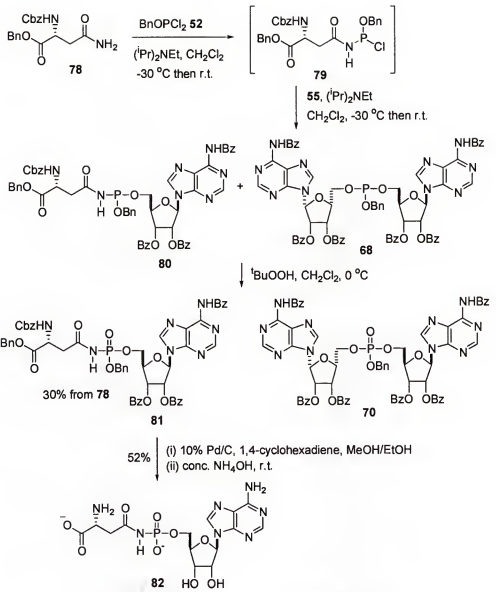

Figure 4-10 "One-pot" synthesis of D-β-asparaginyladenylate **82**.

"One-pot" preparation of β-asparaginyladenylate **45** and **82** is a concise, novel coupling protocol. This simple procedure appears to be compatible with standard protecting groups, and may represent a general approach for the preparation of *N*-acylphosphoramidates from unreactive amides that do not undergo coupling under the conditions of existing literature protocols.

Biological Evaluation of β-Asparaginyladenylates

L-β-Asparaginyladenylate (**45**) inhibits enzyme with IC_{50} of ~200 nM. D-β-asparaginyladenylate (**82**) inhibits the enzyme 200-fold less active than L-β-asparaginyladenylate (**45**). L-β-Asparaginyladenylate (**45**) does not bind to the free enzyme, but binds to a form that is produced during catalytic turnover.[59]

Experimental Section

Melting points were recorded using a Fisher-Johns melting point apparatus, and are uncorrected. Optical rotations were measured using a Polyscience Model SR-6 polarimeter. ^{1}H, ^{13}C, ^{19}F and ^{31}P NMR spectra were obtained at 300, 75.4, 282 and 121 MHz, respectively. For ^{1}H and ^{13}C, chemical shifts are reported in ppm (δ) downfield of tetramethylsilane as an internal reference (δ 0.0), except for measurements in D_2O for which acetone (δ 2.1) was employed as an external standard. In the case of ^{31}P, 85% H_3PO_4 was used as an external standard (δ 0.0). In the case of ^{19}F, $CFCl_3$ was used as an internal standard (δ 0.0). Splitting patterns are abbreviated as follows: s, singlet, d, doublet, t, triplet, q, quartet and m, multiplet. EI, CI and FAB mass spectra were recorded on a Finnegan MAT 25Q (high resolution) spectrometer. Methane was generally employed in obtaining CI mass spectra. Analytical thin layer chromatography (TLC) was performed on silica gel 60F-254 plates. Flash chromatography was performed using standard procedures[55] on Kieselgel (230-400 mesh), and size exclusion chromatography was performed on Sephadex G-10 resin. Semi-preparative reverse-phase (C_{18}) HPLC was carried out on a RAININ system using a DYNAMAX-60A column (2 cm x 30 cm). All reagents were purchased from Aldrich or Fisher Scientific, and were used without

further purification except for chromatography solvents, which were distilled before use. Moisture sensitive reactions were carried out under a nitrogen, or argon, atmosphere in glassware that was flame-dried with an inert gas sweep. THF was freshly distilled from sodium benzophenone ketyl before use.

5'-*O*-*tert*-butyldimethylsilyladenosine (**63**). *tert*-Butyldimethylsilylchloride (10.52 g, 67 mmol) was slowly added to a stirred suspension of adenosine (14.9 g, 55.8 mmol) and imidazole (9.21 g, 134 mmol) in anhydrous DMF (300 mL).[253] The reaction mixture, which became homogeneous, was then stirred overnight at RT before being concentrated under reduced pressure. The oily residue was then purified by flash chromatography (eluant: 10:1 $CHCl_3$/MeOH) to afford the protected adenosine derivative **62** as a white solid: 17.4 g, 82%; mp 178-179 °C [lit.[253] 178-180 °C]; ^{1}H NMR (d_6-DMSO, 300 MHz) δ 0.04 (6 H, s), 0.87 (9 H, s), 3.75 (1 H, dd, J = 11.4, 4.0 Hz), 3.88 (1 H, dd, J = 8.6, 4.0 Hz), 3.96 (1 H, m), 4.19 (1 H, q, J = 5.1 Hz), 4.54 (1H, q, J = 5.1 Hz), 5.22 (1 H, d, J = 5.4 Hz), 5.56 (1 H, d, J = 5.7 Hz), 5.92 (1 H, d, J = 4.8 Hz), 7.30 (2 H, br. s), 8.15 (1 H, s), 8.29 (1 H, s); ^{13}C NMR (d_6-DMSO, 75.4 MHz) δ -5.44 (q), -5.42 (q), 18.09 (s), 25.85 (q), 62.88 (t), 69.88 (d), 73.75 (d), 84.41 (d), 87.41 (d), 119.02 (s), 139.00 (d), 149.39 (s), 152.67 (d), 156.07 (s).

6-*N*-benzoyl-2',3'-*O*-dibenzoyl-5'-*O*-*tert*-butyldimethylsilyl adenosine (**64**). Benzoyl chloride (15.0 mL, 129.67 mmol) was added, over a period of 1.5 h at 0 °C, to a solution of 5'-*O*-*tert*-butyldimethylsilyladenosine **63** (15.2 g, 39.9 mmol) in dry pyridine (300 mL), and the resulting mixture was stirred for another 2 h at RT. After removal of pyridine under the reduced pressure, the residue was dissolved in EtOAc (300 mL) and washed sequentially with water (200 mL), 4% aq. HCl (200 mL), water (200 mL),

saturated $NaHCO_3$ (200 mL), and water (200 mL). The organic layer was dried (Na_2SO_4) and the solvent was removed to yield the crude product. Chromatography (eluant: 4:1, chloroform/ethyl acetate) gave compound **64**, followed by unreacted diol **63** that could be converted into **64** by further reaction with pyridine and benzoyl chloride following the same procedure. Recrystallization (EtOAC/$CHCl_3$) gave the desired derivative **64** as a white solid: 18.83 g, 71%; mp 185-187 °C; ^{1}H NMR ($CDCl_3$, 300 MHz) δ 0.23 (6 H, 2 s), 1.01 (9 H, s), 4.08 (2 H, d, J = 2.1 Hz), 4.59 (1 H, m), 5.93 (1 H, dd, J = 5.0, 2.0 Hz), 6.08 (1 H, dd, J = 7.0, 5.0 Hz), 6.75 (1 H, d, J = 7.0 Hz), 7.29-7.59 (9 H, m), 7.88 (2 H, m), 8.02 (4 H, m), 8.55 (1 H, s), 8.79 (1 H, s), 9.56 (1 H, s); ^{13}C NMR (75.4 MHz, $CDCl_3$) δ -5.44 (q), 18.41 (s), 25.96 (q), 63.33 (t), 72.72 (d), 75.08 (d), 84.83 (d), 85.23 (d), 123.02 (s), 128.03 (d), 128.25 (d), 128.30 (d), 128.38 (d), 128.53 (d), 128.67 (d), 128.86 (d), 129.71 (d), 129.80 (d), 132.67 (s), 133.62 (s), 133.62 (s), 140.91 (d), 149.79 (s), 152.07 (d), 152.75 (s), 164.94 (s), 165.49 (s).

6-*N*-benzoyl-2',3'-*O*-dibenzoyl-adenosine (**55**). Tetra-*n*-butylammonium fluoride (22 mL of a 1 M solution in THF, 22 mmol) was added to a stirred solution of the protected adenosine derivative **64** (11.53 g, 16.63 mmol) in anhydrous THF (30 mL) at 0 °C. The reaction mixture was then stirred at RT for 1 h until starting material had been completely consumed, before being concentrated under reduced pressure to yield an oil that was loaded onto a silica column. Chromatography (eluant: 3:1 $CHCl_3$/EtOAc to 1:2 $CHCl_3$/EtOAc) then gave the desired adenosine derivative **55** as a white solid: 7.81 g, 81%; mp 108-110 °C; ^{1}H NMR ($CDCl_3$, 300 MHz) δ 4.05 (2 H, m), 4.61 (1 H, m), 6.09 (2 H, m), 6.41 (2 H, m), 7.30 (2 H, t, J = 7.8 Hz), 7.43-7.63 (7 H, m), 7.83 (2 H, m), 8.03 (4 H, m), 8.24 (1 H, s), 8.80 (1 H, s), 9.34 (1 H, s); ^{13}C NMR ($CDCl_3$, 75.4 MHz) δ 62.44

(t), 73.22 (d), 73.50 (d), 86.17 (d), 88.52 (d), 124.28 (s), 127.86 (d), 128.17 (d), 128.35 (d), 128.52 (d), 128.74 (d), 128.96 (d), 129.66 (d), 132.80 (s), 133.29 (s), 133.62 (s), 142.41 (d), 150.25 (s), 150.91 (d), 152.36 (s), 164.67 (s), 164.71 (s), 165.32 (s).

O-benzyl-*N*-benzyloxycarbonyl-L-asparagine (**60**). *N*-Benzyloxycarbonyl-L-asparagine **65** (5.61 g, 21.1 mmol) was dissolved in MeOH (190 mL) and water (19 mL), and the solution was titrated to pH 7-8 with 20% aq. Cs_2CO_3 before evaporating to dryness under reduced pressure. The anhydrous salt was then dissolved in anhydrous DMF (100 mL) and reacted overnight with benzyl bromide (2.74 mL, 23 mmol). After removal of the solvent, the residue was re-dissolved in EtOAc (200 mL) and water (200 mL). The organic layer was separated, washed with water (3 x 100 mL), dried (Na_2SO_4), and concentrated. Addition of hexane precipitated the desired ester **60** as a white solid: 7.39 g, 98%; mp 132-133 °C [lit.[244] mp 132 °C]; ^{1}H NMR ($CDCl_3$, 300 MHz) δ 2.71 (1 H, dd, J = 16.2, 4.2 Hz), 2.92 (1 H, dd, J = 16.2, 4.8 Hz), 4.61 (1 H, m), 5.09 (2 H, s), 5.16 (2 H, s), 5.70 (1 H, br. s), 5.80 (1 H, br. s), 6.12 (1 H, d, J = 8.4 Hz), 7.31 (10 H, m); ^{13}C NMR ($CDCl_3$, 75.4 MHz) δ 37.03 (t), 50.69 (d), 66.98 (t), 67.40 (t), 127.92 (d), 128.09 (d), 128.30 (d), 128.48 (d), 135.23 (s), 136.09 (s), 156.14 (s), 170.98 (s), 172.09 (s).

Benzyloxydichlorophosphine (**52**). A solution of benzyl alcohol (63.8 mL, 607 mmol) in Et_2O (300 mL) was added dropwise to a mixture of PCl_3 (53 mL, 607 mmol) and pyridine (50.2 mL, 0.607 mol) dissolved in anhydrous Et_2O (1200 mL) at –78 °C under an inert atmosphere (Ar). Stirring for an additional 15 min, the precipitate formed in the reaction was removed by filtration under Ar, and then washed with Et_2O (2 × 300 mL). After removal of the solvent under reduced pressure, the resulting oily residue was

distilled under reduced pressure to give the dichlorophosphine **52** as a colorless oil, that could be stored without decomposition under Ar at –20 °C: 90 g, 70%; bp 86-89 °C/0.08 mmHg [lit.[247] bp 65 °C/0.2 mmHg]: ^{1}H NMR ($CDCl_3$, 300 MHz) δ 5.20 (2 H, d, $^3J_{HP}$ = 8.1 Hz), 7.36 (5 H, m); ^{13}C NMR ($CDCl_3$, 75.4 MHz) δ 69.71 (dt, $^2J_{CP}$ = 9.8 Hz), 128.35 (d), 128.71 (d), 128.79 (d), 134.68 (d, $^3J_{CP}$ = 2.7 Hz); ^{31}P NMR ($CDCl_3$, 121 MHz) δ 177.41 (s).

O-(6-*N*-Benzoyl-2',3'-*O*-dibenzoyl-adenosine-5'-*O*-yl)-*N*-(*O*-benzyl-*N*-benzyloxycarbonyl-L-asparaginyl)-*O*-benzyloxyphosphoramidite (**67**) The protected asparagine derivative **60** (340 mg, 0.96 mmol) dissolved in anhydrous CH_2Cl_2 (10 mL) was added to a cooled solution of benzyloxydichlorophosphine **52** (880 mg, 0.96 mmol) in anhydrous CH_2Cl_2 (7 mL) at -30 °C. Diisopropylamine (DIPEA) (0.18 mL, 1.04 mmol) was then added, and the resulting mixture was stirred for 1 h at -30 °C, before being warmed to RT. After stirring for a further 6 h, the solution was re-cooled to -30 °C before the sequential addition of the protected adenosine derivative **55** (0.69 g, 1.19 mmol) in anhydrous CH_2Cl_2 (10 mL) and DIPEA (0.36 mL, 2.08 mmol). The resulting solution was slowly warmed to RT and stirred for 4 h, before being concentrated under reduced pressure. The residue was then purified by chromatography (eluant: 3:1 $CHCl_3$/EtOAc to 1:2 $CHCl_3$/EtOAc) giving the known β-cyanoalanine derivative **72**[249]as the first material eluted from the column: 60 mg, 18% (42% based on recovered **60**); mp 105-106 °C [lit.[249] 106-107 °C]; ^{1}H NMR ($CDCl_3$, 300 MHz) δ 2.88 (1 H, dd, *J* = 17.1, 5.1 Hz), 2.98 (1 H, dd, *J* = 17.1, 5.1 Hz), 4.57 (1 H, m), 5.10 (2 H, s), 5.22 (2 H, s), 5.86 (1 H, d, *J* = 6.6 Hz), 7.34 (10 H, m); ^{13}C NMR ($CDCl_3$, 75.4 MHz) δ 21.56 (t), 50.63 (d), 67.43 (t), 68.39 (t), 115.92 (s), 128.08 (d), 128.31 (d), 128.50 (d), 128.52 (d), 128.68 (d),

128.81 (d), 134.31 (s), 135.60 (s), 155.43 (s), 168.45 (s); MS (FAB) 339 (MH^+, 6), 281 (9), 207 (18), 147 (51), 91 (100); exact mass calcd for MH^+ $C_{19}H_{19}N_2O_4$ requires 339.1345, found 339.1346 (FAB).

Further elution yielded the desired coupled product **67** as a white solid (250 mg, ~ 54% based on ^{31}P analysis of this material and the amount of recovered **60**) contamined with a small amount of symmetrically coupled material **68**. This material was sufficiently pure for use in the next step, and further efforts to separate these compounds resulted in extensive decomposition. Continued elution gave a pure sample of **68** as a white foam: 310 mg, 40% (58% based on recovered **55**); ^1H NMR ($CDCl_3$, 300 MHz) δ 4.29 (2 H, m), 4.39 (2 H, m), 4.69 (2 H, m), 5.00 (2 H, d, $^3J_{HP}$ = 8.7 Hz), 6.06 (2 H, m), 6.20 (2 H, dd, *J* = 12.3, 6.3 Hz), 6.67 (2 H, d, *J* = 6.3 Hz), 7.20-7.53 (23 H, m), 7.76 (4 H, m), 7.93 (8 H, m), 8.60 (1 H, s), 8.69 (1 H, s), 8.74 (1 H, s), 8.75 (1 H, s), 9.41 (1 H, s), 9.49 (1 H, s); ^{13}C NMR ($CDCl_3$, 75.4 MHz) δ 62.10 (dt, $^2J_{CP}$ = 10.5 Hz), 62.22 (dt, $^2J_{CP}$ = 10.5 Hz), 64.86 (dt, $^2J_{CP}$ = 10.5 Hz), 71.76 (d), 71.93 (d), 74.18 (d), 74.49 (d), 82.53 (dt, $^3J_{CP}$ = 4.7 Hz), 82.71 (dt, $^3J_{CP}$ = 4.7 Hz), 85.45 (d), 85.59 (d), 123.08 (s), 127.46 (d), 127.89 (d), 127.92 (d), 128.09 (d), 128.23 (d), 128.37 (d), 128.43 (d), 128.52 (d), 129.62 (d), 132.48 (s), 133.49 (s), 137.20 (s), 137.22 (s), 141.33 (d), 141.62 (d), 149.51 (s), 151.81 (d), 151.90 (d), 152.66 (s), 164.81 (s), 164.91 (s), 165.20 (s); ^{31}P NMR ($CDCl_3$, 121 MHz) δ 141.17 (s); MS (FAB) 1317 (MNa^+, 2), 1295 (MH^+, 1), 281 (10), 240 (38), 201 (100); exact mass calcd for MNa^+ $C_{69}H_{55}N_{10}O_{15}PNa$ requires 1317.3484, found 1317.3464 (FAB).

Samples of the starting materials **55** (210 mg) and **60** (190 mg) were also recovered from the column.

O-(6-*N*-Benzoyl-2',3'-*O*-dibenzoyl-adenosine-5'-*O*-yl)-*N*-(*O*-benzyl-*N*-benzyloxycarbonyl-L-asparaginyl)-*O*-benzyloxyphosphoramidate (**69**) The *N*-acylphosphoramidite **67** (369 mg, 0.34 mmol) was dissolved in anhydrous CH_2Cl_2 (5 mL) and degassed with Ar before being cooled to 0 °C. A solution of *t*-BuOOH (0.34 mL of a 5 M solution in anhydrous CH_2Cl_2, 5 equiv) was added slowly at 0 °C, and the reaction mixture stirred for 15 min, after which time TLC analysis showed complete consumption of starting material. The solution was then concentrated under reduced pressure, and the residue purified by chromatography (eluant: 50:1 $CHCl_3$/*i*-PrOH) to afford *N*-acylphosphoramidate **69** as a white foam: 330 mg, 88%; ^{1}H NMR ($CDCl_3$, 300 MHz) δ 3.00 (2 H, m), 4.51-5.17 (10 H, m), 6.00 (1 H, m), 6.10 (1 H, m), 6.55 (1 H, d, J = 8.4 Hz), 6.61 (1 H, d, J = 6.2 Hz), 6.66 (1 H, d, J = 6.0 Hz), 7.15-7.55 (24 H, m), 7.85 (2 H, m), 7.97 (4 H, m), 8.74 (1 H, s), 8.79 (1 H, s), 9.73 (1 H, br s); ^{13}C NMR ($CDCl_3$, 75.4 MHz) δ 38.49 (t), 50.41 (d), 66.63 (dt, $^2J_{CP}$ = 13.0 Hz), 66.64 (t), 67.11 (t), 69.89 (dt, $^2J_{CP}$ = 5.6 Hz), 71.49 (d), 74.18 (d), 81.81 (d, $^2J_{CP}$ = 7.0 Hz), 85.20 (d), 122.76 (s), 127.62 (d), 127.72 (d), 127.76 (d), 127.85 (d), 127.97 (d), 128.05(d), 128.08 (d), 128.19 (d), 128.22 (d), 128.29 (d), 128.33 (d), 128.38 (d), 129.63 (d), 129.65 (d), 132.40 (s), 133.58 (s), 134.74 (s), 134.83 (s), 135.06 (d, $^2J_{CP}$ = 6.0 Hz), 135.91 (s), 141.76 (d), 149.63 (s), 151.71 (d), 152.67 (s), 156.02 (s), 164.80 (s), 165.11 (s), 170.88 (s), 170.95 (s), 172.44 (d, $^2J_{CP}$ = 4.5 Hz); ^{31}P NMR ($CDCl_3$, 121 MHz) δ -1.44, -1.69 (s); MS (FAB) 1110 (MNa^+, 4), 240 (22), 201 (61), 105 (80), 91 (100); exact mass calcd for MNa^+ $C_{57}H_{50}N_7O_{14}PNa$ requires 1110.3051, found 1110.3077 (FAB).

Continued elution gave a sample of the *N*-acylphosphoramidate **70** (formed by oxidation of a small amount of **68** in the starting material) as a white foam; ^{1}H NMR

($CDCl_3$, 300 MHz) δ 4.52 (4 H, m), 4.69 (2 H, m), 5.18 (2 H, d, $^3J_{HP}$ = 9.6 Hz), 6.08 (2 H, m), 6.19 (2 H, m), 6.62 (2 H, d, J = 6.0 Hz), 7.24-7.55 (23 H, m), 7.72-7.99 (12 H, m), 8.52 (1 H, s), 8.54 (1 H, s), 8.75 (1 H, s), 8.77 (1 H, s), 9.31 (1 H, br. s), 9.33 (1 H, br. s); ^{13}C NMR ($CDCl_3$, 75.4 MHz) δ 66.58 (br. dt), 70.15 (dt, $^2J_{CP}$ = 5.7 Hz), 71.02 (d), 71.06 (d), 73.83 (d), 74.11 (d), 81.28 (dt, $^3J_{CP}$ = 4.8 Hz), 81.38 (dt, $^3J_{CP}$ = 4.8 Hz), 85.86 (d), 123.19 (s), 123.26 (s), 127.79 (d), 127.94 (d), 127.97 (d), 127.99 (d), 128.16 (d), 128.25 (d), 128.29 (d), 128.32 (d), 128.37 (d), 128.40 (d), 128.47 (d), 128.62 (d), 129.52 (d), 132.35 (s), 133.36 (s), 133.45 (s), 134.91 (s), 134.99 (s), 141.54 (d), 149.55 (s), 151.62 (d), 152.50 (s), 152.58 (s), 164.69 (s), 164.76 (s), 164.82 (s), 164.87 (s), 165.01 (s), 165.04 (s); ^{31}P NMR ($CDCl_3$, 121 MHz) δ -0.50; MS (FAB) 1333 (MNa^+, 3), 240 (28), 201 (100); exact mass calcd for MNa^+ $C_{69}H_{55}N_{10}PO_{16}Na$ requires 1333.3433, found 1333.3477 (FAB).

O-(Adenosine-5'-*O*-yl)-*N*-(L-asparaginyl)phosphoramidate (**45**) The fully protected *N*-acylphosphoramidate **69** (345 mg, 0.32 mmol) was suspended in a solution of MeOH (6 mL) and EtOH (2 mL) containing 1,4-cyclohexadiene (0.91 mL, 9.6 mmol). After the addition of 10% Pd/C (960 mg), the reaction mixture was vigorously stirred at 30 °C for 4 h, before the addition of further portions of 10% Pd/C (400 mg) and 1,4-cyclohexadiene (0.60 mL). Stirring was then continued for another 3 h at this temperature. Distilled water (5 mL) was then added and the suspension was filtered through celite. The solid residues were washed well using 50% aq. MeOH, and the filtrate was combined with the washings. Removal of the solvent then gave a white solid that was dissolved in conc. NH_4OH (20 mL) and freshly distilled 1,4-dioxane (20 mL). This solution was stirred for 6 h at RT, under an inert N_2 atmosphere, before being concentrated to dryness under

reduced pressure. The resulting white solid was mixed with water (5 mL) and filtered through paper to remove insoluble material. Concentration of the filtrate gave a crude product that was purified on Sephadex G-10 (eluant: H_2O) to afford the ammonium salt of the target *N*-acylphosphoramidate **45**. Further purification by reverse phase HPLC with gradient elution (C_{18} column: solvent flow rate 2 mL/min; from 100:0 H_2O: MeOH + 0.1% TFA to 85:15 H_2O: MeOH + 0.1% TFA over a period of 65 min), with monitoring 260 nm, gave the trifluoroacetate salt of **45** (ret time: 104 min) as a white solid after freeze-drying overnight: 67 mg, 40%; ^{1}H NMR (D_2O, 300 MHz) δ 2.78 (2 H, m), 3.82 (2 H, m), 3.99 (1 H, t, J = 5.1 Hz), 4.04 (1 H, m), 4.11 (1 H, m), 4.40 (1 H, m), 5.83 (1 H, m), 8.10 (1 H, s), 8.30 (1 H, s); ^{13}C NMR (D_2O, 75.4 MHz) δ 48.59 (t), 64.20 (dt, $^2J_{CP}$ = 4.8 Hz), 69.80 (d), 74.14 (d), 83.38 (d), 83.50 (d), 87.45 (d), 115.72 (q, $^1J_{CF}$ = 290.0 Hz), 117.95 (s), 141.97 (d), 144.11 (s), 147.81 (d), 149.31 (s), 162.30 (q, $^2J_{CF}$ = 35.4 Hz), 170.46 (s), 172.08 (s); ^{31}P NMR (D_2O, 121 MHz) δ -5.17; ^{19}F NMR (D_2O, 282 MHz) δ -76.22; MS (FAB) 462 (MH^+, 3), 217 (12), 149 (14), 138 (27), 136 (74), 133 (100); MS (FAB) exact mass calcd for MH^+ $C_{14}H_{21}N_7O_9P$ requires 462.1138, found 462.1139.

O-(6-*N*-benzoyl-2',3'-*O*-dibenzoyl-adenosine-5'-*O*-yl)-*N*-benzyloxycarbonylpropanamide-yl)-*O*-benzyloxyphosphine (**73**). The protected succinamic acid derivative (254 mg, 1.23 mmol) was coupled to the protected adenosine **55** (926 mg, 1.6 mmol) and the phosphine derivative **52** (0.21 mL, 1.23 mmol), using our general "one-pot" procedure, to give the protected *N*-acylphosphoramidite **73** as a white foam: 347 mg, 30% (40% based on recovered amide derivative); ^{1}H NMR ($CDCl_3$, 300 MHz) δ 2.63 (4H, m), 4.17 (2H, m), 4.58 (1H, m), 4.91 (2H, dd, J = 9.4, 19.6 Hz), 5.02 (2H, s), 5.94 (1H, m), 6.19 (1H, dd, J = 5.7, 5.7 Hz), 6.59 (1H, d, J = 5.7 Hz), 7.21-8.00

(26H, m), 8.79 (1H, s), 9.36 (1H, s); ^{13}C NMR ($CDCl_3$, 75.4 MHz) δ 28.21 (t), 29.52 (t), 62.52 (dt, $^2J_{CP}$ = 7.1 Hz), 66.33 (t), 67.34 (dt, $^2J_{CP}$ = 19.9 Hz), 71.99 (d), 74.34 (d), 82.52 (d), 85.78 (d), 123.18 (s), 127.32 (d), 127.46 (d), 127.61 (d), 127.81 (d), 127.90 (d), 127.97 (d), 128.04 (d), 128.20 (d), 128.23 (d), 128.31 (d), 128.37 (d), 128.44 (d), 128.48 (d), 128.63 (d), 129.64 (d), 129.67 (d), 132.58 (s), 133.45 (s), 133.59 (s), 135.56 (s), 137.18 (s), 141.80 (d), 149.58 (s), 151.74 (d), 152.66 (s), 164.81 (s), 164.89 (s), 165.19 (s), 172.26 (s), 175.28 (ds, $^2J_{CP}$ = 9.8 Hz); ^{31}P NMR ($CDCl_3$, 121 MHz) 132.32 (br.); exact mass calcd for MH^+ $C_{49}H_{43}N_6O_{11}H^+$ requires 923.2806, found 923.2805 (FAB).

The reaction produced one by-product, 3-Cyano-proponic benzyl ester (**74**): 70 mg, 28% (37% based on recoverd amide derivative); ^{1}H NMR ($CDCl_3$, 300 MHz) δ 2.68 (4H, m), 5.17 (2H, s), 7.36 (5H, m); ^{13}C NMR ($CDCl_3$, 75.4 MHz) δ 12.84 (d), 29.89 (t), 67.16 (t), 118.34 (s), 128.37 (d), 128.51 (d), 128.60 (d), 135.09 (s), 169.82 (s).

O-(6-*N*-benzoyl-2',3'-*O*-dibenzoyl-adenosine-5'-*O*-yl)-*N*-(*O*-benzyl-*N*-benzyloxycarbonyl-L-glutaminyl)-*O*-benzyloxyphosphoramidate (oxidation product of **75**). The protected derivative of L-glutamine (370 mg, 1 mmol) was coupled to the protected adenosine **55** (752 mg, 1.3 mmol) and the activated phosphine **52** (0.17 mL, 1 mmol), using our general "one-pot" procedure, to give the phosphoramidite derivative **75**: 240 mg, 22% (37% base on recoverd amide derivative) and cyano derivative **76**: 95 mg, 27% (45% based on the recovered amide derivative); ^{1}H NMR ($CDCl_3$, 300 MHz) δ 2.00 (1H, m), 2.23 (1H, m), 3.32 (2H, m), 4.44 (1H, m), 5.09 (2H, s), 5.17 (2H, s), 5.66 (1H, d, J = 7.5 Hz), 7.33 (10H, m); ^{13}C NMR ($CDCl_3$, 75.4 MHz) δ 13.39 (t), 28.35 (t), 52.84 (d), 67.20 (t), 67.71 (t), 118.56 (s), 128.04 (d), 128.22 (d), 128.36 (d), 128.46 (d), 128.62 (d), 128.65 (d), 134.66 (s), 135.80 (s), 155.86 (s), 170.56 (s).

Oxidation of the resulting *N*-acylphosphoramidite intermediate **75** was accomplished by treatment with *t*-BuOOH to give the protected *N*-acylphosphoramidate derivative as a white foam: 192 mg, 79%; ^{1}H NMR ($CDCl_3$, 300 MHz) δ 1.95 (2H, m), 2.41 (2H, m), 4.41 ~ 4.58 (3H, m), 4.93 ~ 5.18 (5H, m), 6.00 (1H, m), 6.11 (1H, m), 6.27 (1H, m), 6.62 (1H, d, J = 6.6 Hz), 7.14 ~ 7.58 (24H, m), 7.84 ~ 8.01 (6H, m), 8.71 (1H, s), 8.81 (1H, s); ^{13}C NMR ($CDCl_3$, 75.4 MHz) δ 27.98 (t), 33.01 (t), 53.48 (d), 66.74 (t), 67.15 (t), 67.42 (t), 70.15 (d), 71.91 (d), 74.49 (d), 82.31 (d), 85.51 (d), 123.14 (s), 128.09 (d), 128.33 (d), 128.61 (d), 128.73 (d), 128.87 (d), 130.01 (s), 132.85 (s), 133.92 (s), 135.92 (s), 136.19 (s), 142.05(d), 149.92 (s), 152.10 (d), 153.11 (s), 156.54 (s), 165.11 (s), 165.49 (s), 172.02 (s), 174.08 (s); ^{31}P NMR ($CDCl_3$, 121 MHz) –0.80, -1.71; exact mass calcd for MH^+ $C_{58}H_{49}N_7PO_{14}$ requires 1102.3310, found 1102.3327 (FAB).

O-(6-*N*-benzoyl-2',3'-*O*-dibenzoyl-adenosine-5'-*O*-yl)-*N*-(benzamide-yl)-*O*-benzyloxyphosphoramidite (**77**). Benzamide (145 mg, 1.2 mmol) was coupled to the protected adenosine **55** (903 mg, 1.56 mmol) and the phosphine **52** (0.21 mL, 1.2 mmol), using our general "one-pot" procedure, to give the protected *N*-acylphosphoramidite **77**: 381 mg, 38%; ^{1}H NMR ($CDCl_3$, 300 MHz) δ 4.27 (2H, m), 4.61 (1H, m), 4.99 (2H, d, $^3J_{HP}$ = 9.3 Hz), 6.01 (1H, dd, J = 3.6, 5.8 Hz), 6.28 (1H, dd, J = 5.8, 5.8 Hz), 6.59 (1H, d, J = 5.8 Hz), 7.23-7.98 (25H, m), 8.61 (1H, s), 8.70 (1H, s), 9.40 (1H, br.); ^{13}C NMR ($CDCl_3$, 75.4 MHz) δ 62.49 (d, $^2J_{CP}$ = 6.8 Hz), 67.41 (d, $^2J_{CP}$ = 16.9 Hz), 71.77 (d), 73.95 (d), 82.39 (d, $^3J_{CP}$ = 4.8 Hz), 85.80 (d), 123.06 (s), 127.15 (d), 127.23 (d), 127.33 (d), 127.44 (d), 127.53 (d), 127.59 (d), 127.70 (d), 127.99 (d), 128.11 (d), 128.21 (d), 128.27 (d), 128.35 (d), 128.43 (d), 128.54 (d), 129.55 (d), 129.59 (d), 132.10 (s), 132.49 (s), 132.66 (s), 133.41 (s), 133.55 (s), 137.20 (d, $^2J_{CP}$ = 4.8 Hz), 141.85 (d), 149.49 (s),

151.52 (d), 152.55 (s), 164.80 (s), 165.16 (s), 170.08 (s), 170.81 (s); ^{31}P NMR ($CDCl_3$, 121 MHz) 132.36, 133.91; exact mass calcd for MH^+ $C_{45}H_{37}N_6O_9$ requires 837.2438, found 837.2435 (FAB).

O-(6-*N*-Benzoyl-2',3'-*O*-dibenzoyl-adenosine-5'-*O*-yl)-*N*-(*O*-benzyl-*N*-benzyloxycarbonyl-D-asparaginyl)-*O*-benzyloxyphosphoramidite (**81**). The protected derivative of D-asparagine **78** (782 mg, 2.2 mmol) was coupled to the protected adenosine **55** (1.65 g, 2.8 mmol) and the activated phosphine **52** (0.36 mL, 2.2 mmol), using our general "one-pot" procedure, and oxidation of the resulting *N*-acylphosphoramidite intermediate **80** was accomplished by treatment with *t*-BuOOH to give the protected *N*-acylphosphoramidate **81** as a white foam: 711 mg, 30% (based on **78**); ^{1}H NMR ($CDCl_3$, 300 MHz) δ 3.00 (2 H, m), 4.57 (2 H, m), 4.80-5.15 (6 H, m), 6.00 (2 H, m), 6.13 (1 H, m), 6.26 (1 H, m), 6.60 (1 H, d, J = 6.6 Hz), 6.68 (1 H, d, J = 6.6 Hz), 6.70 (1 H, d, J = 7.2 Hz), 7.10-7.54 (24 H, m), 7.80-7.99 (6 H, m), 8.81 (1 H, s), 8.82 (1 H, s), 9.78 (1 H, br s); ^{13}C NMR ($CDCl_3$, 75.4 MHz) δ 38.89 (t), 50.29 (d), 66.48 (dt, $^2J_{CP}$ = 10.7 Hz), 66.96 (t), 69.52 (t), 71.43 (dt, $^2J_{CP}$ = 8.9 Hz), 73.83 (d), 74.03 (d), 81.79 (d), 84.84 (d), 122.68 (s), 127.38 (d), 127.52 (d), 127.71 (d), 127.89 (d), 127.93 (d), 128.02 (d), 128.08 (d), 128.12 (d), 128.26 (d), 128.39 (d), 129.51 (d), 132.21 (s), 132.32 (s), 133.47 (s), 134.74 (s), 135.07 (s), 135.89 (s), 141.65 (d), 149.61 (s), 151.65 (d), 152.61 (s), 156.16 (s), 164.63 (s), 164.71 (s), 164.99 (s), 170.87 (s), 172.42 (s); ^{31}P NMR ($CDCl_3$, 121 MHz) δ –1.06, -2.18; MS (FAB) 1088 (MH^+, 8), 240 (14), 201 (98), 105 (26), 91 (100); exact mass calcd for MH^+ $C_{57}H_{51}N_7PO_{14}$ requires 1088.3232, found 1088.3220 (FAB).

O-(Adenosine-5'-*O*-yl)-*N*-(D-asparaginyl)phosphoramidate trifluoroacetate (**82**). The protected derivative **81** (230 mg, 0.2 mmol) was converted to *N*-acylphosphoramidate **82** using an identical procedure to that described for the preparation of **45** from **69**. The trifluoroacetate salt of the desired compound was obtained as a white solid after C_{18} RP-HPLC purification: 51 mg, 45%; ^{1}H NMR (D_2O, 300 MHz) δ 2.78 (2 H, m), 3.81 (2 H, m), 4.01 (2 H, m), 4.11 (1 H, t, J = 4.5 Hz), 4.36 (1 H, dd, J = 5.1, 4.8 Hz), 5.82 (1 H, d, J = 4.8 Hz), 8.08 (1 H, s), 8.29 (1 H, s); ^{13}C NMR (D_2O, 75.4 MHz) δ 48.54 (t), 64.14 (dt, $^{2}J_{CP}$ = 5.0 Hz), 69.67 (d), 74.25 (d), 83.26 (d), 83.39 (d), 87.59 (d), 115.64 (q, $^{1}J_{CF}$ = 290.0 Hz), 117.92 (s), 142.00 (d), 144.06 (s), 147.71 (d), 149.28 (s), 162.17 (q, $^{2}J_{CF}$ = 35.6 Hz), 170.28 (s), 172.08 (s); ^{31}P NMR (D_2O, 121 MHz) δ -5.13; ^{19}F NMR (D_2O, 282.2 MHz) δ -76.23; MS (FAB) 462 (MH^+, 6), 263 (14), 217 (72), 136 (42), 133 (13); exact mass calcd for MH^+ $C_{14}H_{21}N_7PO_9$ requires 462.1138, found 462.1150 (FAB).

CHAPTER 5
COMPUTATIONAL CHARACTERIZATION OF ASPARAGINE SYNTHETASE

Modeling of *E. coli* AS-B

Understanding the structure and catalytic mechanism of asparagine synthetase is of utmost fundamental importance and is crucial for the rational design of specific structure-based and mechanism-based inhibitors. In an effort to both complement and extend our current knowledge of asparagine synthetase, an X-ray crystallographic analysis of asparagine synthetase B from *E. coli* was initiated. The molecular architecture of the catalytically inactive Cys1Ala mutant of the enzyme complexed with L-glutamine and AMP was determined at a resolution of 2.0 Å.[34] *E. coli* asparagine synthetase B (AS-B) contains 553 amino acid residues and functions as a dimer.[254] A ribbon representation of one asparagine synthetase subunit is displayed in Figure 5-1. The monomer consists of two structural motifs formed by Ala1 to Asp194 and Trp195 to Gly516, the N- and C-terminal domains respectively, and at the C-terminal region, Gly517 to Lys553, is missing in the crystal structure. The N-terminal domain, responsible for the hydrolysis of glutamine, is composed mostly of antiparallel β-sheet structure, while the C-terminal domain, which is the synthetase domain, is characterized by a five-stranded paralled β-sheet surrounded by a total of 16 α-helices. Unlike the active site in the glutaminase portion, the C-terminal active site is less well-defined in this complex. As seen in Figure 5-1, it is apparent that the binding pocket for the AMP moiety is quite open.

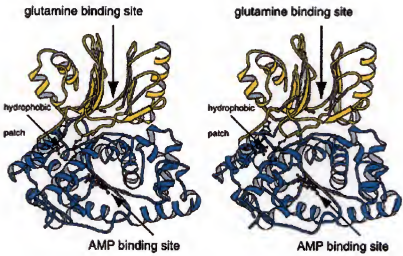

Figure 5-1 Ribbon representation of asparagine synthetase.[34] The N-terminal domain is depicted in yellow, while the C-terminal domain is depicted in blue.

A glutaminase domain is not unique to asparagine synthetase B, a glutamine-dependent amidotransferase. Therefore, the synthetase domain is the inhibition target. Although the C-terminal domain is less well-defined, the general region has been partially defined in the structural analysis and is shown in Figure 5-2. In addition to the bound AMP, three uranium ions are observed in the active site. These metal ions are likely mimicking the binding of magnesium ions. Two specific electrostatic interactions exist between the purine ring and the enzyme: N1 and N6 of the purine moiety and the backbone carbonyl and amide groups of Val272. The 2'-OH of the ribose is linked to the enzyme via the O of Leu232, the O^{γ} of Ser346, and the N of Glu347. Two uranium ions are coordinated by phosphoryl oxygens of the AMP moiety, one of which is further ligated to the enzyme via the carboxylate side chains of Asp238 and Asp351. The second metal ion is surrounded by the carboxylate side chains of Glu352 and Asp384 and the O^{η} of Tyr357.

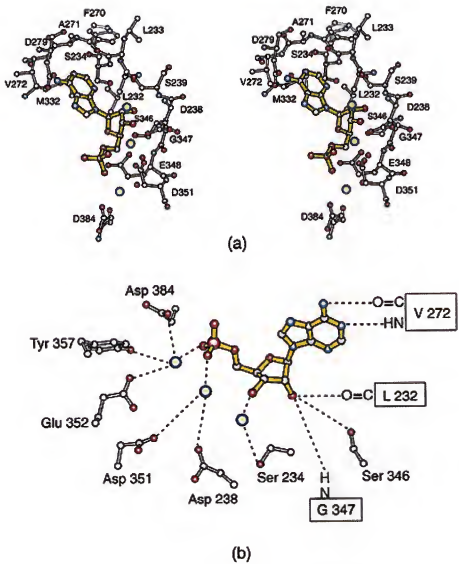

Figure 5-2 Close-up view of the AMP binding region in the C-terminal domain.[34] Those protein atoms located within approximately 4 Å of the AMP are shown in panel a. A cartoon of the possible electrostatic interactions between the protein and the AMP, within 3.2 Å, is displayed in panel b. The bound uranium ions are indicated by the yellow/gray spheres.

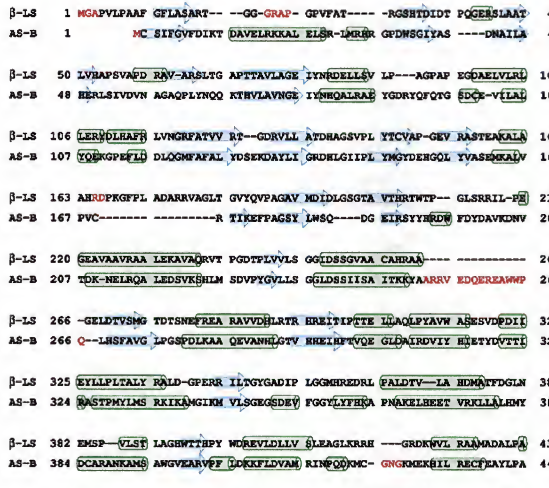

Figure 5-3 Structure-based sequence alignment of β-LS and AS-B.[255]

β-Lactam synthetase (β-LS)[256-258] catalyzes the formation of a β-lactam ring in clavulanic acid, a clinically important β-lactamase inhibitor. Both β-LS and AS-B mediate adenylation of an amino acid, but, in contrast to AS-B, β-LS catalyzes an

intramolecular rather than an intermolecular amide bond formation. The 1.95 Å resolution structure of *Streptomyces clavuligerus* β-LS[255] provides a fully resolved view of the active site in which the substrate, a closely related ATP analogue α, β-methyleneadenosine 5'-triphosphate (AMP-PCP), and a single Mg^{2+} ion are present. As anticipated, sequence alignment (Figure 5-3) shows that β-LS is structurally similar to *E. coli* AS-B. The two enzymes share many secondary and tertiary structural features, including distinct N- and C-terminal domains (Figure 5-4).

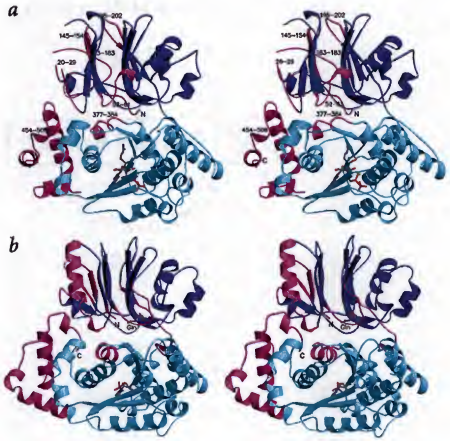

Figure 5-4 Comparison of β-LS and AS-B. a) Stereo view of β-LS. Regions that differ significantly from the corresponding regions in AS-B are colored magenta and labeled by amino acid residue number. b) Stereo view of AS-B in the same orientation as β-LS in (a).[255] N-terminal domain is colored blue and C-terminal domain is colored cyan.

The core regions of the C-terminal synthetase domains of β-LS and AS-B are very similar, both formed by four β-strands and five α-helices, but the β-LS substrate binding cleft is relatively elongated, because the β-LS binding site must accommodate N^2-(carboxyethyl)-L-arginine (CEA), which is substantially longer (~ 12 Å) than aspartic acid (~ 5 Å). In the β-LS active site, the AMP-CPP-Mg^{2+} is very well defined (Figure 5-5). The Mg^{2+} ion is coordinated by one side chain oxygen each from Asp253 and Asp351, by the α, β- and γ-phosphate oxygens, and by a water molecule in a well-organized geometry. The phosphate oxygens also interact with Lys423, Lys443 and the side chain hydroxyl groups of Ser249 and Ser254.

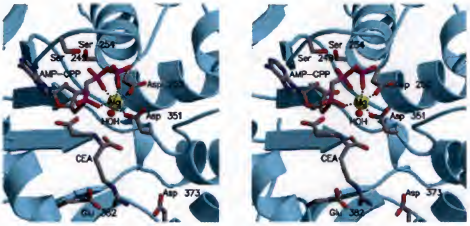

Figure 5-5 Stereo view of the β-LS active site.[255] Key residues that interact with the CEA, AMP-PCP and Mg^{2+} are shown.

The details of the β-LS active site provide new insight into the active site of *E. coli* asparagine synthetase B. In particular, this data can be used to model ATP and Asp into the AS-B structure. The CHARMM molecular modeling package[259-261] was used to do

energy minimization after the ligands were manually docked into the active site by the SYBYL program.

Experimental Procedures

The program ClustalW 18.1[262] was used to do sequence alignment of 15 asparagine synthetase enzymes using the default parameters. The sequences of these enzymes were obtained from the Swiss Port protein database. The SYBYL package (version 6.2) was used for model building and docking. The missing loops were added in SYBYL and the structure was local energy minimized. The structure complexed with the ligands was further refined by the CHARMM 25b2 molecular modeling package.[259-261] CHARMM was also used to add hydrogen atoms. Properties of hydrogen bonds between ligands and the protein and intraproteins were calculated in SYBYL. Structural figures were generated with Snapshot in SYBYL.

The structure of Protein Data Bank (PDB) entry 1CT9 was used for modeling. The 1CT9 structure contains four crystallographically independent subunits of *E. coli* asparagine synthetase B, with each subunit complexed with L-glutamine, AMP and three uranium ions. Three subunits and all the water molecules were removed. According to the crystal structure of β-lactam synthetase, the Mg^{2+} ion is coordinated by one side chain oxygen each from Asp253 and Asp351, which correspond to Asp238 and Asp351 in asparagine synthetase B based on the sequence alignment. In the structure of 1CT9, one of the uranyl ions is coordinated by the side chain oxygens of two Asp residues, Asp238 and Asp351. Hence, the Mg^{2+} ion was placed in the position occupied by this uranyl ion. Another uranyl ion that is coordinated to Tyr357, Asp384 and Glu352 is less likely to play an important role in substrate positioning, because these three residues are not highly

conserved in the sequence alignment of the asparagine synthetase family. Therefore, this uranyl ion along with the third uranyl ion was removed.

The single subunit of structure 1CT9 is missing residues Ala251 to Gln266, Gly423 to Gly425 and Gly517 to Lys553. Because the C-terminal residues are not conserved in the sequence alignment, they likely are not directly involved in substrate and intermediate binding. Besides, it is relatively difficult to use the SYBYL program to search the loop with so many missing residues (37 residues). Therefore, the structure without residues Gly517 to Lys553 was used as the target. The missing residues Ala251 to Gln266 and Gly423 to Gly425 were built in using SYBYL. The basis set used for loop searching in SYBYL is a subset of the Brookhaven Protein Data Bank. The fragments retrieved from the protein database only contain the backbone atoms. After each search, side chains were added and their local geometries were fixed by scanning each rotatable side chain bond in turn until all bad contacts were resolved (or no further changes took place). Finally, local minimization on these two regions was performed using the MINIMIZE SUBSET command. The KOLL_UNI force field (based on AMBER united-atome1) was used since this force field is well parameterized for non-bonding interactions between atoms in proteins. The built loop was specified as a "hot" region for explicit minimization. Surrounding this "hot" region is a rigid region called the "interesting" region, which will contribute non-bonding interactions to the "hot" region. Everything else is considered "uninteresting" and will be ignored by the minimization. The overall structure is not expected to change much.

The starting coordinates of the ligands and the enzyme for energy minimization in CHARMM were taken from the structure obtained from local minimization in SYBYL.

All unknown hydrogens and lone pairs were added in CHARMM. The structure was then minimized in 500 steps using the Steepest Descents (SD) algorithm. Further minimization was exacted using the Adopted Basis Newton-Raphson (ABNR) algorithm until convergence of 0.01 kcal/mol ⊕ r.m.s deviation. No constrains were set on the ligands or the residues. The parameters for the AMP were borrowed from that of ADP and ATP in CHARMM version 22 proteins and nucleic acids force field.[259,260] The optimized structure was further energy minimized using the Generalized Born Solvation Energy and Forces Module.[263] The energy minimization was performed with the CHARMM 25b2 package using the param22 parameter set.

Using the existing AMP in the structure obtained from local minimization in SYBYL as a guide, ATP was built in a similar conformation as that of β-LS in SYBYL. ATP was manually docked in the active site to get the best interaction with the residues around it. Then, local energy minimization of the ATP binding site gave a more relaxed structure. Next, aspartate was similarly built into the active site. Finally, one water molecule was built in the active site, about 2 Å to Mg^{2+} ion. Hydrogens and lone pairs were added in CHARMM. Energy minimization in CHARMM with and without solvent gave two optimized structures.

The optimized structure (without solvation) of the ATP/Asp complex was the target to dock aspartyladenylate and pyrophosphate in the active site. After local energy minimization in SYBYL, the complex was refined in CHARMM.

Results and Discussion

Sequence alignment of the glutamine-dependent asparagine synthetases (Figure 5-6) showed that ASs have high sequence identity, especially in the C-terminal synthetase

domain. The completely conserved residues highlighted in red may be the core of the enzyme which participates in the recognition of the substrates and intermediate and which helps keeping the enzyme in the right conformation.

```
ASNS_MESAU  CGIWALFGSDDCLSVQCLS--AMKIA----HRGPDAFRFENVNGYTNCCFGFHRLAVVD
ASNS_MOUSE  CGIWALFGSDDCLSVQCLS--AMKIA----HRGPDAFRFENVNGYTNCCFGFHRLAVVD
ASNS_RAT    CGIWALFGSDDCLSVQCLS--AMKIA----HRGPDAFRFENVNGYTNCCFGFHRLAVVD
ASNS_HUMAN  CGIWALFGSDDCLSVQCLS--AMKIA----HRGPDAFRFENVNGYTNCCFGFHRLAVVD
ASNS_SANAU  CGILAVLGCSDDSQAKRVR--VLELSRRLKHRGPD---WSGLDHHGDCYLAHQRLAIID
ASNS_TRIVS  CGILAVLGCSDDSQAKRVR--VLELSRRLKHRGPD---WSGIHHHGDCYLAHQRLAIVD
ASN2_LOTJA  CGILAVLGCSDDSQAKRVR--VLELSRRLKHRGPD---WSGLHQHGDNFLAHQRLAIVD
ASN1_PEA    CGILAVLGCSDDSQAKRVR--ILELSRRLKHRGPD---WSGLHQHGDNYLAHQRLAIVD
ASN2_PEA    CGILAVLGCSDPSRAKRVR--VLELSRRLKHRGPE---WSGLHQHGDCYLAQQRLAIVD
ASN1_LOTJA  CGILAVLGCSDFTQAKRVR--VLELSRRLKHRGPD---WSGLHQHGDCYLAHQRLAIVD
ASNS_ARATH  CGILAVLGCSDDSQAKRVR--VLELSRRLRHRGPD---WSGLYQNGDNYLAHQRLAVID
ASNS_BRAOL  CGILAVLGCSDDSQAKRVR--VLELSRRLRHRGPD---WSGIYQNGFNYLAHQRLAIID
ASNS_MAIZE  CGILAVLGVVEVSLAKRSR--IIELSRRLRHRGPD---WSGLHCHEDCYLAHQRLAIID
ASNS_ORYSA  CGILAVLGVADVSLAKRSR--IIELSRRLRHRGPD---WSGIHCYQDCYLAHQRLAIVD
ASNB_ECOLI  CSIFGVFDIKTDAVELRKK--ALELSRLMRHRGPD---WSGIYASDNAILAHERLSIVD

ASNS_MESAU  PLFGMQPIRVKKYPYLWLCYNGEIYNHKALQQRFEF--EYQTNVDGEIILHLYDKGGIE
ASNS_MOUSE  PLFGMQPIRVRKYPYLWLCYNGEIYNHKALQQRFEF--EYQTNVDGEIILHLYDKGGIE
ASNS_RAT    PLFGMQPIRVRKYPYLWLCYNGEIYNHKALQQRFEF--EYQTNVDGEIILHLYDKGGIE
ASNS_HUMAN  PLFGMQPIRVKKYPYLWLCYNGEIYNHKKMQQHFEF--EYQTKVDGEIILHLYDKGGIE
ASNS_SANAU  PASGDQPLYNEDK-TIIVTVNGEIYNHEELRKGLPG-HTFRTGSDCEVIAHLYEEHG-E
ASNS_TRIVS  PASGDQPLFNEDK-RIAVTVNGEIYNHEELRALLPN-HKFRTGSDCDVIAHLYEEYG-E
ASN2_LOTJA  PASGDQPLFNEDQ-SIIVTVNGEIFNHEELRKQLPN-HKFRTGCDCDVIAHLYEEHG-E
ASN1_PEA    PASGDQPLFNEDK-SIIVTVNGEIYNHEELRKQLPN-HKFFTQCDCDVIAHLYEEHG-E
ASN2_PEA    PASGDQPLFNEDN-PSIVTVNGEIYNHEDLRKQLSN-HTFRTGSDCDVIAHLYEEYG-E
ASN1_LOTJA  PASGDQPLFNEDK-SIIVTVNGEIYNHEELRKQLPN-HQFRTGSDCDVIAHLYEEHG-E
ASNS_ARATH  PASGDQPLFNEDK-TIVVTVNGEIYNHEELRKRLKN-HKFRTGSDCEVIAHLYEEYG-V
ASNS_BRAOL  PDSGDQPLFNEDK-SIVVTVNGEIYNHEELRKGLKN-HKFHTGSDCDVIAHLYEEHG-E
ASNS_MAIZE  PTSGDQPLYNEDK-TVVVTVNGEIYNHEELKAKLKT-HEFQTGSDCEVIAHLYEEYG-E
ASNS_ORYSA  PTSGDQPLYNEDK-SVVVTVNGEIYNHEELKANLKS-HKFQTASDCEVIAHLYEEYG-E
ASNB_ECOLI  VNAGAQPLYNQQK-THVLAVNGEIYNHQALRAEYGDRYQFQTGSDCEVILALYQEKG-P

ASNS_MESAU  QTICMLDGVFAFILLDTANKKVFLGRDTYGVRPLFKAMTEDGFLAVCSEAKGLVSLK
ASNS_MOUSE  KTICMLDGVFAFILLDTANKKVFLGRDTYGVRPLFKAMTEDGFLAVCSEAKGLVSLK
ASNS_RAT    KTICMLDGVFAFILLDTANKKVFLGRDTYGVRPLFKALTEDGFLAVCSEAKGLVSLK
ASNS_HUMAN  QTICMLDGVFAFVLLDTANKKVFLGRDTYGVRPLFKAMTEDGFLAVCSEAKGLVTLK
ASNS_SANAU  SFIHMLDGIFSFVLLDSRNNSFVAARDAIGVTPLYIGWGLDGSVWISSEMKGLN---
ASNS_TRIVS  NFVEMLDGMFSFVLLDSRDNTFIAARDAFGITSLYIGWGLDGSVWISSELKGLH---
ASN2_LOTJA  NFVDMLDGIFSFVLLDTRDNSFLVARDAIGVTSLYIGYGLDGSVWIASELKGLN---
ASN1_PEA    NFVDMLDGIFSFVLLDTRDNSFIVARDAIGVTSLYIGWGLDGSVWIASELKGLN---
ASN2_PEA    DFVDMLDGIFSFVPLDTRDNSYIVARDAIGVTSLYIGWGLDGSVWISSEMKGLN---
ASN1_LOTJA  NFMDMLDGIFSFVLLDTRDNTFIVARDAIGVTSLYIGWGLDGSVWISSEMKGLN---
ASNS_ARATH  DFVDMLDGIFSFVLLDTRDNSFMVARDAIGVTSLYIGWGLDGSVWISSEMKGLN---
ASNS_BRAOL  NFVDMLDGIFSFVLLDTRDNSFMVARDAVGVTSLYIGWGLDGSLWVSSEMKGLH---
ASNS_MAIZE  EFVDMLDGMFSFVLLDTRDKSFIAARDAIGICPLYMGWGLDGSVWFSSEMKALS---
ASNS_ORYSA  EFVDMLDGMFAFVLLDTRDKSFIAARDAIGICPLYMGWGLDGSVWFSESMKALS---
ASNB_ECOLI  EFLDDLQGMFAFALYDSEKDAYLIGRDHLGIIPLYMGYDEHGQLYVASEMKALV---
```

```
ASNS_MESAU  HSTTPFLKVEPFLPGHYEVLDLKPNGKVASVEMVKYHHCRDEPLHALYDSVEKLFP
ASNS_MOUSE  HSTTPFLKVEPFLPGHYEVLDLKPNGKVASVEMVKYHHCTDEPLHAIYDSVEKLFP
ASNS_RAT    HSTTPFLKVEPFLPGHYEVLDLKPNGKVASVEMVKYHHCTDEPLHAIYDSVEKLFP
ASNS_HUMAN  HSATPFLKVEPFLPGHYEVLDLKPNGKVASVEMVKYHHCRDVPLHALYDNVEKLFP
ASNS_SANAU  ---DDCEHFKFFPPGHLYSSKEGS-----------FKRWYNPPWFSEV------IP
ASNS_TRIVS  ---DECENFEVFPPGHVYSSKTEG-----------FRRWYNPPWFSEA------IP
ASN2_LOTJA  ---DDCEHFELFPPGHLYSSKEKE-----------FRRWYNPPWFSEA------IP
ASN1_PEA    ---DECEHFEVFPPGHLYSSKERE-----------FRRWYNPPWFNEAI-----IP
ASN2_PEA    ---DDCEHFECFPPGHLYSSKDSG-----------FRRWYNPSWYSEA------IP
ASN1_LOTJA  ---DDCEHFEVFPPGHLYSSRERA-----------FRRWYNPTWFSES------IP
ASNS_ARATH  ---DDCEHFETFPPGHFYSSKLGG-----------FKQWYNPPWFNES------VP
ASNS_BRAOL  ---EDCEHFEAFPPGHLYSSKSGGG----------FKQWYNPPWFNES------VP
ASNS_MAIZE  ---DDCERFITFPPGHLYSSKTGG-----------LRRWYNPPWFSET------VP
ASNS_ORYSA  ---DDCERFISFPPGHLYSSKTGG-----------LRRWYNPPWFSES------IP
ASNB_ECOLI  ---PVCRTIKEFPAGSYLWSQDGE-----------IRSYYHRDWFDYDA-----VK

ASNS_MESAU  GFELETVKSNLRILFDNAVRKRLMTDRRIVCLLSGGLDSSLVASSL----LKQLKEAQV
ASNS_MOUSE  GFDLETVKNNLRILFDNAIKKRLMTDRRIGCLLSGGLDSSLVAASL----LKQLKEAQV
ASNS_RAT    GFEIETVKNNLRILFNNAIKKRLMTDRRIGCLLSGGLDSSLVAASL----LKQLKEAQV
ASNS_HUMAN  GFEIETVKNNLRILFNNAVKKRLMTDRRIGCLLSGGLDSSLVAATL----LKQLKEAQV
ASNS_SANAU  SVPFDPLA--LRKAFEDAVIKRLMTDVPFGVLLSGGLDSSLVASVT----ARYLEGTKA
ASNS_TRIVS  STPYDPLV--LRGAFEQAVIKRLMTDVPFGVLLSGGLDSSLVAAVT----ARHLAGTKA
ASN2_LOTJA  SAPYDPLA--LRQAFEKAIIKRLMTDVPFGVLLSGGLDSSLVASVT----ARYLADTKA
ASN1_PEA    STPYDPLV--LRNAFEKAVIKRLMTDVPFGVLLSGGLDSSLVASVT----ARYLAGTKA
ASN2_PEA    SAPYDPLA--LRHAFEKAVVKRLMTDVPFGVLLSGGLDSSLVASIT----SRYLATTKA
ASN1_LOTJA  SAPYDPLA--VRHAFEKAVIKRLMTDVPFGVLLSGGLDSSLVASIT----SRYLATTKA
ASNS_ARATH  STPYEPLA--IRRAFENAVIKRLMTDVPFGVLLSGGLDSSLVASIT----ARHLAGTKA
ASNS_BRAOL  STPYEPLA--IRSAFEDAVIKRLMTDVPFGVLLSGGLDSSLVASIT----ARHLAGTKA
ASNS_MAIZE  STPYNALF--LREMFEKAVIKRLMTDVPFGVLLSGGLDSSLVASVA----SRHLNETKV
ASNS_ORYSA  STPYNPLL--LRQSFEKAIIKRLMTDVPFGVLLSGGLDSSLVASVV----SRHLAEAKV
ASNB_ECOLI  DNVTDKNE--LRQALEDSVKSHLMSDVPYGVLLSGGLDSSIISAITKKYAARRVEDQER

ASNS_MESAU  Q----YPLQTFAIGMEDSPDLLAARKVANYIGSEHHEVLFNSEEGIQALDEVIFSLETY
ASNS_MOUSE  Q----YPLQTFAIGMEDSPDLLAARKVANYIGSEHHEVLFNSEEGIQALDEVIFSLETY
ASNS_RAT    P----YALQTFAIGMEDSPDLLAARKVANYIGSEHHEVLFNSEEGIQSLDEVIFPLETY
ASNS_HUMAN  Q----YPLQTFAIGMEDSPDLLAARKVADHIGSEHYEVLFNSEEGIQALDEVIFSLETY
ASNS_SANAU  AELWGTQLHSFCVGLEGSPDLKAAKEVANFLGTIHHEFHFTVQDGIADIEDVIYHVETY
ASNS_TRIVS  AKRWGSQLHSFCVGLEGSPDLKAGKEVADYLGTVHHEFLFTVQDGIADIEDVIYHIETY
ASN2_LOTJA  AKQWGSKLHSFCVGLEGAPDLKAARERVADYIGTVHHEFQYTIQDGIADIEDVIYHVETY
ASN1_PEA    AKQWGAKLPSFCVGLKGAPDLKAGKEVADFLGTVHHEFEFTIQDGIADEDVIYHTETY
ASN2_PEA    AEQWGSKLHSFCVGLEGSPDLKAGKEVADYLGTVHHEFTFTVQDGIADIEDVIYHVETY
ASN1_LOTJA  AEQWGSKLHSFCVGLEGSPDLKAAKEVADYLGTVHHEFTFTVQDGIADIEEVIYHVETY
ASNS_ARATH  AKQWGPQLHSFCVGLEGSPDLKAGKEVAEYLGTVHHEFHFSVQDGIADIEDVIYHVETY
ASNS_BRAOL  AKRWGPQLHSFCVGLEGSPDLKAGKEVAEYLGTVHHEFHFTVQDGIADIEDVIYHVETY
ASNS_MAIZE  DRQWGNKLHTFCIGLKGSPDLKAARERVADYLSTVHHEFHFTVQEGIADLEEVIYHIETY
ASNS_ORYSA  AAQWGNKLHTFCIGLKGSPDLRAAKEVADYLGTVHHELHFTVQEGIADLEEVIYHVETY
ASNB_ECOLI  SEAWWPQLHSFAVGLPGSPDLKAAQEVANHLGTVHHEIHFTVQEGLDAIRDVIYHIETY

ASNS_MESAU  DITTVRASVGMYLISKYIRKNTDSVVIFSGEGSDELTQGYIYFHKAPSPEKAEEESERL
ASNS_MOUSE  DITTVRASVGMYLISKYIRKNTDSVVIFSGEGSDELTQGYIYFHKAPSPEKAEEESERL
ASNS_RAT    DITTVRASVGMYLISKYIRKNTDSVVIFSGEGSDELTQGYIYFHKAPSPEKAEEESERL
ASNS_HUMAN  DITTVRASVGMYLISKYIRKNTDSVVIFSGEGSDELTQGYIYFHKAPSPEKAEEESERL
ASNS_SANAU  DVTTIRASTPMFLMSRKIKS-LGVKMVISGEGSDEIFGGYLYFHKAPNKEELHLETCHK
ASNS_TRIVS  DVTTIRASTPMFLMSRKIKS-LGVKMVISGEGSDEIFGGYLYFHKAPNKEEFHRETCRK
ASN2_LOTJA  DVTTIRAGTPMFLMSRKIKS-LGVKMVLSGEGSDEIFAGYLYFHKAPNKEELHQETCSK
```

```
ASN1_PEA    DVTTIRAATPMFLMSRKIKS-SGVKWVISGEGSDEIFGGYLYFHKAPNREEFHQETCRK
ASN2_PEA    DVTSIRASTPMFLMSRKIKS-LGVKWVISGEGSDEIFGGYLYFHKAPNKEEFHEETCRK
ASN1_LOTJA  DVTTIRASTPMFLMSRKIKS-LGVKWVISGEGSDEIFGGYLYFHKAPNKEEFHETETCRK
ASNS_ARATH  DVTTIRASTPMFLMSRKIKS-LGVKMVLSGEGADEIFGGYLYFHKAPNKKEFHQETCRK
ASNS_BRAOL  DVTTIRASTPMFLMSRKIKS-LGVKMVLSGEGSDEIFGGYLYFHKAPNKQEFHQETCRK
ASNS_MAIZE  DVTTIRASTPMFLMSRKIKS-LGVKMVISGEGSDEIFGGYLYFHKAPNKKEFLEETCRK
ASNS_ORYSA  DVTTIRASTPMFLMSRKIKS-LGVKMVLSGEGSDEIFGGYLYFHKAPNKKEFHEETCRK
ASNB_ECOLI  DVTTIRASTPMYLMSRKIKA-MGIKMVLSGEGSDEVFGGYLYFHKAPNAKELHEETVRK

ASNS_MESAU  LKELYLFDVLRADRTTAAHGLELRVPFLDHRFSSYYLSLPPEMRVPKN---GIEKHLL
ASNS_MOUSE  LKELYLFDVLRADRTTAAHGLELRVPFLDHRFSSYYLSLPPDMRIPKN---GIEKHLL
ASNS_RAT    LKELYLFDVLRADRTTAAHGLELRVPFLDHRFSSYYLSLPPEMRIPKD---GIEKHLL
ASNS_HUMAN  IRELYLFDVLRADRTTAAHGLELRVPFLDHRFSSYYLSLPPEMRIPKN---GIEKHLL
ASNS_SANAU  IKALHQYDCLRANKATSAWGLEARVPFLDKEFVNVAMSIDPEWKMIKPDIGRIEKWIL
ASNS_TRIVS  IKALHQYDCLRANKATSAWGLEARVPFLDKEFVNLAMSIDPEAKMIKPDQGRIEKWIL
ASN2_LOTJA  IKALHKYDCLRANKSTYAWGLEARVPFLDKKFIDVAMGIDPENKMIKRDEGRIEKWVL
ASN1_PEA    IKALHRYDCLRANKSTYAWGLEARVPFLDKDFIKVAMDIDPEFKMIKHDEGRIEKWIL
ASN2_PEA    IKALHQYDCQRANKSTYAWGLEARVPFLDKAFINVAMNIDPENKMIKRDEGRIEKYIL
ASN1_LOTJA  IKALHQYDCLRANKSTFAWGLEARVPFLDKEFINVAMNIDPEYKMIKRDEGRIEKYIL
ASNS_ARATH  IKALHKYDCLRANKSTSAFGLEARVPFLDKDFINTAMSLDPESKMIKPEEGRIEKWVL
ASNS_BRAOL  IKALHKYDCLRANKATSAFGLEARVPFLDKEFINTAMSLDPESKMIKPEEGRIEKWVL
ASNS_MAIZE  IKALHLYDCLRANKATSAWGVEARVPFLDKSFISVAMDIDPEWNMIKRDLGRIEKWVM
ASNS_ORYSA  IKALHLYDCLRANKSTSAWGVEARVPFLDKNFINVAMDIDPEWKMIKRDLGRIEKWVL
ASNB_ECOLI  LLALHMYDCARANKAMSAWGVEARVPFLDKKFLDVAMRINPQDKMCGN--GKMEKHIL

ASNS_MESAU  RETFEDSN--LLPKEILWRPKEAFSDGITSVKNSWFKILQDYVEHQVDDAMMATAAQKF
ASNS_MOUSE  RETFEDCN--LLPKEILWRPKEAFSDGITSVKNSWFKILQDYVEHQVDDEMMSAASQKF
ASNS_RAT    RETFEDSN--LLPKEILWRPKEAFSDGITSVKNSWFKILQDFVEYQVDDAMMSEASQKF
ASNS_HUMAN  RETFEDSN--LIPKEILWRPKEAFSDGITSVKNSWFKILQEYVEHQVDDAMMANAAQKF
ASNS_SANAU  RRAFDDEENPYLPKHILYRQKEQFSDGVG---YSWIDGLKAHSALHVTDKMMLNAAHIY
ASNS_TRIVS  RKAFDDEERPYLPKHILYRQKEQFSDGVG---YSWIDGLKAHAEQHVTDKMMLNAGHIF
ASN2_LOTJA  RKAFDDEENPYLPKHILYRQKEQFSDGVG---YGWIDGLKDHAAKHVTDKMMLNASNIY
ASN1_PEA    RKAFDDEENPYLPKHILYRQKEQFSDGVG---YGWIDGIKDHAAKHVTDRMMFNASHIF
ASN2_PEA    RKAFDDEENPYLPKHILYRQKEQFSDGVG---YSWIDGLKDHAAKHVTDKMMLNAGNIF
ASN1_LOTJA  RRAFDDEEKPYLPKHILYRQKEQFSDGVG---YSWIDGLKDHAAKHVTDKMILNAGNIF
ASNS_ARATH  RRAFDDEERPYLPKHILYRQKEQFSDGVG---YSWIDGLKDHAAQNVNDKMMSNAGHIF
ASNS_BRAOL  RRAFDDEERPYLPKHILYRQKEQFSDGVG---YSWIDGLKAHAAENVNDKMMSKAAFIF
ASNS_MAIZE  RKAFDDDEHPYLPKHILYRQKEQFSDGVG---YNWIDGLKSFTEQQVTDEMMNNAAQMF
ASNS_ORYSA  RNAFDDEEKPYLPKHILYRQKEQFSDGVG---YSWIDGLKDHANEHVSDSMMMNASFVY
ASNB_ECOLI  RECFEA----YLPASVAWRQKEQFSDGVG---YSWIDTLKEVAAQQVSDQQLETARFRF

ASNS_MESAU  PFNTPKTKEGYFYRQIFEHHYPGRADWLT----------------HYWMPKWINATDP
ASNS_MOUSE  PFNTPKTKEGYFYRQIFERHYPGRADWLT----------------HYWMPKWINATDP
ASNS_RAT    PFNTPQTKEGYYYRQIFEHHYPGRADWLT----------------HYWMPKWINATDP
ASNS_HUMAN  PFNTPKTKEGYYYRQVFERHYPGRADWLS----------------HYWMPKWINATDP
ASNS_SANAU  PHNTPTTKEAYYYRMIFERFFPQ-----------------------IDSPWRSKCG-
ASNS_TRIVS  PHNTPTTKEGYYYRMIFERFFPQNSAKLTVPGGPSVACSTAT--AVAWDASWSKNLDP
ASN2_LOTJA  PFNTPNTKEAYYYRMIFERFFPQNSARLSVPGGASIACSTEK--AIEWDAAWSNNLDP
ASN1_PEA    PFNTPNTKEAYYYRMIFERFFPQNSARLTVPGGPSVACSTEK--AIEWDASWSNNLDP
ASN2_PEA    PHNTPNTKEAYYYRMIFERFFPQNSARLTVPGGPTVACSTAK--AVEWDAAWSNNLDP
ASN1_LOTJA  RHNTPLTKEAYYYRMIFERFFPQNSARLTVPGGPTVACSTAK--AVEWDAAWSNNLDP
ASNS_ARATH  PHNTPNTKEAYYYRMIFERFFPQNSARLTVPGGATVACSTAK--AVEWDASWSNNMDP
ASNS_BRAOL  PHNTPLTKEAYYYRMIFERFFPQNSARLTVPGGATVACSTAK--AVEWDASWSNNMDP
ASNS_MAIZE  PYNTPVNKEAYYYRMIFERLFPQDSARETVPWGPSIACSTPA--AIEWVEQWKASNDP
ASNS_ORYSA  PENTPVTKEAYYYRTIFEKFFPKNAARLTVPGGPSVACSTAK--AVEWDAAWSKNLDP
ASNB_ECOLI  PYNTPTSKEAYLYREIFELFPLPSAAECVPGGPSVACSSAK--AIEWDEAFKKMDDP
```

```
ASNS_MESAU  SARTLTHYKSAAKA---------------------------------- 560
ASNS_MOUSE  SARTLTHYKSAAKA---------------------------------- 560
ASNS_RAT    SARTLTHYKSTAKA---------------------------------- 560
ASNS_HUMAN  SARTLTHYKSAVKA---------------------------------- 560
ASNS_SANAU  ------LQHSKSY----------------------------------- 524
ASNS_TRIVS  SGRAATGVHDLAYEN-HVPIGNLKSKKMDSVSLGNAVGPQELTIRS---- 585
ASN2_LOTJA  SGRAALGVHDSAYDD-QLNKSVSKGVEPEKIIPKMEVSPLGVAILS---- 585
ASN1_PEA    SGRAALGVHVSAYEH-QIN-PVTKGVEPEKIIPKIGVSPLGVAIQT---- 585
ASN2_PEA    SGRAALGVHDSAYEN--HNKVN-KTVEFEKIIP-LEAAPVELAIQG---- 582
ASN1_LOTJA  SGRAALGVHLSAYDDKQNNLINNKPVEFEKLIP-MEAPSLGVAIHS---- 585
ASNS_ARATH  SGRAAIGVHLSAYDG--KNVALTIP-PLKAIDNMPMMMGQGVVIQS---- 583
ASNS_BRAOL  SGRAAIGVHLSAYDG--SKVALPLPAPHKAIDDIPMMMGQEVVIQT---- 585
ASNS_MAIZE  SGR-FISSHDSAATDHTAVSRRWPTAAAR----PANGTVNGKDVPVPIAV 585
ASNS_ORYSA  SGRAALGVHDAAYEDTLQKSPASANPVLDNGFGPALGESMVKTVASATAV 590
ASNB_ECOLI  SGR-AVGVHQSAYK---------------------------------- 553
```

Figure 5-6 Sequence alignment of asparagine synthetases.

The results of the CHARMM computational experiments yields information about preferred binding models complexed with AMP and ATP/Asp with and without solvent. The structures were visualized in SYBYL and hydrogen bonds in the active site were viewed.

In the complex of AMP and *E. coli* asparagine synthetase B (Figure 5-7), there are still two specific electrostatic interactions between N1 and N6 of the purine ring and the backbone carbonyl and amino groups of Val272. In addition, there is one more hydrogen bond between N6 of the purine ring and the carboxyl side chain of Asp279. Both Asp279 and Val272 are located within about 4 Å of AMP in the crystal structure. The 2'-hydroxyl group of the ribose is hydrogen-bonded with the N of Glu347 and the O^{γ} of Ser346. The hydrogen-bond between the 2'-OH group and the backbone carbonyl group of Leu232 which has been seen in the crystal structure was not found in this model. This residue moved slightly away from the 2'-OH in the model. There is another hydrogen-bond between the ribose moiety and the enzyme: the N of Gly347 and the 3'-hydroxyl group. The side chain of Lys449 interacted with one phosphate oxygen via a hydrogen-bond.

This interaction was not seen in the crystal structure. Lys449 is a completely conserved residue in the asparagine synthetase family. From the sequence alignment of β-lactam synthetase and asparagine synthetase, Lys449 of AS-B corresponds to Lys443 of β-LS, which is hydrogen-bonding with the phosphate oxygen of AMP-PCP. It is very likely that this residue participates in substrate binding. The Mg^{2+} is coordinated with two phosphate oxygens and one side chain oxygen each from Asp238 and Asp351.

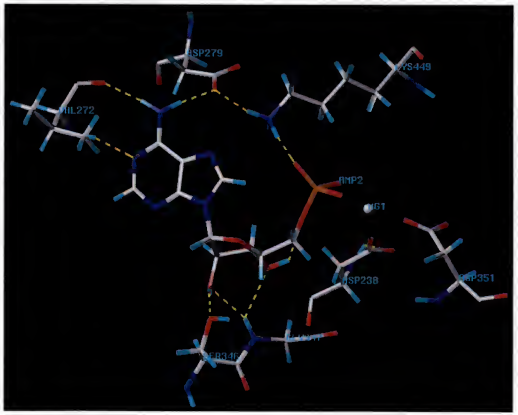

Figure 5-7 AMP binding model in *E. coli* asparagine synthetase B. Dotted lines in yellow denote hydrogen-bond interactions.

In the solvation model, the AMP binding site is very similar to that of the model without solvation. There are the same hydrogen-bonds between the enzyme and the AMP ligand. The only big difference is that there is no hydrogen-bond between the side chain

of Asp279 and the side chain of Lys449 as seen in the model without solvation, which forces the phosphate and the adenine moieties into closer proximaty. Residue Lys449 moves slightly away from Asp279 in the solvation model.

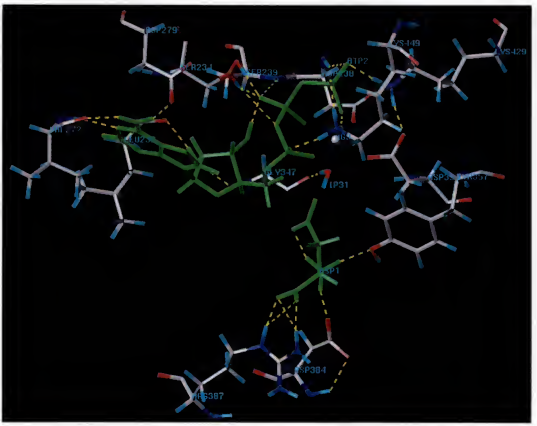

Figure 5-8 ATP/Asp binding model in *E. coli* AS-B. The structures of ATP and Asp are depicted in green. Dotted lines denote hydrogen-bond interactions between the enzyme and the substrates.

In the model of the ATP and asparate complex, the ligands are binding with the enzyme by many electrostatic interactions (Figure 5-8). There are three electrostatic interactions between the purine ring of ATP and the protein: two from backbone of Val272 and one from side chain of Asp279. The 2'-hydroxyl group hydrogen-bonds to the backbone carbonyl group of Leu232 and the backbone amide group of Gly347. The

3'-hydroxyl group hydrogen-bonds with one β-phosphate oxygen. The phosphate moiety interacts with several hydrophilic residues. The α-phosphate oxygen hydrogen-bonds with the side chain of Lys449. One β-phosphate oxygen is hydrogen bonded to the O^{γ} each from Ser234 and Ser239 and the N of Ser239. The γ-phosphate oxygens make hydrogen bonds with the side chains of Lys449 and Lys429, and backbone amide group of Asp238. The Mg^{2+} ion is coordinated by one side chain oxygen each from Asp238 and Asp351, by α-, β- and γ-phosphate oxygens, and by a water molecule in a well-organized octahedral geometry. The distance between the Mg^{2+} ion and these coordinated oxygens is about 1.9 Å. The water molecule is also hydrogen-bonded with the backbone carbonyl group of Gly347.

The backbone carbonyl and amide groups of asparate are situated between the positive charged residue Arg387 and negatively charged residue Asp384. The carboxyl group of aspartate is hydrogen bonded to the side chain of Arg387, while the amino group of aspartate is linked to the side chain of Asp384. There is another hydrogen-bond interaction between the amino group of aspartate and the side chain of Tyr357.

The solvation model of the ATP/Asp complex is slightly different (Figure 5-9). The binding site is loosened by the solvent effect. The binding of the adenine moiety is the same as before, with interaction with Val272 and Asp279. The ribose moiety makes only one hydrogen bond with the enzyme at Gly347. The interaction with Leu232 is missing. The phosphate oxygens still interact with residues Ser234, Ser239, Lys449, Lys429 and Asp238. The Mg^{2+} ion has the same coordination. The binding of aspartate is not as rigid as in the case without solvation, though there are still two hydrogen bonds between the carboxyl and amino groups of aspartate and the side chains of Arg387 and Asp384.

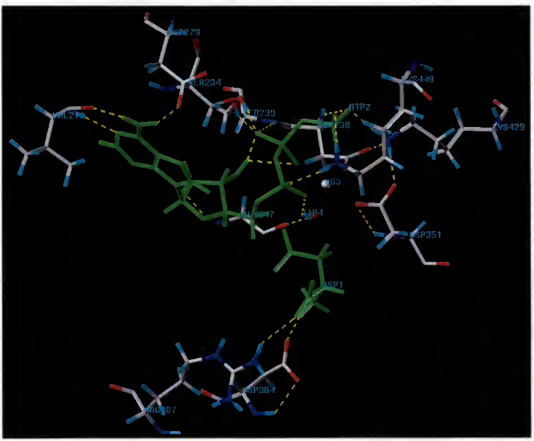

Figure 5-9 ATP/Asp binding model with solvation in *E. coli* AS-B. The structures of ATP and Asp are depicted in green. Dotted lines denote hydrogen-bond interactions between the enzyme and the substrates.

In the crystal structure of *E. coli* AS-B, there are two water molecules in the AMP binding site. Both of them bind uranium ions, which are also interacting with phosphoryl oxygens. In the crystal structure of β-lactam synthetase, one water molecule is coordinated with a Mg^{2+} ion. Since the ATP analogue complexed in the structure is stable to hydrolysis, it is possible that the water molecule can exist in the crystal structure. However, whether the water molecule really situates in the active site of AS-B and coordinates with Mg^{2+} is still a question. Crystallographic studies have revealed in many cases that Mg^{2+} is bound to enzymes or substrates in part through water-mediated

interactions.[264] The first-order rate of exchange of Mg^{2+} with water is of the order of 10^5 s^{-1}, which compares with 10^8 s^{-1} for Ca^{2+} and 3×10^7 s^{-1} for Mn^{2+}.[265] The slower exchange rate of Mg^{2+} with water has direct implications for its role in enzymatic catalysis. The study of metal-ligand interactions in relevant small molecules has shown Mg^{2+} to always have six coordinating oxygen ligands.[266] We modeled the complex of ATP/Asp and enzyme without water molecular to see whether there is any residue that might coordinate with Mg^{2+}. It turned out that the binding of ATP and Asp is very similar to that of the structure with the water molecule (Figure 5-10). The only big difference is the coordination of Mg^{2+}, which changed from six-coordination to five-coordination. No more residues in the active site can possibly coordinate with Mg^{2+}. Hence, it is very possible that the water molecule just participates in the coordination with Mg^{2+}, and it leaves with pyrophosphate after aspartate attacks ATP. It is less likely that it will react with ATP or the β-AspAMP intermediate.

In the model of the aspartyladenylate and pyrophosphate complex (Figure 5-11), the binding of the ligands is very similar to that of ATP and aspartate complex. The binding of the adenine moiety is the same as before, with interactions with Val272 and Asp279. There are two hydrogen bonds between the 2'-OH of ribose ring and the backbones of Leu232 and Gly347. The carboxyl and amino groups of aspartate are hydrogen bonded to the side chains of Arg387, Asp384 and Tyr357. Pyrophosphate is stabilized by hydrogen-bonding with the side chains of Ser234, Ser239, Lys429 and Lys449, and by coordinating with the Mg^{2+} ion. The Mg^{2+} ion is coordinated by the side chain carboxylate groups of Asp238 and Asp351, a water molecule and the phosphoryl

oxygen of aspartyladenylate as well. The solvation model of aspartyladenylate and pyrophosphate complex is very similar.

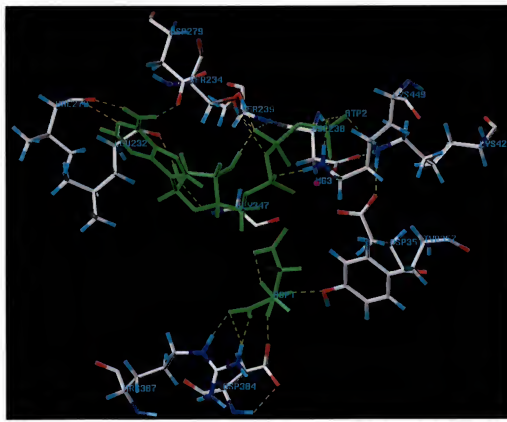

Figure 5-10 ATP/Asp binding model in *E. coli* AS-B without H_2O molecule in the active site. The structures of ATP and Asp are depicted in green. Dotted lines denote hydrogen-bond interactions between the enzyme and the substrates.

The oxygen of the mixed anhydride bond is not recognized by the enzyme. We expect that the replacement of oxygen with an NH group will not affect its binding with the enzyme. The inhibitor L-asparaginyladenylate should have very similar interactions with the enzyme as aspartyladenylate, which would explain its inhibition of the enzyme. D-asparaginyladenylate should not have interactions between its amino acid moiety and

the residues, Asp284 and Arg387, which would explain its very low inhibition activity compared with L-asparaginyladenylate.

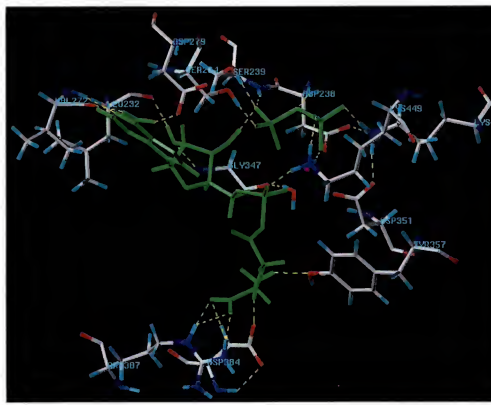

Figure 5-11 Aspartyladenylate and pyrophosphate binding model in *E. coli* AS-B. The structures of aspartyladenylate and pyrophosphate are depicted in green. Dotted lines denote hydrogen-bond interactions between the enzyme and the substrates.

Homology Modeling of Human AS

General scientific interest in human AS has been stimulated by the inverse correlation between the capacity for intracellular asparagine biosynthesis and the susceptibility of leukemia cells to drug therapy. The X-ray crystal structure of the human enzyme is not available yet. We wanted to use homology-based methods to model the

structure of human AS, and hence predict the binding of the substrates, intermediate and inhibitors.

Significant progress has been made in constructing structural models of soluble proteins using comparative, or homology, methods.[267,268] Given the high sequence identity between human and bacterial AS, it is likely that a reasonable model of the human enzyme can be built if its structure can not be solved by X-ray crystallography.

Experimental Procedures

The optimized structure of *E. coli* AS-B complexed with AMP, Gln and Mg^{2+} was used as the target. According to the sequence alignment, the loop segments of *E. coli* AS-B were deleted or replaced by cognate residues in human.[269,270] Conversely, loops of the human enzyme were inserted into the bacterial structure. Both of these operations were performed within Biopolymer module implemented in SYBYL 6.2 (Tripos Inc.) in which loops and side chain structures were obtained. Local minimization was performed using the MINIMIZE SUBSET command after the side chain had been added and fixed.

Constrained molecular dynamics (MD) in combination with simulated annealing algorithms,[271] followed by energy minimization, was used to refine the model. Key hydrogen bonds, that maintain core secondary structures and protein-ligand interactions, were maintained in these simulations by constraint potentials. All simulations were carried out in CHARMM using the CHARMM force field. The model was subjected to 5000 cycles of steepest descent followed by Adopted Basis Newton-Raphson algorithms until convergence of 0.01 kcal/mol ⊕ r.m.s deviation. No distance constraint was applied at this point. The minimized structure was further refined using the following simulated annealing protocal. The system with a 5.0 kcal/mol distance constraint applied to the

backbone hydrogen bonds was gradually heated to 600 K over a period of 12 ps with ΔT = 5 K every 0.1 ps, followed by 20 ps of equilibration at 600 K. Next, the structure was cooled to 300 K gradually with 3 additional 2 ps constant temperature simulations at 500 K, 400 K and 300 K. The constraints applied to the hydrogen bonds that maintain core secondary structure and protein ligand interactions were reduced gradually from 5 kcal/mol $\oplus^2$ to 2 kcal/mol $\oplus^2$ during the annealing process. The structure obtained at 300 K was further refined at 300 K by 4 additional 20 ps simulations with constraints of 1.5 kcal/mol $\oplus^2$, 1.0 kcal/mol $\oplus^2$, 0.5 kcal/mol $\oplus^2$ and zero. The refined structure obtained at 300 K was fully minimized with steepest descent and Adopted Basis Newton-Raphson algorithms.

Using AMP as a guide, ATP, Asp and a water molecule were built into the unrefined structure of the enzyme in SYBYL (version 6.2). They were manually docked in the synthetase active site. Using the same simulated annealing protocol, the structure was refined in CHARMM 25b2.

The molecular simulations and energy minimization were performed with the CHARMM 25b2 package using the param22 parameter set. Molecular dynamics were carried out using the Verlet leapfrog algorithm with a distance-dependent dielectric constant $\varepsilon = r$. Long-range electrostatic forces were cut off at 13 $\oplus$ by means of a shifting function, and van der Waals forces were cut off between 9 and 13 $\oplus$ by means of a switching function. The nonbonded list was kept to 14 $\oplus$ and updated every 10 steps. A step wise of 1 fs was used, and the velocities were scaled every 50 steps to keep the temperature within 10 degrees of 300 K during the equilibration. All bonds containing hydrogens were held rigid by the SHAKE algorithm.[272]

Results and Discussion

Sequence alignment of *E. coli* asparagine synthetase B and human asparagine synthetase is shown in Figure 5-12. The sequence identity is up to 37% for the whole sequence and 39% for the C-terminal domain. In the model of the ATP/Asp complex with *E. coli* AS-B, Leu232, Ser234, Asp238, Ser239, Val272, Gly347, Asp351, Tyr357, Asp384, Arg387, Lys429 and Lys449 are involved in the recognition of ATP and Asp. These residues are all highly conserved in the sequence alignment. In the human asparagine synthetase, they correspond to Leu255, Ser257, Asp261, Ser262, Ile287, Gly363, Asp367, Tyr373, Asp400 and Arg387, Lys444 and Lys466.

```
        1                                                    47
ecoli   CSIFGVFDIK TDAVELRKKA LELSRLMRHR GPDWSGIYAS DN...AILAH
human   CGIWALFG.S DDCLS..VQC LS.AMKIAHR GPDAFRFENV NGYTNCCFGF
        1                                                    46
        48                                                   96
ecoli   ERLSIVDVNA GAQPLYNQQK THV.LAVNGE IYNHQALRAE YGDRYQFQTG
human   HRLAVVDPLF GMQPIRVKKY PYLWLCYNGE IYNHKKMQQH F..EFEYQTK
        47                                                   94
        97                                                  145
ecoli   SDCEVILALY QEKGPEF.LD DLQGMFAFAL YDSEKDAYLI GRDHLGIIPL
human   VDGEIILHLY DKGGIEQTIC MLDGVFAFVL LDTANKKVFL GRDTYGVRPL
        95                                                  144
        146                                                 181
ecoli   YMGYDEHGQL YVASEMKALV .......PVC RTIKEFPAGS Y....L...W
human   FKAMTEDGFL AVCSEAKGLV TLKHSATPFL K.VEPFLPGH YEVLDLKPNG
        145                                                 193
        182                                                 220
ecoli   SQDGEIRSYY HRDWFD.... .YDAVK.... ..DNVTDKNE LRQALEDSVK
human   KVASVEMVKY HHCRDVPLHA LYDNVEKLFP GFEIETVKNN LRILFNNAVK
        194                                                 243
        221                                                 270
ecoli   SHLMSDVPYG VLLSGGLDSS IISAITKKYA ARRVEDQERS EAWWPQLHSF
human   KRLMTDRRIG CLLSGGLDSS LVAATLLKQL KEAQV..... ..QYP.LQTF
        244          * *   **                               285
        271                                                 320
ecoli   AVGLPGSPDL KAAQEVANHL GTVHHEIHFT VQEGLDAIRD VIYHIETYDV
human   AIGMEDSPDL LAARKVADHI GSEHYEVLFN SEEGIQALDE VIFSLETYDI
        286                                                 335
        321                                                 369
ecoli   TTIRASTPMY LMSRKI.KAM GIKMVLSGEG SDEVFGGYLY FHKAPNAKEL
human   TTVRASVGMY LISKYIRKNT DSVVIFSGEG SDELTQGYIY FHKAPSPEKA
        336                          *    *       *       385
```

```
       370                                                    419
ecoli  HEETVRKLLA LHMYDCARAN KAMSAWGVEA RVPFLDKKF LDVAMRINPQD
human  EEESERLLRE LYLFDVLRAD RTTAAHGLEL RVPFLDHRF SSYYLSLPPEM
       386            *  *                                   435
       420                                                    464
ecoli  KMCGNGKMEK HILRECFE.. AYLPASVAWR QKEQFSDG.. .VGYSWIDTL
human  RIPKNG.IEK HLLRETFEDS NLIPKEILWR PKEAFSDGIT SVKNSWFKIL
       436      *                  *                          484
       465                                                    513
ecoli  KEVAAQQVSD QQLETARFRF PYNTPTSKEA YLYREIFEEL FPLPSAAEC.
human  QEYVEHQVDD AMMANAAQKF PFNTPKTKEG YYYRQVFERH YPGRADWLSH
       485                                                    534
       514                                          553
ecoli  ..VPGGPSVA CSSAKAI.EW DEAFKKMDDP SGRAVGVHQ SAYK
human  YWMPKWINAT DPSARTLTHY KSAVKA~~~~~~~~ ~~~~~~~~~
       535                      560
```

Figure 5-12 Sequence alignment of *E. coli* AS-B and human AS. Residues that are conserved are highlighted in red. Residues that are similar are highlighted in blue. The residues involved in the substrates recognition in *E. coli* AS-B are marked star.

A 2D representation of human asparagine synthetase complexed with AMP, glutamine and Mg^{2+} is given in Figure 5-13. The N-terminal domain is composed mostly of antiparallel β-sheet structure, while the larger C-terminal domain is composed mostly of α-helices. Comparison of the structures of human AS and *E. coli* AS-B (Figure 5-13) showed that the two enzymes share secondary and tertiary structural features. In the AMP binding domain of human AS (Figure 5-14), the residues that recognize AMP and Mg^{2+} are very similar to that of *E. coli* enzyme. There are two specific electrostatic interactions between the purine ring of the nucleotide and the protein: the backbone carbonyl and amide groups of Ile287, corresponding to Val272 of *E. coli* AS-B, and N1 and N6 of the purine moiety. The hydrogen-bond between the N6 of the adenine ring and the side chain of Asp294 does not exist. This bond is found in *E. coli* AS-B. The 2'-hydroxyl group of the ribose moiety is linked to the protein via the backbone carbonyl group of Leu255, corresponding to Leu232 of *E. coli* AS-B. Gly363 does not hydrogen-bond with the 2'- or

3'-hydroxyl group, as Gly347 does in *E. coli* AS-B. But, this residue is in a very close position to the 2'- and 3'-OH. The side chain of Lys 466, like that of Lys 449 in *E. coli* AS-B, is hydrogen-bonding with one phosphoryl oxygen. The Mg^{2+} ion is coordinated with two phosphoryl oxygens and one side oxygen each from Asp261 and Asp367, corresponding to Asp238 and Asp351 in *E. coli* AS-B. Though the residues of human AS that participate in the binding of AMP are very similar to that of *E. coli* enzyme, the positions of some residues, such as Lys466 are slightly different.

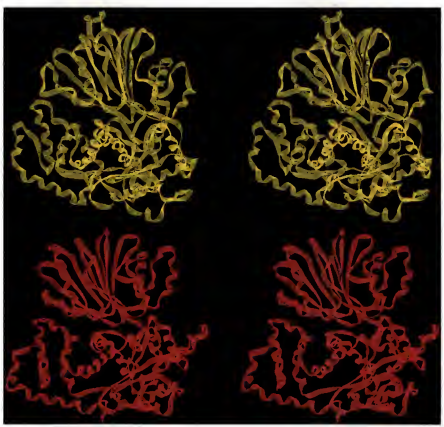

Figure 5-13 Stereo view of the modeled structure of human AS (in yellow) and the energy minimized structure of *E. coli* AS-B (in red).

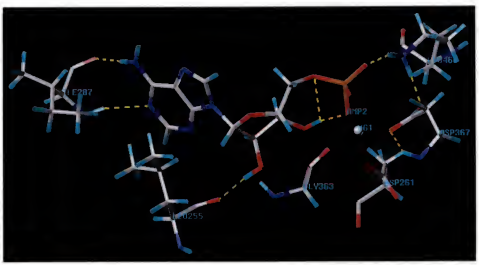

Figure 5-14 AMP binding model in human AS. Dotted lines in yellow denote possible hydrogen-bond interactions.

In the model of the ATP and Asp complex, the ligands bind to the enzyme through hydrogen-bonds (Figure 5-15). There are 2 electrostatic interactions between the purine ring of ATP and the protein: one occurs between the backbone carbonyl group of Ile287 and the amino group at position 6 of the adenine ring; the second occurs between the side chain of Asp294 and N6 of the purine moiety. In the *E. coli* AS-B complex, there is one more interaction between the backbone amide group of Val272 (corresponding to Ile287 in the human enzyme) and N1 of the purine moiety. The 2'-hydroxyl group hydrogen-bonds with the backbone carbonyl group of Leu255 and backbone amide group of Gly363, like that of Leu232 and Gly347 in *E. coli* AS-B. The 3'-hydroxyl group hydrogen-bonds with the backbone amide group of Gly363 also. In the *E. coli* AS-B complex, the 3'-hydroxyl group is hydrogen-bonding with one α-phosphoryl oxygen. The phosphate moiety interacts with several hydrophilic residues. One β-phosphoryl oxygen is hydrogen bonded to the O^{γ} of Ser262 and the N of Ser262. In *E. coli* AS-B, the β-phosphoryl oxygen also hydrogen-bonds with the O^{γ} of Ser234, which is Ser257 in the

human enzyme. The γ-phosphoryl oxygens make hydrogen bonds with the side chains of Lys449 and Lys429, and the N of Asp261, which are the same as those seen for the *E. coli* enzyme. The Mg^{2+} ion is coordinated by one side oxygen each from Asp261 and Asp367, (Asp238 and Asp351 in *E. coli* AS-B), by α-, β- and γ-phosphate oxygens, and by a water molecule in a well-organized octahedral geometry. The distance between the Mg^{2+} ion and these coordinated oxygens is about 1.9 Å. The water molecule is also hydrogen-bonding with the backbone carbonyl group of Gly363, like Gly347 in *E. coli* AS-B.

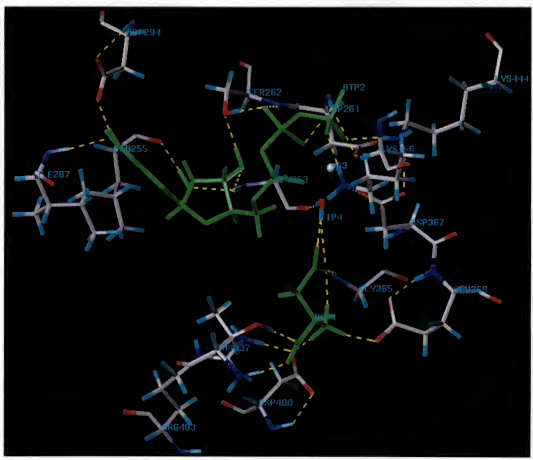

Figure 5-15 ATP/ASP binding model in human asparagines synthetase. The structures of ATP and Asp are depicted in green. Dotted lines denote hydrogen-bond interactions between the enzyme and the substrates.

Aspartate is recognized by the residues Arg403 and Asp400 in the human enzyme, corresponding to Arg387 and Asp384 in the *E. coli* enzyme. The carboxyl group of aspartate is hydrogen bonded to the side chain of Arg387, while the amino group of aspartate is linked to the side chain of Asp384. There are several other interactions between the enzyme and asparate that have not been seen in the *E. coli* AS-B complex. The side chain of Glu368 hydrogen-bonds with the amino group of aspartate. The backbone amide group of Gly365 hydrogen-bonds with the side chain carboxyl group of aspartate. The side chain of Thr337 hydrogen-bonds with the backbone carboxyl group of aspartate. All three of these residues, Gly365, Glu368 and Thr337 are completely conserved in the family of asparagine synthetases (Figure 5-6). In the *E. coli* AS-B complex, though they are not making hydrogen bonds with the aspartate substrate, they are very close to the substrate. They might participate in holding the enzyme in the right conformation. Tyr373, which hydrogen-bonds with aspartate in *E. coli* AS-B, is slightly moved away from aspartate. There are two hydrogen-bonds between the water molecule and the carboxyl side chain of aspartate, which have not been seen in *E. coli* AS-B.

If there was no water molecule in the synthetase active site of human asparagine synthetase, after molecular simulations and energy minimization, no residue was found coordinating with Mg^{2+} ion as a substitute of water.

Conclusion

The modeled structure of human asparagine synthetase shares secondary and tertiary structural features with bacterial asparagine synthetase B. In the synthetase domains of human AS and bacterial AS-B, the recognition of ATP and aspartate is very

similar, which means the active sites of these two enzymes have very similar electrostatic and steric properties. We anticipate β-asparaginyladenylate, the inhibitor of *E. coli* AS-B, will inhibit human AS as well.

CHAPTER 6
CONCLUSION AND FUTURE WORK

Molecular modeling of asparagine synthetase B indicates that the enzyme recognizes ATP and aspartate through the interactions between the purine ring and Val272, 2'-hydroxyl group of ribose and Gly347, Leu232, phosphoryl oxygens and Lys429, Lys449, Ser234, Ser239, aspartic acid and Asp384, Arg387. The Mg^{2+} ion is coordinated with two aspartate residues: Asp238 and Asp351. These residues are highly conserved in the asparagine synthetase family. The unreacted substrates in the synthetase active site are bound in a geometry that favors the adenylation reaction catalyzed by this enzyme.

We proposed, as the reaction progresses, the side carboxylate of aspartate attacks the α-phosphate of ATP. Pyrophosphate will leave with Mg^{2+}, and the negative charges on the pyrophosphate moiety are stabilized through the cation and two serine residues bound with β-phosphoryl oxygen. Very similar to the arginine, histidine and serine residue in class II aminoacy-tRNA synthetase, Lys429 and Lys449, together with Ser234 and Ser239, stabilize the pyrophosphate group and help the leaving of pyrophosphate. The formed intermediate is recognized by the enzyme through the interaction between Val272 and purine ring, between Asp384, Arg387 and amino acid moiety. The oxygen atom of the mixed anhydride bond is not recognized by the enzyme. Therefore, the substitution of this unrecognizable atom with nitrogen will not affect the enzyme recognition ability and L-conformation of β-asparaginyladenylate shows high inhibition

activity. The D-conformation of β-asparaginyladenylate has 200-fold less activity, presumably because its amino acid moiety fails to bind to the residues of Asp384 and Arg387. The binding is thus greatly lessened, compared to L-conformation compound.

The results of molecular modeling indicate Asp384 and Arg387 are important residues in the binding of the substrates and intermediate. To prove this hypothesis, the efforts will be made to co-crystallize the enzyme and β-asparaginyladenylate complex, which will give the information about the binding of the inhibitor. These two residues can be mutated to Asp384Asn, Arg387Ala. The enzyme mutants may exhibit diminished, or no detectable synthetase activity but retain their function as glutaminases. This work is still under progress in our group. Further mutation on Lys429, Lsy449, and Ser239 can be conducted. These residues are proposed to bind with ATP and pyrophosphate and help the leaving of pyrophosphate. Without these residues, the rate of the reaction might be slowed down, or the enzyme may lose the activity. These are the work that can be done in the future.

Another avenue for future work on asparagine synthetase is to design, synthesize and characterize more novel β-aspartyladenylate analogues as inhibitors of asparagine synthetase. Figure 6-1 lists the compounds that can be designed as the analogues of β-aspartyladenylate. First, the amino acid moiety will be modified. β-carboxyl proline **23** was proved to be an inhibitor of AS-B. Hence, proline is chosen to mimic the aspartyl moiety of the intermediate. In compound **83** (Figure 6-1), the phosphonate linker can be either 5'-N-, or 5'-O-sulfamoyl linkage. The carboxylate group of the proline moiety will be replaced with different functionality such as amide, ester, and hydroxamate. Second, the adenosine part will be modified. Replacement of the adenine ring with a variety of

heterocycles has been seen in the inhibitors of aminoacyl-tRNA synthetase. Thiazole derivatives and tetrazole derivatives will be introduced as the substituent of the adenine ring (**84** and **85**). Also, the adenine ring can be replaced with vanilloid, isovanilloid or nitrophenyl derivative (**86**).

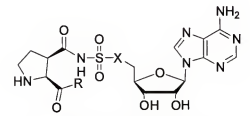

83 X = NH, O
R = OH, NH_2, OCH_3, NHOH

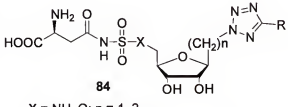

84
X = NH, O; n = 1, 2
R = amino, alkyl, aryl, cycloalkyl, alkoxy and aryloxy

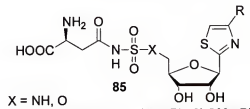

85
X = NH, O
R: 4'-cyano-furanyl, 2'-OMe-Ph, 3'-OMe-Ph, PhOPh, 4'-OMe-Ph, 6'-OMe-2-naphthyl, CH_2CH_2Ph

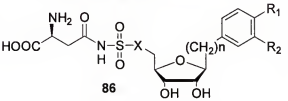

86
X = NH, O; n = 0, 1;
R_1, R_2 = OH, OMe or H, NO_2

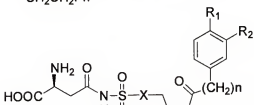

87 X = NH, O; n = 0, 1
R_1, R_2 = OH, OMe, or H, NO_2
R_3 = H, OH

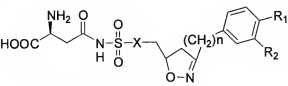

88 X = NH, O; n = 0, 1
R_1, R_2 = OH, OMe, or H, NO_2

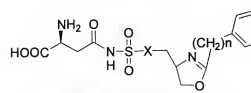

89 X = NH, O; n = 0, 1
R_1, R_2 = OH, OMe, or H, NO_2

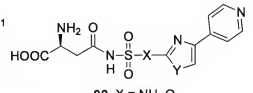

90 X = NH, O
Y = NH, S

Figure 6-1 Structures of some β-aspartyladenylate analogues.

The ribose can be substituted by its biosteres, such as acyclic amide and hydroxamate (**87**), dihydroisooxazole (**88**) and dihydrooxazole (**89**). These ribose surrogates have been successfully utilized for pharmacologically active adenylates in drug design.[131] The adenine moiety can be vanilloid, isovanilloid, nitrophenyl derivatives, thiazole derivatives, tetrazole derivatives, or adenine itself.

Another variety of β-aspartyladenylate analogue is imidazole pyridine and thiazole pyridine derivative (**90**). Imidazole pyridine and thiazole pyridine have been utilized to replace the adenosine moiety in the drug design.

Separate modifications on the adenosine moiety and amino acid moiety provide the substituents for adenosine and amino acid. The compounds that contain both of these two substituent moieties that are linked by sulfomyl linkage are expected to have good inhibition activity against the enzyme. These compounds lacking the charged amino and carboxylate groups should be able to enter cells more easily than β-asparaginyladenylate. They are more drug-like. These SARs and libraries will enable the development of small molecules able to function as potent, specific inhibitors of asparagine synthetase.

REFERENCES

(1) Cooney, D. A.; Handschu.Re *Annual Review of Pharmacology* **1970**, *10*, 421-&.

(2) Swain, A. L.; Jaskolski, M.; Housset, D.; Rao, J. K. M.; Wlodawer, A. *Proceedings of the National Academy of Sciences of the United States of America* **1993**, *90*, 1474-1478.

(3) Broome, J. D. *Journal of Experimental Medicine* **1968**, *127*, 1055-1072.

(4) Broome, J. D. *Journal of Experimental Medicine* **1963**, *118*, 99-148.

(5) Ertel, I. J.; Nesbit, M. E.; Hammond, D.; Weiner, J.; Sather, H. *Cancer Research* **1979**, *39*, 3893-3896.

(6) Sanz, G. F.; Sanz, M. A.; Rafecas, F. J.; Martinez, J. A.; Martinaragones, G.; Marty, M. L. *Cancer Treatment Reports* **1986**, *70*, 1321-1323.

(7) Ohnuma, T.; Holland, J. F.; Meyer, P. *Cancer* **1972**, *30*, 376-381.

(8) Barr, R. D.; Deveber, L. L.; Pai, K. M.; Andrew, M.; Halton, J.; Cairney, A. E.; Whitton, A. C. *American Journal of Pediatric Hematology Oncology* **1992**, *14*, 136-139.

(9) Terebelo, H. R.; Anderson, K.; Wiernik, P. H.; Cuttner, J.; Cooper, R. M.; Faso, L.; Berenberg, J. L. *American Journal of Clinical Oncology-Cancer Clinical Trials* **1986**, *9*, 411-415.

(10) Kiriyama, Y.; Kubota, M.; Takimoto, T.; Kitoh, T.; Tanizawa, A.; Akiyama, Y.; Mikawa, H. *Leukemia* **1989**, *3*, 294-297.

(11) Lobel, J. S.; Obrien, R. T.; McIntosh, S.; Aspnes, G. T.; Capizzi, R. L. *Cancer* **1979**, *43*, 1089-1094.

(12) Capizzi, R. L.; Bertino, J. R.; Skeel, R. T.; Creasey, W. A.; Zanes, R.; Olayon, C.; Peterson, R. G.; Handschu.Re *Annals of Internal Medicine* **1971**, *74*, 893-901.

(13) Chakrabarti, R.; Schuster, S. M. *International Journal of Pediatric Hematology/Oncology* **1997**, *4*, 597-611.

(14) Hersh, E. M. *Transplantation* **1971**, *12*, 368-376.

(15) Uren, J. R.; Chang, P. K.; Handschumacher, R. E. *Biochemical Pharmacology* **1977**, *26*, 1405-1410.

(16) Richards, N. G. J.; Schuster, S. M. In *Advances in Enzymology, Vol 72* 1998; Vol. 72, p 145-198.

(17) Hinchman, S. K.; Henikoff, S.; Schuster, S. M. *Journal of Biological Chemistry* **1992**, *267*, 144-149.

(18) Ramos, F.; Wiame, J. M. *European Journal of Biochemistry* **1979**, *94*, 409-417.

(19) Tsai, F. Y.; Coruzzi, G. M. *Embo Journal* **1990**, *9*, 323-332.

(20) Lam, H. M.; Peng, S. S. Y.; Coruzzi, G. M. *Plant Physiology* **1994**, *106*, 1347-1357.

(21) Burchall, J. J.; Reichelt, E. C.; Wolin, M. J. *Journal of Biological Chemistry* **1964**, *239*, 1794-1798.

(22) Ravel, J. M.; Shive, W.; Norton, S. J.; Humphreys, J. S. *Journal of Biological Chemistry* **1962**, *237*, 2845-2849.

(23) Reitzer, L. J.; Magasanik, B. *Journal of Bacteriology* **1982**, *151*, 1299-1313.

(24) Hongo, S.; Sato, T. *Biochimica Et Biophysica Acta* **1983**, *742*, 484-489.

(25) Luehr, C. A.; Schuster, S. M. *Archives of Biochemistry and Biophysics* **1985**, *237*, 335-346.

(26) Andrulis, I. L.; Duff, C.; Evansblackler, S.; Worton, R.; Siminovitch, L. *Molecular and Cellular Biology* **1983**, *3*, 391-398.

(27) Smith, J. L. *Biochemical Society Transactions* **1995**, *23*, 894-898.

(28) Tso, J. Y.; Zalkin, H.; Vancleemput, M.; Yanofsky, C.; Smith, J. M. *Journal of Biological Chemistry* **1982**, *257*, 3525-3531.

(29) Badetdenisot, M. A.; Rene, L.; Badet, B. *Bulletin De La Societe Chimique De France* **1993**, *130*, 249-255.

(30) Vanoni, M. A.; Edmondson, D. E.; Rescigno, M.; Zanetti, G.; Curti, B. *Biochemistry* **1991**, *30*, 11478-11484.

(31) Cedar, H.; Schwartz, J. H. *Journal of Biological Chemistry* **1969**, *244*, 4112-4121.

(32) Cedar, H.; Schwartz, J. H. *Journal of Biological Chemistry* **1969**, *244*, 4122-4127.

(33) Nakatsu, T.; Kato, H.; Oda, J. *Nature Structural Biology* **1998**, *5*, 15-19.

(34) Larsen, T. M.; Boehlein, S. K.; Schuster, S. M.; Richards, N. G. J.; Thoden, J. B.; Holden, H. M.; Rayment, I. *Biochemistry* **1999**, *38*, 16146-16157.

(35) Boehlein, S. K.; Stewart, J. D.; Walworth, E. S.; Thirumoorthy, R.; Richards, N. G. J.; Schuster, S. M. *Biochemistry* **1998**, *37*, 13230-13238.

(36) Boehlein, S. K.; Richards, N. G. J.; Walworth, E. S.; Schuster, S. M. *Journal of Biological Chemistry* **1994**, *269*, 26789-26795.

(37) Boehlein, S. K.; Richards, N. G. J.; Schuster, S. M. *Journal of Biological Chemistry* **1994**, *269*, 7450-7457.

(38) Zalkin, H. *Advanced Enzymology Related Areas Molecular Biology* **1993**, *66*, 203-309.

(39) Richards, N. G. J.; Schuster, S. M. *Febs Letters* **1992**, *313*, 98-102.

(40) Miles, E. W.; Rhee, S.; Davies, D. R. *Journal of Biological Chemistry* **1999**, *274*, 12193-12196.

(41) Lipinski, C. A.; Lombardo, F.; Dominy, B. W.; Feeney, P. J. *Advanced Drug Delivery Reviews* **1997**, *23*, 3-25.

(42) Veber, D. F.; Johnson, S. R.; Cheng, H. Y.; Smith, B. R.; Ward, K. W.; Kopple, K. D. *Journal of Medicinal Chemistry* **2002**, *45*, 2615-2623.

(43) Proudfoot, J. R. *Bioorganic & Medicinal Chemistry Letters* **2002**, *12*, 1647-1650.

(44) Pike, D. C.; Beevers, L. *Biochimica Et Biophysica Acta* **1982**, *708*, 203-209.

(45) Zhukov, Y. N.; Biryukov, A. I.; Khomutov, R. M. *Bioorganicheskaya Khimiya* **1988**, *14*, 969-972.

(46) Koizumi, M.; Hiratake, J.; Nakatsu, T.; Kato, H.; Oda, J. *Journal of the American Chemical Society* **1999**, *121*, 5799-5800.

(47) Mokotoff, M.; Bagaglio, J. F.; Parikh, B. S. *Journal of Medicinal Chemistry* **1975**, *18*, 354-358.

(48) Handschu.Re; Bates, C. J.; Chang, P. K.; Andrews, A. T.; Fischer, G. A. *Science* **1968**, *161*, 62-63.

(49) Jayaram, H. N.; Cooney, D. A.; Ryan, J. A.; Neil, G.; Dion, R. L.; Bono, V. H. *Cancer Chemotherapy Reports Part 1* **1975**, *59*, 481-491.

(50) Jayaram, H. N.; Cooney, D. A.; Milman, H. A.; Homan, E. R.; Rosenbluth, R. J. *Biochemical Pharmacology* **1976**, *25*, 1571-1582.

(51) Cooney, D. A.; Driscoll, J. S.; Milman, H. A.; Jayaram, H. N.; Davis, R. D. *Cancer Treatment Reports* **1976**, *60*, 1493-1557.

(52) Cooney, D. A.; Jones, M. T.; Milman, H. A.; Young, D. M.; Jayaram, H. N. *International Journal of Biochemistry* **1980**, *11*, 519-539.

(53) Andrulis, I. L.; Argonza, R.; Cairney, A. E. L. *Somatic Cell and Molecular Genetics* **1990**, *16*, 59-65.

(54) Parr, I. B.; Boehlein, S. K.; Dribben, A. B.; Schuster, S. M.; Richards, N. G. J. *Journal of Medicinal Chemistry* **1996**, *39*, 2367-2378.

(55) Foote, J.; Lauritzen, A. M.; Lipscomb, W. N. *Journal of Biological Chemistry* **1985**, *260*, 9624-9629.

(56) Turnbull, J. L.; Waldrop, G. L.; Schachman, H. K. *Biochemistry* **1992**, *31*, 6562-6569.

(57) Horowitz, B.; Meister, A. *Journal of Biological Chemistry* **1972**, *247*, 6708-&.

(58) Colman, R. F. *The enzymes*; 3rd ed.; Academic Press: San Diego, 1990; Vol. XIX.

(59) Boehlein, S. K.; Nakatsu, T.; Hiratake, J.; Thirumoorthy, R.; Stewart, J. D.; Richards, N. G. J.; Schuster, S. M. *Biochemistry* **2001**, *40*, 11168-11175.

(60) Schimmel, P. *Annual Review of Biochemistry* **1987**, *56*, 125-158.

(61) Eriani, G.; Delarue, M.; Poch, O.; Gangloff, J.; Moras, D. *Nature* **1990**, *347*, 203-206.

(62) Hudson, I. R. B. *Journal of Hospital Infection* **1994**, *27*, 81-98.

(63) Arnez, J. G.; Moras, D. *Trends in Biochemical Sciences* **1997**, *22*, 211-216.

(64) Moras, D. *Trends in Biochemical Sciences* **1992**, *17*, 159-164.

(65) Brick, P.; Bhat, T. N.; Blow, D. M. *Journal of Molecular Biology* **1989**, *208*, 83-98.

(66) Rould, M. A.; Perona, J. J.; Soll, D.; Steitz, T. A. *Science* **1989**, *246*, 1135-1142.

(67) Rath, V. L.; Silvian, L. F.; Beijer, B.; Sproat, B. S.; Steitz, T. A. *Structure with Folding & Design* **1998**, *6*, 439-449.

(68) Brunie, S.; Zelwer, C.; Risler, J. L. *Journal of Molecular Biology* **1990**, *216*, 411-424.

(69) Doublie, S.; Bricogne, G.; Gilmore, C.; Carter, C. W. *Structure* **1995**, *3*, 17-31.

(70) Nureki, O.; Vassylyev, D. G.; Katayanagi, K.; Shimizu, T.; Sekine, S.; Kigawa, T.; Miyazawa, T.; Yokoyama, S.; Morikawa, K. *Science* **1995**, *267*, 1958-1965.

(71) Nureki, O.; Vassylyev, D. G.; Tateno, M.; Shimada, A.; Nakama, T.; Fukai, S.; Konno, M.; Hendrickson, T. L.; Schimmel, P.; Yokoyama, S. *Science* **1998**, *280*, 578-582.

(72) Cavarelli, J.; Delagoutte, B.; Eriani, G.; Gangloff, J.; Moras, D. *Embo Journal* **1998**, *17*, 5438-5448.

(73) Cusack, S.; Yaremchuk, A.; Tukalo, M. *Embo Journal* **2000**, *19*, 2351-2361.

(74) Fukai, S.; Nureki, O.; Sekine, S.; Shimada, A.; Tao, J. S.; Vassylyev, D. G.; Yokoyama, S. *Cell* **2000**, *103*, 793-803.

(75) Cusack, S.; Berthetcolominas, C.; Hartlein, M.; Nassar, N.; Leberman, R. *Nature* **1990**, *347*, 249-255.

(76) Cusack, S.; Yaremchuk, A.; Tukalo, M. *Embo Journal* **1996**, *15*, 2834-2842.

(77) Belrhali, H.; Yaremchuk, A.; Tukalo, M.; Larsen, K.; Berthetcolominas, C.; Leberman, R.; Beijer, B.; Sproat, B.; Alsnielsen, J.; Grubel, G.; Legrand, J. F.; Lehmann, M.; Cusack, S. *Science* **1994**, *263*, 1432-1436.

(78) Belrhali, H.; Yaremchuk, A.; Tukalo, M.; Berthetcolominas, C.; Rasmussen, B.; Bosecke, P.; Diat, O.; Cusack, S. *Structure* **1995**, *3*, 341-352.

(79) Biou, V.; Yaremchuk, A.; Tukalo, M.; Cusack, S. *Science* **1994**, *263*, 1404-1410.

(80) Logan, D. T.; Mazauric, M. H.; Kern, D.; Moras, D. *Embo Journal* **1995**, *14*, 4156-4167.

(81) Arnez, J. G.; Dock-Bregeon, A. C.; Moras, D. *Journal of Molecular Biology* **1999**, *286*, 1449-1459.

(82) Arnez, J. G.; Harris, D. C.; Mitschler, A.; Rees, B.; Francklyn, C. S.; Moras, D. *Embo Journal* **1995**, *14*, 4143-4155.

(83) Arnez, J. G.; Augustine, J. G.; Moras, D.; Francklyn, C. S. *PNAS* **1997**, *94*, 7144-7149.

(84) Aberg, A.; Yaremchuk, A.; Tukalo, M.; Rasmussen, B.; Cusack, S. *Biochemistry* **1997**, *36*, 3084-3094.

(85) Cusack, S.; Yaremchuk, A.; Krikliviy, I.; Tukalo, M. *Structure* **1998**, *6*, 101-108.

(86) Reshetnikova, L.; Moor, N.; Lavrik, O.; Vassylyev, D. G. *Journal of Molecular Biology* **1999**, *287*, 555-568.

(87) Goldgur, Y.; Mosyak, L.; Reshetnikova, L.; Ankilova, V.; Lavrik, O.; Khodyreva, S.; Safro, M. *Structure* **1997**, *5*, 59-68.

(88) Mosyak, L.; Reshetnikova, L.; Goldgur, Y.; Delarue, M.; Safro, M. G. *Nature Structural Biology* **1995**, *2*, 537-547.

(89) Berthet-Colominas, C.; Seignovert, L.; Hartlein, M.; Grotli, M.; Cusack, S.; Leberman, R. *Embo Journal* **1998**, *17*, 2947-2960.

(90) Onesti, S.; Miller, A. D.; Brick, P. *Structure* **1995**, *3*, 163-176.

(91) Cusack, S.; Yaremchuk, A.; Tukalo, M. *Embo Journal* **1996**, *15*, 6321-6334.

(92) Desogus, G.; Todone, F.; Brick, P.; Onesti, S. *Biochemistry* **2000**, *39*, 8418-8425.

(93) Ruff, M.; Krishnaswamy, S.; Boeglin, M.; Poterszman, A.; Mitschler, A.; Podjarny, A.; Rees, B.; Thierry, J. C.; Moras, D. *Science* **1991**, *252*, 1682-1689.

(94) Cavarelli, J.; Eriani, G.; Rees, B.; Ruff, M.; Boeglin, M.; Mitschler, A.; Martin, F.; Gangloff, J.; Thierry, J. C.; Moras, D. *Embo Journal* **1994**, *13*, 327-337.

(95) Delarue, M.; Poterszman, A.; Nikonov, S.; Garber, M.; Moras, D.; Thierry, J. C. *Embo Journal* **1994**, *13*, 3219-3229.

(96) Poterszman, A.; Delarue, M.; Thierry, J. C.; Moras, D. *Journal of Molecular Biology* **1994**, *244*, 158-167.

(97) Schmitt, E.; Moulinier, L.; Fujiwara, S.; Imanaka, T.; Thierry, J. C.; Moras, D. *Embo Journal* **1998**, *17*, 5227-5237.

(98) Sankaranarayanan, R.; Dock-Bregeon, A. C.; Romby, P.; Caillet, J.; Springer, M.; Rees, B.; Ehresmann, C.; Ehresmann, B.; Moras, D. *Cell* **1999**, *97*, 371-381.

(99) Schimmel, P.; Tao, J. S.; Hill, J. *Faseb Journal* **1998**, *12*, 1599-1609.

(100) Wendler, P.; Silverman, J. A. *Current Opinion in Anti-infect. Invest. Drugs* **2000**, *2*, 125-132.

(101) Gallant, P.; Finn, J.; Keith, D.; Wendler, P. *Emer. Ther. Targets* **2000**, *4*, 1-10.

(102) Takashi, N.; Osamu, N.; Shigeyuki, Y. *journal of Biological Chemistry* **2001**, *276*, 47387-47393.

(103) Airas, R. K. *European Journal of Biochemistry* **1996**, *240*, 223-231.

(104) Tao, J. S.; Schimmel, P. *Expert Opinion on Investigational Drugs* **2000**, *9*, 1767-1775.

(105) Capobianco, J. O.; Zakula, D.; Coen, M. L.; Goldman, R. C. *Biochemical and Biophysical Research Communications* **1993**, *190*, 1037-1044.

(106) Tanaka, K.; Tamaki, M.; Watanabe, S. *Biochimica Et Biophysica Acta* **1969**, *195*, 244-245.

(107) Kohno, T.; Kohda, D.; Haruki, M.; Yokoyama, S.; Miyazawa, T. *Journal of Biological Chemistry* **1990**, *265*, 6931-6935.

(108) Werner, R. G.; Thorpe, L. F.; Reuter, W.; Nierhaus, K. H. *European Journal of Biochemistry* **1976**, *68*, 1-3.

(109) Schachvonwitten.M; Els, H. *Journal of the American Chemical Society* **1963**, *85*, 3425-&.

(110) Witty, D. R.; Walker, G.; Bateson, J. H.; O'Hanlon, P. J.; Cassels, R. *Bioorganic & Medicinal Chemistry Letters* **1996**, *6*, 1375-1380.

(111) Cochereau, C.; Sanchez, D.; Bourhaoui, A.; Creppy, E. E. *Toxicology and Applied Pharmacology* **1996**, *141*, 133-137.

(112) Houge-Frydrych, C. S. V.; Readshaw, S. A.; Bell, D. J. *Journal of Antibiotics* **2000**, *53*, 351-356.

(113) Qiu, X. Y.; Janson, C. A.; Smith, W. W.; Green, S. M.; McDevitt, P.; Johanson, K.; Carter, P.; Hibbs, M.; Lewis, C.; Chalker, A.; Fosberry, A.; Lalonde, J.; Berge, J.; Brown, P.; Houge-Frydrych, C. S. V.; Jarvest, R. L. *Protein Science* **2001**, *10*, 2008-2016.

(114) Stefanska, A. L.; Fulston, M.; Houge-Frydrych, C. S. V.; Jones, J. J.; Warr, S. R. *Journal of Antibiotics* **2000**, *53*, 1346-1353.

(115) Lee, J.; Kang, M. K.; Chun, M. W.; Jo, Y. J.; Kwak, J. H.; Kim, S. *Bioorganic & Medicinal Chemistry Letters* **1998**, *8*, 3511-3514.

(116) Tosa, T.; Pizer, L. I. *Journal of Bacteriology* **1971**, *106*, 966-&.

(117) Lee, J.; Kang, S. U.; Kim, S. Y.; Kim, S. E.; Kang, M. K.; Jo, Y. J.; Kim, S. *Bioorganic & Medicinal Chemistry Letters* **2001**, *11*, 961-964.

(118) Brown, P.; Richardson, C. M.; Mensah, L. M.; O'Hanlon, P. J.; Osborne, N. F.; Pope, A. J.; Walker, G. *Bioorganic & Medicinal Chemistry* **1999**, *7*, 2473-2485.

(119) Bernier, S.; Dubois, D. Y.; Therrien, M.; Lapointe, J.; Chenevert, R. *Bioorganic & Medicinal Chemistry Letters* **2000**, *10*, 2441-2444.

(120) Desjardins, M.; Garneau, S.; Desgagnes, J.; Lacoste, L.; Yang, F.; Lapointe, J.; Chenevert, R. *Bioorganic Chemistry* **1998**, *26*, 1-13.

(121) Forrest, A. K.; Jarvest, R. L.; Mensah, L. M.; O'Hanlon, P. J.; Pope, A. J.; Sheppard, R. J. *Bioorganic & Medicinal Chemistry Letters* **2000**, *10*, 1871-1874.

(122) Pope, A. J.; Moore, K. J.; McVey, M.; Mensah, L.; Benson, N.; Osbourne, N.; Broom, N.; Brown, M. J. B.; O'Hanlon, P. *Journal of Biological Chemistry* **1998**, *273*, 31691-31701.

(123) Goring, G.; Cramer, F. *Chemische Berichte-Recueil* **1973**, *106*, 2460-2467.

(124) Moriguchi, T.; Yanagi, T.; Kunimori, M.; Weda, T.; Sekine, M. *Journal of Organic Chemistry* **2000**, *65*, 8229-8238.

(125) Moriguchi, T.; Yanagi, T.; Wada, T.; Sekine, M. *Tetrahedron Letters* **1998**, *39*, 3725-3728.

(126) Ueda, H.; Shoku, Y.; Hayashi, N.; Mitsunaga, J.; In, Y.; Doi, M.; Inoue, M.; Ishida, T. *Biochimica Et Biophysica Acta* **1991**, *1080*, 126-134.

(127) Isono, K.; Uramoto, M.; Kusakabe, H.; Miyata, N.; Koyama, T.; Ubukata, M.; Sethi, S. K.; McCloskey, J. A. *Journal of Antibiotics* **1984**, *37*, 670-672.

(128) Heacock, D.; Forsyth, C. J.; Shiba, K.; MusierForsyth, K. *Bioorganic Chemistry* **1996**, *24*, 273-289.

(129) Lee, J.; Kang, S. U.; Kang, M. K.; Chun, M. W.; Jo, Y. J.; Kwak, J. H.; Kim, S. *Bioorganic & Medicinal Chemistry Letters* **1999**, *9*, 1365-1370.

(130) Lee, J.; Kang, S. U.; Kim, S. Y.; Kim, S. E.; Jo, Y. J.; Kim, S. *Bioorganic & Medicinal Chemistry Letters* **2001**, *11*, 965-968.

(131) Kleinman, E. F.; Campbell, E.; Giordano, L. A.; Cohan, V. L.; Jenkinson, T. H.; Cheng, J. B.; Shirley, J. T.; Pettipher, E. R.; Salter, E. D.; Hibbs, T. A.; DiCapua, F. M.; Bordner, J. *Journal of Medicinal Chemistry* **1998**, *41*, 266-270.

(132) Hill, J. M.; Yu, G. X.; Shue, Y.; Zydowsky, T. M.; Rebek, J. In *United States Patent* United States, 1998.

(133) Yu, X. Y.; Hill, J. M.; Yu, G.; Wang, W.; Kluge, A. F.; Wendler, P.; Gallant, P. *Bioorganic & Medicinal Chemistry Letters* **1999**, *9*, 375-380.

(134) Desjardins, M.; Desgagnes, J.; Lacoste, L.; Yang, F.; Morin, M.-P.; Lapointe, J.; Chenevert, R. *Bioorganic & Medicinal Chemistry Letters* **1997**, *7*, 2363-2366.

(135) Biryukov, A. I.; Ishmuratov, B. K.; Khomutov, R. M. *Febs Letters* **1978**, *91*, 249-252.

(136) Nakama, T.; Nureki, O.; Yokoyama, S. *J. Biol. Chem.* **2001**, *276*, 47387-47393.

(137) Brown, M. J. B.; Mensah, L. M.; Doyle, M. L.; Broom, N. J. P.; Osbourne, N.; Forrest, A. K.; Richardson, C. M.; O'Hanlon, P. J.; Pope, A. J. *Biochemistry* **2000**, *39*, 6003-6011.

(138) Stefanska, A. L.; Cassels, R.; Ready, S. J.; Warr, S. R. *Journal of Antibiotics* **2000**, *53*, 357-363.

(139) Houge-Frydrych, C. S. V.; Gilpin, M. L.; Skett, P. W.; Tyler, J. W. *Journal of Antibiotics* **2000**, *53*, 364-372.

(140) Banwell, M. G.; Crasto, C. F.; Easton, C. J.; Forrest, A. K.; Karoli, T.; March, D. R.; Mensah, L.; Nairn, M. R.; O'Hanlon, P. J.; Oldham, M. D.; Yue, W. M. *Bioorganic & Medicinal Chemistry Letters* **2000**, *10*, 2263-2266.

(141) Konrad, I.; Roschenthaler, R. *Febs Letters* **1977**, *83*, 341-347.

(142) Creppy, E. E.; Mayer, M.; Kern, D.; Schlegel, M.; Steyn, P. S.; Vleggaar, R.; Dirheimer, G. *Biochimica Et Biophysica Acta* **1981**, *656*, 265-268.

(143) Vocadlo, D. J.; Mayer, C.; He, S. M.; Withers, S. G. *Biochemistry* **2000**, *39*, 117-126.

(144) Namchuk, M. N.; McCarter, J. D.; Becalski, A.; Andrews, T.; Withers, S. G. *Journal of the American Chemical Society* **2000**, *122*, 1270-1277.

(145) Gu, X. R.; Liu, Y. Q.; Santi, D. V. *Proceedings of the National Academy of Sciences of the United States of America* **1999**, *96*, 14270-14275.

(146) Michel, D.; Schlosser, M. *Tetrahedron* **2000**, *56*, 4253-4260.

(147) De Jonghe, S.; Van Overmeire, I.; Gunst, J.; De Bruyn, A.; Hendrix, C.; Van Calenbergh, S.; Busson, R.; De Keukeleire, D.; Philippe, J.; Herdewijn, P. *Bioorganic & Medicinal Chemistry Letters* **1999**, *9*, 3159-3164.

(148) Gerfen, G. J.; van der Donk, W. A.; Yu, G. X.; McCarthy, J. R.; Jarvi, E. T.; Matthews, D. P.; Farrar, C.; Griffin, R. G.; Stubbe, J. *Journal of the American Chemical Society* **1998**, *120*, 3823-3835.

(149) Kim, D. H.; Park, J. I. *Bioorganic & Medicinal Chemistry Letters* **1996**, *6*, 2967-2970.

(150) Park, B. K.; Kitteringham, N. R. *Drug Metabolism Reviews* **1994**, *26*, 605-643.

(151) Resnati, G. *Tetrahedron* **1993**, *49*, 9385-9445.

(152) Egron, M. J.; Leclercq, F.; Antonakis, K.; Bennanibaiti, M. I.; Frayssinet, C. *Carbohydrate Research* **1993**, *248*, 143-150.

(153) Dubois, J.; Dugave, C.; Foures, C.; Kaminsky, M.; Tabet, J. C.; Bory, S.; Gaudry, M.; Marquet, A. *Biochemistry* **1991**, *30*, 10506-10512.

(154) Dax, K.; Albert, M.; Ortner, J.; Paul, B. J. *Current Organic Chemistry* **1999**, *3*, 287-307.

(155) Dolbier, W. R. *Chemical Reviews* **1996**, *96*, 1557-1584.

(156) Schlosser, M. *Angewandte Chemie-International Edition* **1998**, *37*, 1497-1513.

(157) Coward, J. K.; McGuire, J. J.; Galivan, J. *Acs Symposium Series* **1991**, *456*, 196-204.

(158) Ito, H.; Saito, A.; Taguchi, T. *Tetrahedron-Asymmetry* **1998**, *9*, 1989-1994.

(159) Tian, F.; Bartberger, M. D.; Dolbier, W. R. *Journal of Organic Chemistry* **1999**, *64*, 540-546.

(160) Saunders, W. H. *Journal of Organic Chemistry* **1999**, *64*, 861-865.

(161) Li, A. R.; Shtarev, A. B.; Smart, B. E.; Yang, Z. Y.; Lusztyk, J.; Ingold, K. U.; Bravo, A.; Dolbier, W. R. *Journal of Organic Chemistry* **1999**, *64*, 5993-5999.

(162) Headley, A. D.; Starnes, S. D. *Journal of Computational Chemistry* **2000**, *21*, 426-431.

(163) Hoffmann, M.; Rychlewski, J.; Rychlewska, U. *Journal of the American Chemical Society* **1999**, *121*, 1912-1921.

(164) Barbarich, T. J.; Rithner, C. D.; Miller, S. M.; Anderson, O. P.; Strauss, S. H. *Journal of the American Chemical Society* **1999**, *121*, 4280-4281.

(165) Tsushima, T.; Kawada, K.; Shiratori, O.; Uchida, N. *Heterocycles* **1985**, *23*, 45-49.

(166) Tsukamoto, T.; Kitazume, T.; McGuire, J. J.; Coward, J. K. *Journal of Medicinal Chemistry* **1996**, *39*, 66-72.

(167) McGuire, J. J.; Hart, B. P.; Haile, W. H.; Rhee, M. S.; Galivan, J.; Coward, J. K. *Archives of Biochemistry and Biophysics* **1995**, *321*, 319-328.

(168) McGuire, J. J.; Hart, B. P.; Haile, W. H.; Magee, K. J.; Rhee, M.; Bolanowska, W. E.; Russell, C.; Galivan, J.; Paul, B.; Coward, J. K. *Biochemical Pharmacology* **1996**, *52*, 1295-1303.

(169) Hart, B. P.; Haile, W. H.; Licato, N. J.; Bolanowska, W. E.; McGuire, J. J.; Coward, J. K. *Journal of Medicinal Chemistry* **1996**, *39*, 56-65.

(170) Zalkin, H.; Smith, J. L. In *Advances in Enzymology, Vol 72* 1998; Vol. 72, p 87-+.

(171) Buchanan, J. M. *Advances in Enzymology and Related Areas of Molecular Biology* **1973**, *39*, 91-183.

(172) Gong, S. S.; Basilico, C. *Nucleic Acids Research* **1990**, *18*, 3509-3513.

(173) Barbosa-Tessmann, I. P.; Chen, C.; Zhong, C.; Schuster, S. M.; Nick, H. S.; Kilberg, M. S. *Journal of Biological Chemistry* **1999**, *274*, 31139-31144.

(174) Barbosa-Tessmann, I. P.; Chen, C.; Zhong, C.; Siu, F.; Schuster, S. M.; Nick, H. S.; Kilberg, M. S. *Journal of Biological Chemistry* **2000**, *275*, 26976-26985.

(175) Tsukamoto, T.; Coward, J. K. *Journal of Organic Chemistry* **1996**, *61*, 2497-2500.

(176) Konas, D. W.; Coward, J. K. *Organic Letters* **1999**, *1*, 2105-2107.

(177) Kitagawa, O.; Hashimoto, A.; Kobayashi, Y.; Taguchi, T. *Chemistry Letters* **1990**, 1307-1310.

(178) Hudlicky, M. *Journal of Fluorine Chemistry* **1993**, *60*, 193-210.

(179) Avent, A. G.; Bowler, A. N.; Doyle, P. M.; Marchand, C. M.; Young, D. W. *Tetrahedron Letters* **1992**, *33*, 1509-1512.

(180) Kroger, S.; Haufe, G. *Amino Acids* **1997**, *12*, 363-372.

(181) Hudlicky, M.; Merola, J. S. *Tetrahedron Letters* **1990**, *31*, 7403-7406.

(182) Hart, B. P.; Coward, J. K. *Tetrahedron Letters* **1993**, *34*, 4917-4920.

(183) Taguchi, T.; Mitsuhashi, S.; Yamanouchi, A.; Kobayashi, Y.; Sai, H.; Ikekawa, N. *Tetrahedron Letters* **1984**, *25*, 4933-4936.

(184) Sutherland, A.; Willis, C. L. *Natural Product Reports* **2000**, *17*, 621-631.

(185) Li, K. Q.; Leriche, C.; Liu, H. W. *Bioorganic & Medicinal Chemistry Letters* **1998**, *8*, 1097-1100.

(186) Tolman, V.; Sedmera, P. *Journal of Fluorine Chemistry* **2000**, *101*, 5-10.

(187) Tolman, V.; Simek, P. *Journal of Fluorine Chemistry* **2000**, *101*, 11-14.

(188) Kokuryo, Y.; Nakatani, T.; Kobayashi, K.; Tamura, Y.; Kawada, K.; Ohtani, M. *Tetrahedron-Asymmetry* **1996**, *7*, 3545-3551.

(189) Rose, N. G. W.; Blaskovich, M. A.; Wong, A.; Lajoie, G. A. *Tetrahedron* **2001**, *57*, 1497-1507.

(190) Rife, J.; Ortuno, R. M.; Lajoie, G. A. *Journal of Organic Chemistry* **1999**, *64*, 8958-8961.

(191) Blaskovich, M. A.; Lajoie, G. A. *Journal of the American Chemical Society* **1993**, *115*, 5021-5030.

(192) Blaskovich, M. A.; Lajoie, G. A. *Tetrahedron Letters* **1993**, *34*, 3837-3840.

(193) Percy, J. M. In *Organofluorine Chemistry* 1997; Vol. 193, p 131-195.

(194) Tozer, M. J.; Herpin, T. F. *Tetrahedron* **1996**, *52*, 8619-8683.

(195) Welch, J. T. *Tetrahedron* **1987**, *43*, 3123-3197.

(196) Kukhar, V. P.; Soloshonok, V. A. *Fluorine-containing amino acids, synthesis and properties*, 1995.

(197) Vayron, P.; Renard, P. Y.; Valleix, A.; Mioskowski, C. *Chemistry-a European Journal* **2000**, *6*, 1050-1063.

(198) Kotoris, C. C.; Chen, M. J.; Taylor, S. D. *Journal of Organic Chemistry* **1998**, *63*, 8052-8057.

(199) Nakano, T.; Makino, M.; Morizawa, Y.; Matsumura, Y. *Angewandte Chemie-International Edition in English* **1996**, *35*, 1019-1021.

(200) Davis, F. A.; Han, W.; Murphy, C. K. *Journal of Organic Chemistry* **1995**, *60*, 4730-4737.

(201) Differding, E.; Ofner, H. *Synlett* **1991**, 187-189.

(202) Benincasa, M.; Forti, L.; Ghelfi, F.; Libertini, E.; Pagnoni, U. M. *Synthetic Communications* **1996**, *26*, 4113-4122.

(203) Robinson, R. P.; Donahue, K. M. *Journal of Organic Chemistry* **1992**, *57*, 7309-7314.

(204) Takahashi, L. H.; Radhakrishnan, R.; Rosenfield, R. E.; Meyer, E. F.; Trainor, D. A. *Journal of the American Chemical Society* **1989**, *111*, 3368-3374.

(205) Chou, T. S.; Heath, P. C.; Patterson, L. E.; Poteet, L. M.; Lakin, R. E.; Hunt, A. H. *Synthesis-Stuttgart* **1992**, 565-570.

(206) Xu, Y. L.; Tian, F.; Dolbier, W. R. *Journal of Organic Chemistry* **1999**, *64*, 5599-5602.

(207) Xu, Y. L.; Dolbier, W. R. *Journal of Organic Chemistry* **1997**, *62*, 6503-6506.

(208) Xu, Y. L.; Dolbier, W. R.; Rong, X. X. *Journal of Organic Chemistry* **1997**, *62*, 1576-1577.

(209) Rittle, K. E.; Homnick, C. F.; Ponticello, G. S.; Evans, B. E. *Journal of Organic Chemistry* **1982**, *47*, 3016-3018.

(210) Lubell, W. D.; Rapoport, H. *Journal of the American Chemical Society* **1987**, *109*, 236-239.

(211) Lubell, W.; Rapoport, H. *Journal of Organic Chemistry* **1989**, *54*, 3824-3831.

(212) Lubell, W. D.; Jamison, T. F.; Rapoport, H. *Journal of Organic Chemistry* **1990**, *55*, 3511-3522.

(213) King, H. *Journal of Chemical Society* **1942**, 432.

(214) Cha, J. S.; Kwon, S. S. *Journal of Organic Chemistry* **1987**, *52*, 5486-5487.

(215) Anh, N. T. *Topics in Current Chemistry* **1980**, *88*, 145-163.

(216) Bartlett, P. A. *Tetrahedron* **1980**, *36*, 3-72.

(217) Xu, Y. L.; Dolbier, W. R. *Journal of Organic Chemistry* **2000**, *65*, 2134-2137.

(218) Xu, Y. L.; Dolbier, W. R. *Tetrahedron Letters* **1998**, *39*, 9151-9154.

(219) Kim, K. S.; Qian, L. G. *Tetrahedron Letters* **1993**, *34*, 7195-7196.

(220) Beckwith, A. L. J.; Crich, D.; Duggan, P. J.; Yao, Q. W. *Chemical Reviews* **1997**, *97*, 3273-3312.

(221) Barton, D. H. R.; Dorchak, J.; Jaszberenyi, J. C. *Tetrahedron* **1992**, *48*, 7435-7446.

(222) Barton, D. H. R. *Tetrahedron* **1992**, *48*, 2529-2544.

(223) Barton, D. H. R.; Jang, D. O.; Jaszberenyi, J. C. *Tetrahedron* **1993**, *49*, 2793-2804.

(224) Sheehan, J. C.; Goodman, M.; Hess, G. P. *Journal of the American Chemical Society* **1956**, *78*, 1367-1369.

(225) Worster, P. M.; Leznoff, C. C.; McArthur, C. R. *Journal of Organic Chemistry* **1980**, *45*, 174-175.

(226) McArthur, C. R.; Worster, P. M.; Okon, A. U. *Synthetic Communications* **1983**, *13*, 311-318.

(227) Corey, E. J.; Raju, N. *Tetrahedron Letters* **1983**, *24*, 5571-5574.

(228) Barton, D. H. R.; Jang, D. O.; Jaszberenyi, J. C. *Tetrahedron Letters* **1991**, *32*, 7187-7190.

(229) Carpino, L. A.; Han, G. Y. *Journal of Organic Chemistry* **1972**, *37*, 3404-&.

(230) Carpino, L. A. *Accounts of Chemical Research* **1987**, *20*, 401-407.

(231) Still, W. C.; Kahn, M.; Mitra, A. *Journal of Organic Chemistry* **1978**, *43*, 2923-2925.

(232) Blaskovich, M. A.; Evindar, G.; Rose, N. G. W.; Wilkinson, S.; Luo, Y.; Lajoie, G. A. *Journal of Organic Chemistry* **1998**, *63*, 3631-3646.

(233) Moriguchi, T.; Asai, N.; Okada, K.; Seio, K.; Sasaki, T.; Sekine, M. *Journal of Organic Chemistry* **2002**, *67*, 3290-3300.

(234) Phillips, D. R.; Uramoto, M.; Isono, K.; McCloskey, J. A. *Journal of Organic Chemistry* **1993**, *58*, 854-859.

(235) Moriguchi, T.; Wada, T.; Sekine, M. *Journal of Organic Chemistry* **1996**, *61*, 9223-9228.

(236) Challis, B. C.; Iley, J. N. *Journal of the Chemical Society-Perkin Transactions 2* **1987**, 1489-1494.

(237) Hendrickse, T. F.; Mizrahi, V.; Modro, T. A. *Phosphorus Sulfur and Silicon and the Related Elements* **1984**, *20*, 93-105.

(238) Mizrahi, V.; Modro, T. A. *Journal of Organic Chemistry* **1982**, *47*, 3533-3539.

(239) Chakravarty, P. K.; Greenlee, W. J.; Parsons, W. H.; Patchett, A. A.; Combs, P.; Roth, A.; Busch, R. D.; Mellin, T. N. *Journal of Medicinal Chemistry* **1989**, *32*, 1886-1890.

(240) Zioudrou, C. *Tetrahedron* **1962**, *18*, 197-204.

(241) Desmarch.Jm; Fukuto, T. R. *Journal of Organic Chemistry* **1972**, *37*, 4218-4220.

(242) Robles, J.; Pedroso, E.; Grandas, A. *Journal of Organic Chemistry* **1995**, *60*, 4856-4861.

(243) Takaku, H.; Ueda, S. *Bulletin of the Chemical Society of Japan* **1983**, *56*, 1424-1427.

(244) Bergmann, M.; Zervas, L.; Salzmann, L. *Chemische Berichte* **1933**, *66*, 1288-1290.

(245) Kaczmarek, J.; Smagowski, H.; Grzonka, Z. *Journal of the Chemical Society-Perkin Transactions 2* **1979**, 1670-1674.

(246) Finnegan, W. G.; Henry, R. A.; Lofquist, R. *Journal of the American Chemical Society* **1958**, *80*, 3908-3911.

(247) Bannwarth, W.; Trzeciak, A. *Helvetica Chimica Acta* **1987**, *70*, 175-186.

(248) Ogilvie, K. K.; Theriault, N. Y.; Seifert, J. M.; Pon, R. T.; Nemer, M. J. *Canadian Journal of Chemistry-Revue Canadienne De Chimie* **1980**, *58*, 2686-2693.

(249) Ressler, C.; Nagaraja.Gr; Kirisawa, M.; Kashelik.Dv *Journal of Organic Chemistry* **1971**, *36*, 3960-3966.

(250) Ressler, C.; Nagaraja.Gr; Lauinger, C. *Biochimica Et Biophysica Acta* **1969**, *184*, 578-582.

(251) Saneii, H.; Spatola, A. F. *Tetrahedron Letters* **1982**, *23*, 149-152.

(252) Davidson, D.; Skovronek, H. *Journal of the American Chemical Society* **1958**, *80*, 376-379.

(253) Ogilvie, K. K.; Beaucage, S. L.; Schifman, A. L.; Theriault, N. Y.; Sadana, K. L. *Canadian Journal of Chemistry-Revue Canadienne De Chimie* **1978**, *56*, 2768-2780.

(254) Scofield, M. A.; Lewis, W. S.; Schuster, S. M. *Journal of Biological Chemistry* **1990**, *265*, 12895-12902.

(255) Miller, M. T.; Bachmann, B. O.; Townsend, C. A.; Rosenzweig, A. C. *Nature Structural Biology* **2001**, *8*, 684-689.

(256) Bachmann, B. O.; Li, R. F.; Townsend, C. A. *Proceedings of the National Academy of Sciences of the United States of America* **1998**, *95*, 9082-9086.

(257) McNaughton, H. J.; Thirkettle, J. E.; Zhang, Z. H.; Schofield, C. J.; Jensen, S. E.; Barton, B.; Greaves, P. *Chemical Communications* **1998**, 2325-2326.

(258) Bachmann, B. O.; Townsend, C. A. *Biochemistry* **2000**, *39*, 11187-11193.

(259) Mackerell, A. D.; Wiorkiewiczkuczera, J.; Karplus, M. *Journal of the American Chemical Society* **1995**, *117*, 11946-11975.

(260) MacKerell, A. D.; Bashford, D.; Bellott, M.; Dunbrack, R. L.; Evanseck, J. D.; Field, M. J.; Fischer, S.; Gao, J.; Guo, H.; Ha, S.; Joseph-McCarthy, D.; Kuchnir, L.; Kuczera, K.; Lau, F. T. K.; Mattos, C.; Michnick, S.; Ngo, T.; Nguyen, D. T.; Prodhom, B.; Reiher, W. E.; Roux, B.; Schlenkrich, M.; Smith, J. C.; Stote, R.; Straub, J.; Watanabe, M.; Wiorkiewicz-Kuczera, J.; Yin, D.; Karplus, M. *Journal of Physical Chemistry B* **1998**, *102*, 3586-3616.

(261) Brooks, B. R.; Bruccoleri, R. E.; Olafson, B. D.; States, D. J.; Swaminathan, S.; Karplus, M. *Journal of Computational Chemistry* **1983**, *4*, 187-217.

(262) Thompson, J. D.; Higgins, D. G.; Gibson, T. J. *Nucleic Acids Research* **1994**, *22*, 4673-4680.

(263) Dominy, B. N.; Brooks, C. L. *Journal of Physical Chemistry B* **1999**, *103*, 3765-3773.

(264) Matte, A.; Delbaere, L. T. J. *Magnesium-Activated Enzyme Systems*; Marcel Dekker, Inc.: New York, 2001.

(265) Hughes, M. N. *The Inorganic Chemistry of Biological Processes*; 2nd ed.; John Wiley & Sons: Chichester, U.K., 1985.

(266) Harding, M. M. *Acta Crystallographica Section D-Biological Crystallography* **1999**, *55*, 1432-1443.

(267) Johnson, M. S.; Srinivasan, N.; Sowdhamini, R.; Blundell, T. L. *Critical Reviews in Biochemistry and Molecular Biology* **1994**, *29*, 1-68.

(268) Sanchez, R.; Sali, A. *Current Opinion in Structural Biology* **1997**, *7*, 206-214.

(269) Johnson, M. S.; Sali, A.; Blundell, T. L. *Methods in Enzymology* **1990**, *183*, 670-690.

(270) Greer, J. *Proteins-Structure Function and Genetics* **1990**, *7*, 317-334.

(271) Kirkpatrick, S.; Gelatt, C. D.; Vecchi, M. P. *Science* **1983**, *220*, 671-680.

(272) Vangunsteren, W. F.; Berendsen, H. J. C. *Molecular Physics* **1977**, *34*, 1311-1327.

BIOGRAPHICAL SKETCH

Yun Ding was born on February 4, 1971 in Zhejiang, China. She graduated with a bachelor's degree in medicinal chemistry from East China University of Science and Technology, Shanghai, China, with Outstanding Graduate Award from the Shanghai Higher Education Commission in July 1993. In four-year's undergraduate study, she also finished the course requirements for the second major of English. She was awarded the Outstanding Student Award from the Shanghai Higher Education Commission in the academic year of 1991 and 1992, respectively. In August 1993, she was admitted as a graduate student by the Shanghai Institute of Organic Chemistry, Chinese Academy of Sciences without having to take the entrance examination. She received a Master of Science degree in organic chemistry in July 1996. Yun is currently anticipating graduation in December of 2002 from the University of Florida with a Doctor of Philosophy degree in organic chemistry.

I certify that I have read this study and that in my opinion it conforms to acceptable standards of scholarly presentation and is fully adequate, in scope, and quality, as a dissertation for the degree of Doctor of Philosophy.

Nigel G. J. Richards, Chair
Associate Professor of Chemistry

I certify that I have read this study and that in my opinion it conforms to acceptable standards of scholarly presentation and is fully adequate, in scope, and quality, as a dissertation for the degree of Doctor of Philosophy.

William R. Dolbier, Jr.
Professor of Chemistry

I certify that I have read this study and that in my opinion it conforms to acceptable standards of scholarly presentation and is fully adequate, in scope, and quality, as a dissertation for the degree of Doctor of Philosophy.

J. Eric Enholm
Professor of Chemistry

I certify that I have read this study and that in my opinion it conforms to acceptable standards of scholarly presentation and is fully adequate, in scope, and quality, as a dissertation for the degree of Doctor of Philosophy.

Steven A. Benner
Distinguished Professor of Chemistry

I certify that I have read this study and that in my opinion it conforms to acceptable standards of scholarly presentation and is fully adequate, in scope, and quality, as a dissertation for the degree of Doctor of Philosophy.

Sheldon M. Schuster
Professor of Biochemistry and
Molecular Biology

This dissertation was submitted to the Graduate Faculty of the Department of Chemistry in the College of Liberal Arts and Sciences and to the Graduate School and was accepted as partial fulfillment of the requirements for the degree of Doctor of Philosophy.

December 2002

_____

Dean, Graduate School